94-72

International Journal of Bifurcation and Chaos, Vol. 6, No. 12A (1996) 2237–2297
© World Scientific Publishing Company

COARSE-GRAINING INVARIANT ORBITS OF ONE-DIMENSIONAL $\mathbb{Z}_p$-LINEAR CELLULAR AUTOMATA

ANDRÉ M. BARBÉ*
Katholieke Universiteit Leuven,
Department of Electrical Engineering,
Kard. Mercierlaan 94, B-3001 Leuven, Belgium

Received April 26, 1995; Revised November 22, 1995

This paper studies the properties of state-time evolution patterns of one-dimensional linear cellular automata over the field $\mathbb{Z}_p$ (p prime) which are invariant under certain coarse-graining operations.

A procedure is developed for finding all solutions to this invariance problem. The resulting patterns display a complexity which may range from periodic over self-similar, quasi-periodic, quasi-randomlike towards randomlike. Conditions for the existence of periodic solutions are derived.

1. Introduction

A one-dimensional cellular automaton (CA) produces a two-dimensional orbit pattern (i.e. state-time evolution pattern) which is completely determined by the initial state configuration and the CA's local evolution rule. A coarse-graining operation provides a rescaled view on such a pattern, by replacing regularly constructed agglomerates of cells in this pattern by a single cell whose state depends in a well-defined way on the state of the other cells in the agglomerate.

Coarse-graining operations are well known from renormalization techniques for analyzing critical phenomena in physics (e.g. ferromagnetism, critical state of fluids, percolation. See, for example, [Bruce & Wallace, 1989], [Wilson, 1979]). It is characteristic at critical points that certain features of the underlying system are invariant under a proper coarse-graining operation.

This paper deals with CA orbit patterns which are *coarse-graining invariant* (CGI), and can be seen as a broad generalization of the particular 2-state case presented in an earlier paper [Barbé *et al.*, 1995]. The generalization concerns (a) the *number of states* of a cell in the automaton: this will be p (p prime); (b) the *size* of the agglomerate to be coarse-grained: $p^n \times p^n (n \in \mathbb{N})$ instead of 2×2; (c) the *shape* of the agglomerates, which may be quite arbitrary; (d) the *way of combining* the cells within the agglomerates into a new cell (in the earlier paper, this was addition modulo 2 of all four cells in the square agglomerate); (e) the very concept of "invariance" will be broadened to "invariance modulo a shift".

The research presented here breaks with the tradition of considering cellular automata which evolve solely under a local rule, by requiring that the evolution also be governed by a global law (here

*E-mail: Andre.Barbe@esat.kuleuven.ac.be

the coarse-graining invariance). This results in the emergence of a specific set of orbit patterns with an interesting complexity, a phenomenon which has been observed before for a CA with an imposed conservation-type global law [Barbé, 1990].

Section 2 starts with a general formulation of the dynamics of CA over $\mathbb{Z}_l$ (set of integers modulo l). Then it is shown how an orbit pattern of a $\mathbb{Z}_p$-automaton (p prime) remains an orbit pattern for the same automaton when only cells at interdistance p^n are considered while all other cells are deleted (this is called p^n-decimation). This property is of crucial importance in the further developments.

Section 3 introduces coarse-graining operations on orbit patterns of $\mathbb{Z}_p$-automata. This needs the definition of admissible tilings of the lattice on which the orbits are displayed. Then we discuss the way in which all cells in a tile can be combined together through a proper weighting. It is then shown how an admissible coarse-graining of an orbit pattern produces a new orbit pattern (satisfying the same CA-rule). This is a direct consequence of the decimation property from Sec. 2.

Section 4 derives the conditions for coarse-graining invariance of an orbit pattern and introduces the concept of *complete* coarse-graining invariance. This is a situation for which the number of solutions to the CGI-problem is finite. We give a constructive proof of this, which provides a set of recursive equations for deriving the initial state of the CA which generates a CGI-orbit. There recursive equations are of a particular kind. We show how to obtain the initial conditions from which these equations can be solved, and will thereby introduce the notion of seed, seedcode, freecells and depcells of a particular solution. Subsection 4.4 discusses the (Abelian) group structure of the solution set for a given CGI-problem.

In contrast to the cases presented in the earlier paper [Barbé *et al.*, 1995], where only quasi-periodic and Sierpinsky-like patterns emerged, the generalization in the present paper produces patterns which may be periodic (fully or partially), quasi-periodic, visually self-similar, complex, quasi-randomlike, randomlike. Examples of this are given in Sec. 5.

Section 6 analyzes the conditions for periodicity of solutions. We formulate a theorem concerning the possible periods. Sufficient conditions are given which allow to find all solution patterns to the CGI-problem which are fully or partially periodic.

2. One-Dimensional Linear Cellular Automata over $\mathbb{Z}_p$

2.1. *Preliminaries: Additive automata over* $\mathbb{Z}_l, l \in \mathbb{N}$

Consider a double-infinite string of cells as shown in Fig. 1. Each cell has an address $c \in \mathbb{Z}$, according to its natural position with respect to a fixed reference cell with address 0. Also, at each discrete time moment $r \in \mathbb{N}$,[1] the cell at location c is attributed a state $a(r, c)$ which is an integer from $\mathbb{Z}_l \triangleq \{0, 1, \ldots, l-1\}$, the set of integers modulo l. This string of cells forms a one-dimensional linear cellular automaton (CA) when it is provided with a dynamics that updates the cell states from one time-instance to the next one, according to the *local evolution rule*

$$a(r, c) = \sum_{k=d_l}^{d_r} q(k)a(r-1, c-k) \pmod{l}, \quad (1)$$

where $q(k) \in \mathbb{Z}_l$, and where d_l and d_r are integers satisfying $d_l < d_r$.

The double-infinite string or sequence

$$S_r \triangleq \langle a(r, c)\rangle_{c\in\mathbb{Z}} = \ldots a(r, -2)a(r, -1)a(r, 0)a(r, 1)a(r, 2)\ldots \quad (2)$$

represents the *state of the automaton at time* r.

We also introduce the *rule-sequence* R defined as

$$R \triangleq \langle r(c)\rangle_{c\in\mathbb{Z}} \text{ where } r(c) = q(c) \text{ when } d_l \le c \le d_r \quad r(c) = 0 \text{ otherwise}. \quad (3)$$

Equation (1) then shows that S_r can be obtained from S_{r-1} by convoluting S_r with R.

The automaton obeying the rule of Eq. (1) is called *linear* or *additive*, because Eqs. (1) and (2) show that when S'_{r-1} and S''_{r-1} are two different states at time $(r-1)$ which are linearly combined to form the state $S_{r-1} = c'S'_{r-1} + c''S''_{r-1} (\mathrm{mod}\, l)$, ($c'$ and $c'' \in \mathbb{Z}_l$), then $S_r = c'S'_r + c''S''_r$, where S'_r and S''_r are the states derived from S'_{r-1} and S''_{r-1} separately according to Eq. (1).

[1] We use the convention $\mathbb{N} = \{0, 1, 2, \ldots\}, \mathbb{N}_0 = \mathbb{N}\backslash\{0\}$.

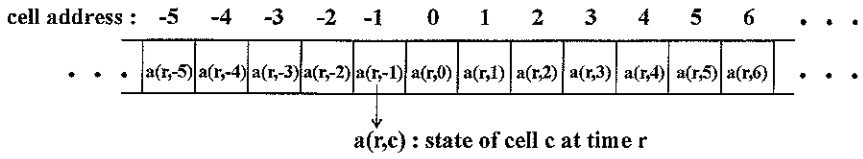

(a)

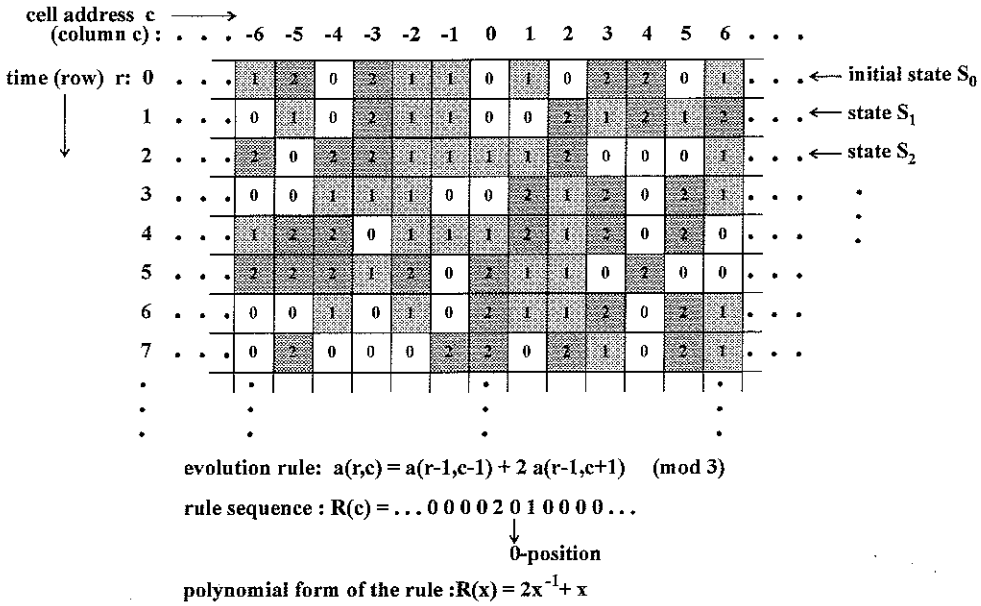

(b)

Fig. 1. (a) The double-infinite cellular automaton configuration at time r. (b) The orbit $O_R(S_o)$ (trajectory, state-time evolution) of a cellular automaton in $\mathbb{Z}_3$.

The complete *state-time evolution* (or *orbit*, *trajectory*) of the automaton, as given by the two-dimensional sequence $\langle a(r, c)\rangle_{(r,c)\in\mathbb{N}\times\mathbb{Z}}$, can be graphically represented on a half-infinite two-dimensional square lattice of cells as shown in Fig. 1(b), where each cell is given an attribute (number, color, symbol) which is in 1-1 correspondence with its state in $\mathbb{Z}_l$. In the many illustrations that will follow, this will be a color. In this way the state-time evolution of a one-dimensional automaton produces a two-dimensional orbit pattern $O_R(S_0)$. As indicated, this pattern is completely determined by the initial state S_0 and by the particular local rule (sequence) R. Assuming that the context fixes R and S_0, we will continue to use $a(r, c)$ for the state of the (r, c)th cell in this pattern, whereby (r, c) have now become associated with the row-number and column-number in the array on which the pattern is displayed.

2.2. *Polynomial formalism for studying additive CA*

Observe the 1-1 correspondence between an arbitrary sequence $\langle b(k)\rangle_{k\in\mathbb{Z}}$ and the associated polynomial

$$B(x) \triangleq \sum_{k\in\mathbb{Z}} b(k)x^k .$$

Now consider the corresponding polynomials for the sequences R and S_r:

$$R(x) \triangleq \sum_{c\in\mathbb{Z}} r(c)x^c = \sum_{k=d_l}^{d_r} q(k)x^k \qquad (4)$$

$$S_r(x) \triangleq \sum_{c\in\mathbb{Z}} a(r, c)x^c , \qquad (5)$$

where d_l and d_r now appear as the lower and upper degree of $R(x)$. Then the convolution of Eq. (1)

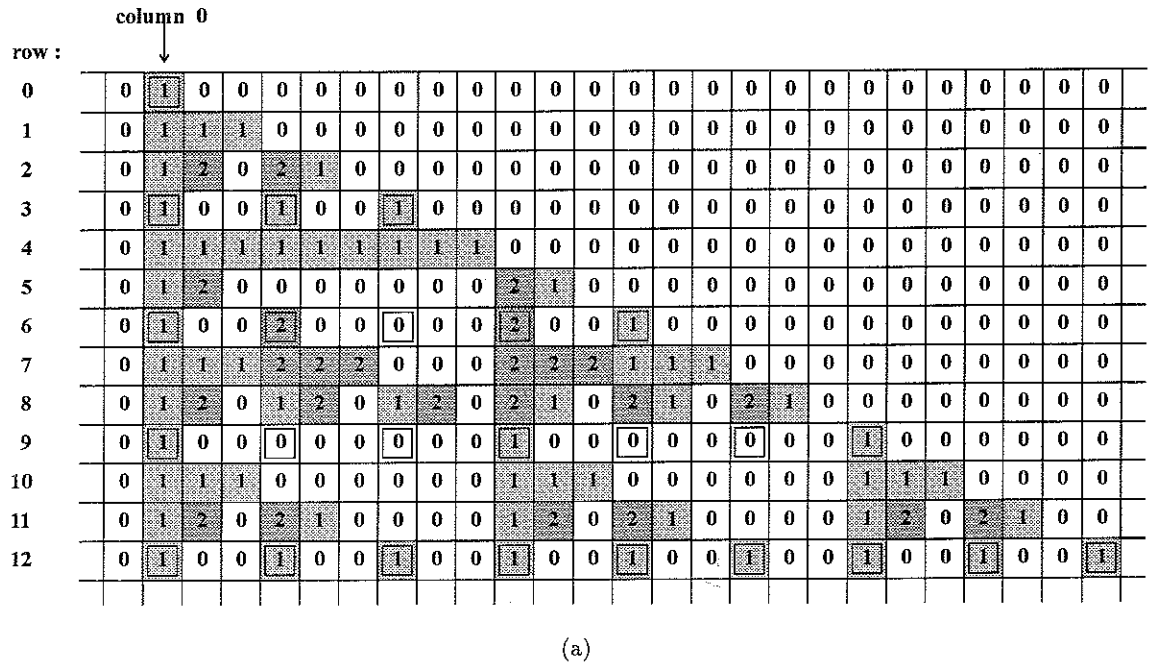

(a)

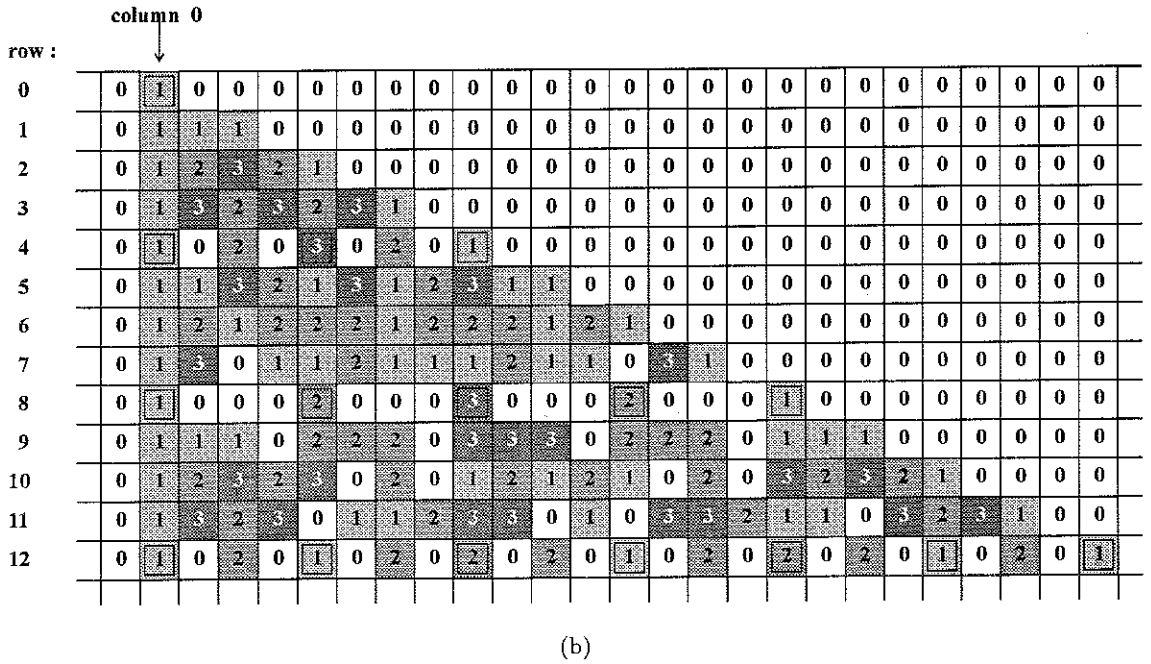

(b)

Fig. 2. Rule orbit patterns for (a) $R(x) = 1 + x + x^2 \in \mathbb{Z}_3[x]$ and (b) $R(x) = 1 + x + x^2 \in \mathbb{Z}_4[x]$. The first case is invariant under (0, 0)3-decimation, the second case is *not* invariant under (0, 0)4-decimation (the decimation is indicated by the doubly-squared cells).

can be transformed into the equivalent polynomial product form

$$S_r(x) = R(x) \cdot S_{r-1}(x) \tag{6}$$

(all operations modulo l, the polynomials $R(x)$ and $S_r(x)$ belong to the class $\mathbb{Z}_l[x]$ of polynomials with coefficients in $\mathbb{Z}_l$). From Eq. (6), it follows directly that

$$S_r(x) = (R(x))^r \cdot S_0(x)\,. \tag{7}$$

$R(x)$ completely determines the rule of the automaton. It is sometimes called the *characteristic*

polynomial or *generating function* (see e.g. [Martin *et al.*, 1984]). We will just refer to it as the (polynomial form of the) CA-rule.

Let the initial state for the automaton be such that $S_0(x) = 1$. This corresponds to the initial state which has a 1 in the 0th cell, while all other cells are 0, and this particular sequence will be denoted by U_0. Equation (7) then produces

$$S_r(x) = (R(x))^r\,, \tag{8}$$

and the corresponding orbit pattern $O_R(U_0)$ displays on the rth row the sequence associated with the polynomial $(R(x))^r$, i.e. the sequence which is the $(r-1)$-fold convolution of the sequence R with itself (for $r \geq 2$). This particular orbit pattern will be called the *rule orbit pattern*, and the corresponding state of the cell at row r and column c will be represented by $\rho(r, c)$. Observe that $\rho(r, c) = 0$ for $c < rd_l$ and $c > rd_r$. An example is given in Fig. 2 for $R(x) = 1+x+x^2 \in \mathbb{Z}_3[x]$ and $R(x) = 1+x+x^2 \in \mathbb{Z}_4[x]$.

Equation (7) can also be written in the slightly more general form

$$S_r(x) = (R(x))^m \cdot S_{r-m}(x)\,, \quad 0 \leq m \leq r\,. \tag{9}$$

Re-interpreted in the sequence-domain, this means that the rth row in $O_R(S_0)$ can be obtained from the mth row above it (i.e. row $(r-m)$), by convoluting the latter one with the mth row of the rule orbit pattern $O_R(U_0)$. Formally:

$$\forall r \in \mathbb{N},\, m \leq r:$$

$$a(r, c) = \sum_{j=md_l}^{md_r} \rho(m, j)a(r-m, c-j)\,. \tag{10}$$

2.3. *Particular properties for $\mathbb{Z}_p$-automata, p being prime*

We start by formulating a key-property, because all further developments in this paper crucially depend on it. Observe that selecting p prime in $\mathbb{Z}_p$, makes $(\mathbb{Z}_p, +, \cdot)$ a field.

Property 2.1. *For polynomials $B(x) \in \mathbb{Z}_p[x]$ with p prime, it holds that*

$$(B(x))^p = B(x^p) \quad (mod\, p) \tag{11}$$

and, by extension

$$\forall n \in \mathbb{N}_0 : (B(x))^{p^n} = B(x^{p^n}) \quad (mod\, p)\,. \tag{12}$$

This property is closely related to Fermat's (little) theorem, and a proof can be found in Hardy & Wright [1978, chapter VI]. Cellular automata with a rule $R(x) \in \mathbb{Z}_p[x]$, p prime, belong to the class of so-called Strong Fermat Automata (w.r.t. p) [see (F. von Haeseler *et al.*, 1993)]. In what follows, p will always denote a prime number, and all equations and arithmetic expressions concerning the CA-behavior will be modulo p. Henceforth, the (mod p) indication will mostly be dropped.

Definition 2.1.

— Let $r_0, c_0 \in \mathbb{N}$ and $r_0, c_0 < p^n$. The $(r_0, c_0)p^n$-decimation of a CA-orbit pattern $O_R(S_0)$ in $\mathbb{Z}_p$ is the pattern $D_{p^n}^{(r_0, c_0)}O_R(S_0)$ with elements

$$d(r, c) = a(r_0 + rp^n, c_0 + cp^n)$$
$$(\text{for } r \in \mathbb{N} \;\&\; r_0 + rp^n \geq 0,\, c \in \mathbb{Z}) \tag{13}$$

— With l a positive integer, the sequence $\langle b'(i)\rangle_{i\in\mathbb{Z}}$ is the *l-expansion* of the sequence $\langle b(i)\rangle_{i\in\mathbb{Z}}$ when

$$\begin{cases} b'(i) = b\left(\dfrac{i}{l}\right) \text{ for } i = kl,\, k \in \mathbb{Z} \\ b'(i) = 0 \text{ otherwise}\,, \end{cases}$$

i.e. $\langle b'(i)\rangle$ inserts $(l-1)$ zeroes between each term of $\langle b(i)\rangle$. When $B'(x)$ and $B(x)$ are the associated polynomials, this means that $B'(x) = B(x^l)$.

Property 2.2. *The rule orbit pattern $O_R(U_0)$ is invariant under $(0, 0)p^n$-decimation, i.e.*

$$D_{p^n}^{(0,0)}O_R(U_0) = O_R(U_0)\,. \tag{14}$$

Proof. $(R(x))^m$ corresponds to the mth row in the rule orbit pattern. Equation (12) implies that $(R(x))^{rp^n} = (R(x^{p^n}))^r$, i.e. the rp^nth row in the rule orbit pattern is the p^n-expansion of its rth row:

$$\rho(rp^n, c) = \rho\left(r, \frac{c}{p^n}\right) \text{ when } c = mp^n,\, m \in \mathbb{Z}$$
$$= 0 \text{ when } c \neq mp^n \tag{15}$$

This also implies:

$$\rho(rp^n, cp^n) = \rho(r, c) \text{ for } r \in \mathbb{N},\, c \in \mathbb{Z} \tag{16}$$

From Eq. (13) we obtain that the $(0, 0)p^n$-decimation of $O_R(U_0)$ returns $O_R(U_0)$:

$$d(r, c) \overset{(13)}{=} \rho(rp^n, cp^n) \overset{(16)}{=} \rho(r, c)\,. \quad \blacksquare$$

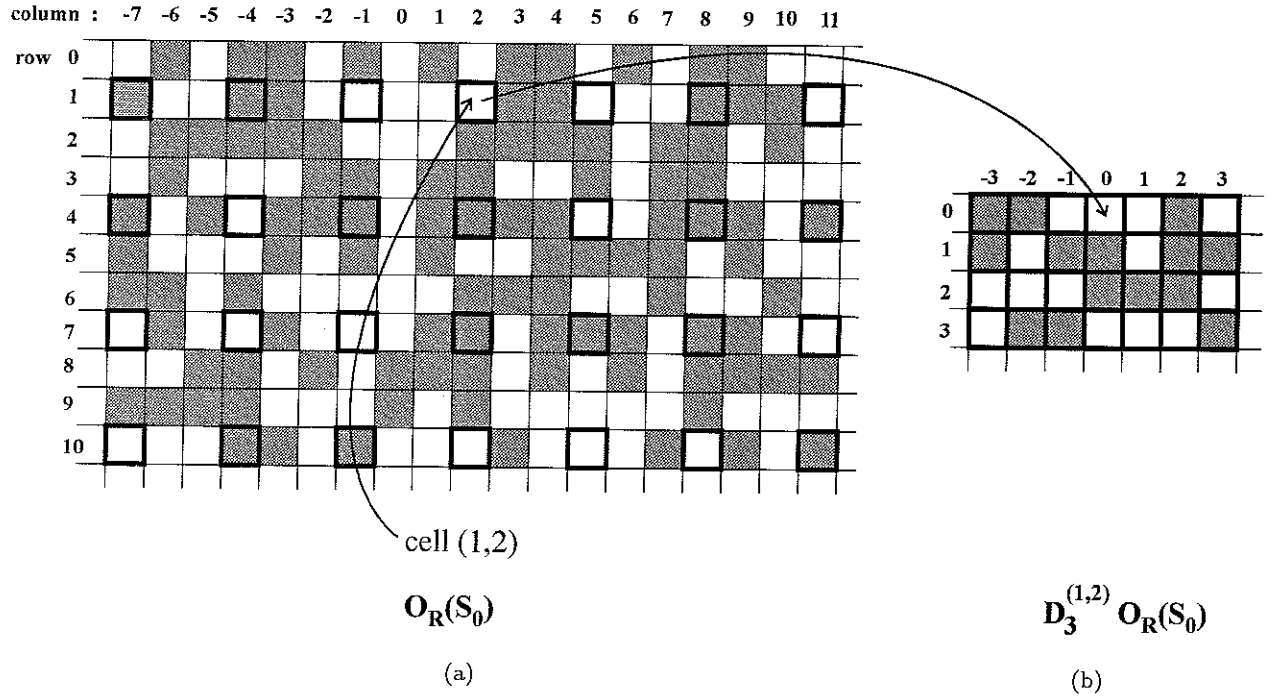

(a) (b)

Fig. 3. (a) An orbit pattern $O_R(S_0)$ and the cells selected for 3-decimation (highlighted cells). $(r_0, c_0) = (1, 2)$ is the location of the decimation reference cell. (b) Joining the highlighted cells in the proper order forms the $D_3^{(1,2)}O_R(S_0)$ decimation pattern of $O_R(S_0)$.

Property 2.2 is easily checked in Fig. 2(a) (rule in $\mathbb{Z}_3$): rows 3, 6, 9, 12... are the 3-expansions of rows 1, 2, 3, 4... (in general row $k3^n$ is the 3^n-expansion of row k). Observe that a similar property does *not* hold for Fig. 2(b) (rule in $\mathbb{Z}_4$): rows 4, 8, 12,... are clearly not 4-extensions of the rows 1, 2, 3,...

Property 2.3. *The $(r_0, c_0)p^n$-decimation of any orbit pattern $O_R(S_0)$ satisfies the rule R; or, with $d(r, c)$ a general element of $D_{p^n}^{(r_0, c_0)}O_R(S_0)$:*

$$d(r, c) = \sum_{k=md_l}^{md_r} \rho(m, k)d(r-m, c-k), \quad 0 \le m \le r\,. \tag{17}$$

Proof

$$d(r, c) \overset{(13)}{=} a(r_0 + rp^n, c_0 + cp^n)$$

$$\overset{(10)}{=} \sum_{j=mp^n d_l}^{mp^n d_r} \rho(mp^n, j)a(r_0 + rp^n - mp^n, c_0 + cp^n - j)$$

$$\overset{(15)}{=} \sum_{k=md_l}^{md_r} \rho(mp^n, kp^n)a(r_0 + rp^n - mp^n, c_0 + cp^n - kp^n)$$

$$\overset{(13)}{=} \sum_{k=md_l}^{md_r} \rho(m, k)d(r - m, c - k)\,. \quad \blacksquare$$

3. Coarse-Graining Operations

3.1. *Admissible tilings of the square lattice*

The lattice on which the orbit pattern of a cellular automaton is displayed, is the half-infinite two-dimensional square lattice with address space $\{(r, c)|r \in \mathbb{N}, c \in \mathbb{Z}\}$. We will partition it in a regular tiling.

Definition 3.1.

- A *p^n-tile* of the half-infinite square lattice is any agglomerate of $p^n \times p^n$ lattice-cells which, by horizontal shifts over distances $kp^n (k \in \mathbb{Z})$ and by vertical shifts over distances $lp^n (l \in \mathbb{N})$, completely covers the lattice without overlap.

  Such a tile consists of a set of cells whose addresses belong to the set

$$\mathcal{A}_{p^n,\beta,\Gamma}(rp^n, c) \triangleq \{(rp^n + i, c + \beta_i + j + \gamma_{i,j}p^n) \mid i, j = 0, 1, \ldots, p^n - 1\}\,, \tag{18}$$

with $r \in \mathbb{N}$ and $c \in \mathbb{Z}$, r and c fixed; and with $\beta \triangleq (0, \beta_1, \ldots, \beta_{p^n-1})$, $\beta_i \in \mathbb{Z}$ and $\Gamma \triangleq p^n \times p^n$

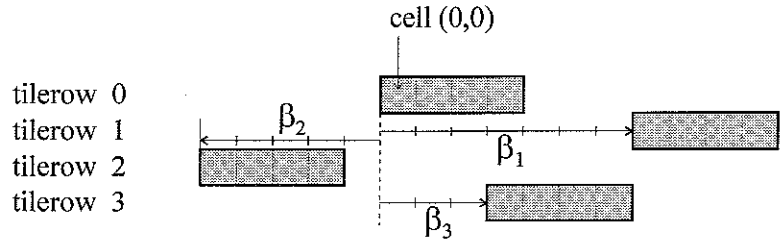

tile configuration vector $\beta = (0, \beta_1, \beta_2, \beta_3) = (0,7,-5,3)$

a.

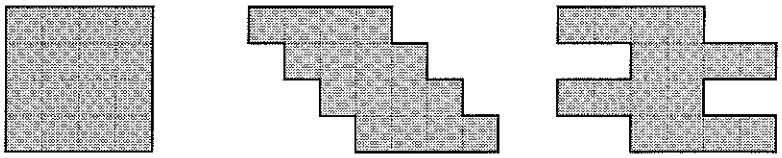

b. **c.** **d.**

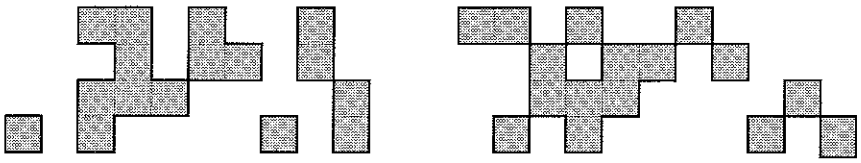

e. **f.**

Fig. 4. A selection of possible 2^2-tile-configurations. The configuration parameters are (a) $\beta = (0, \beta_1, \beta_2, \beta_3) = (0, 7, -5, 3)$, $\Gamma = [0]$; (b) $\beta = (0, 0, 0, 0)$, $\Gamma = [0]$; (c) $\beta = (0, 1, 2, 3)$, $\Gamma = [0]$; (d) $\beta = (0, 2, 0, 2)$, $\Gamma = [0]$; (e) $\beta = (0, 0, 0, 0)$ and $\Gamma = \begin{bmatrix} 0 & 0 & 1 & 0 \\ 1 & 0 & 1 & 0 \\ 0 & 0 & 0 & 1 \\ 0 & 1 & -1 & 1 \end{bmatrix}$; (f) $\beta = (0, 1, 2, 3)$ and Γ as under (e).

matrix with elements $\gamma_{i,j} \in \mathbb{Z}$ $(i, j = 0, 1, \ldots, p^n - 1)$. As shown in Fig. 4, different tile-shapes are possible, dependent on β and Γ. Therefore, β will be called the *tile configuration vector*, and Γ the *tile configuration matrix*. The cells in a tile are not necessarily connected, but they all belong to p^n successive rows. Each row in a tile will be called a *tilerow*: they are numbered from 0 to $p^n - 1$ from top to bottom. When $\Gamma = [0]$, all cells in each tilerow are connected (like in Figs. 4(a) to 4(d). β_i is the relative shift of the ith tilerow with respect to the 0th tilerow: $\beta_i > 0$ corresponds to a shift over β_i cells to the right, $\beta_i < 0$ to a shift to the left. Obviously $\beta_0 = 0$. When $\gamma_{i,j} \neq 0$, it means that the jth cell in the ith tilerow will be relocated from its horizontal position $(c + \beta_i + j)$ to $(c + \beta_i + j + \gamma_{i,j} p^n)$, and so cells may become disconnected in a tilerow [Figs. 4(e) and 4(f)].

- It will be convenient to introduce the *global tile configuration matrix* Ξ with elements

$$\xi_{i,j} \triangleq \beta_i + \gamma_{i,j} p^n .$$

The following concepts are illustrated in Fig. 5(a).

- The *basis-tile* is the tile corresponding to Eq. (18) with $r = c = 0$.
- The p^n-*tiling* obtained by covering the lattice by vertical and horizontal p^n-shifts of the basis-tile

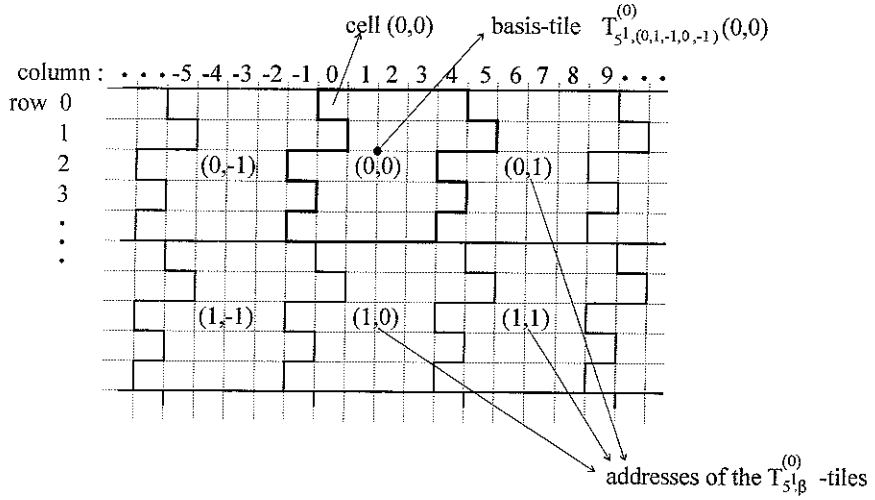

(a)

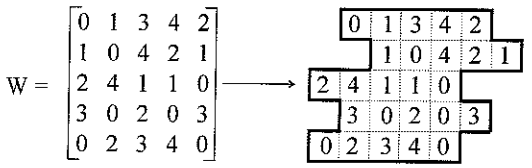

(b)

Fig. 5. (a) The basic $\mathcal{T}^{(0)}_{5^1,\beta}$-tiling ($\beta = (0, 1, -1, 0, -1)$). The σ-shifted tiling $\mathcal{T}^{(\sigma)}_{5^1,\beta}$ ($\sigma = 0, 1, 2, 3, 4$ for this example) would shift all tiles over σ cells to the right. (b) Weighting the tile-cells according to the weight matrix W.

will be called the *basic p^n-tiling*. It will be represented by $\mathcal{T}^{(0)}_{p^n,\Xi}$. Each tile in this tiling will be given an address (r, c). The tile with address (r, c) in tiling $\mathcal{T}^{(0)}_{p^n,\Xi}$ will be denoted by $T^{(0)}_{p^n,\Xi}(r, c)$: it is the tile that covers the cells located at $(rp^n + i, cp^n + \xi_{i,j} + j)$, with $i, j \in \{0, 1, \ldots, p^n - 1\}$. When $\Gamma = [0]$, the notation $\mathcal{T}^{(0)}_{p^n,\beta}$ will be used.

- For a given tile configuration, there are p^n different p^n-tilings. They are obtained by shifting the basic p^n-tiling horizontally over $0, 1, 2, \ldots, p^n - 1$ cells. The tiling obtained by shifting the basic tiling over σ cells will be represented by $\mathcal{T}^{(\sigma)}_{p^n,\Xi}$. The (r, c)th tile in this σ-shifted tiling will be denoted by $T^{(\sigma)}_{p^n,\Xi}(r, c)$ and contains the cells with addresses $(rp^n + i, cp^n + \xi_{i,j} + \sigma + j)$; $i, j \in \{0, 1, \ldots, p^n - 1\}$.

3.2. *Coarse-graining of an orbit pattern*

A given orbital pattern $O_R(S_0)$ can be submitted to a *coarse-graining transformation* as follows:

1. Fix a p^n-tiling, say $\mathcal{T}^{(\sigma)}_{p^n,\Xi}$.
2. Consider each tile $\mathcal{T}^{(\sigma)}_{p^n,\Xi}(r, c)$ as a new single cell whose value $\theta^{(\sigma)}(r, c)$ is a weighted sum of the values of all cells in $O_R(S_0)$ which are covered by the tile:

$$\theta^{(\sigma)}(r, c) = \sum_{0 \le i, j \le p^n - 1} w(i, j)\, a(rp^n + i, cp^n + \xi_{i,j} + \sigma + j) \tag{19}$$

   with $w(i, j) \in \mathbb{Z}_p$.
3. The set of all new (coarse-grained) cells $\theta^{(\sigma)}(r, c)$ ($r \in \mathbb{N}$, $c \in \mathbb{Z}$) constitutes a new pattern which is the coarse-grained version of the original orbit pattern $O_R(S_0)$. It will be represented by $[\mathcal{T}^{(\sigma)}_{p^n,\Xi}, W]O_R(S_0)$, where W is the $p^n \times p^n$ *weight-matrix* $W \triangleq [w(i, j)]$, $0 \le i, j \le p^n - 1$.

The elements in the weight matrix can also be thought of as values attributed to the cells in the tile-configuration [see Fig. 5(b)]. A coarse-graining

operation based on the tiling $\mathcal{T}^{(\sigma)}_{p^n,\Xi}$ and weight matrix W will be called a $[\mathcal{T}^{(\sigma)}_{p^n,\Xi}, W]$-coarse-graining.

Let $\Delta_{u,v}$ be a $p^n \times p^n$ matrix whose entries are all zero except the one at (u, v) which is 1. If we take $W = \Delta_{u,v}$ in Eq. (19), then the coarse-graining operation reduces to a pure p^n*-decimation operation*; i.e. the $[\mathcal{T}^{(\sigma)}_{p^n,\Xi}, \Delta_{u,v}]$-coarse graining of $O_R(S_0)$ equals $D^{(u,v+\xi_{u,v}+\sigma)}_{p^n} O_R(S_0)$ with elements

$$d^{(u,v+\xi_{u,v}+\sigma)}(r, c) = a(u + rp^n, v + \xi_{u,v} + \sigma + cp^n)\ r \in \mathbb{N},\ c \in \mathbb{Z}. \tag{20}$$

Property 3.1. *Any* $[\mathcal{T}^{(\sigma)}_{p^n,\Xi}, W]$*-coarse-graining of an orbit pattern* $O_R(S_0)$ *satisfies the rule* R*. That is, when* $\theta^{(\sigma)}(r, c)$ *denotes the* (r, c)*th cell of this coarse-graining, we have*

$$\theta^{(\sigma)}(r, c) = \sum_{k=md_l}^{md_r} \rho(m, k)\theta^{(\sigma)}(r - m, c - k),\ 0 \le m \le r$$

(recall: $\rho(m, k)$ *is the* (m, k)*th cell of the rule orbit pattern).*

Proof

$$\theta^{(\sigma)}(r, c) \overset{(19)}{=} \sum_{0 \le i,j \le p^n - 1} w(i, j)a(rp^n + i, cp^n + \xi_{i,j} + \sigma + j)$$

$$\overset{(20)}{=} \sum_{0 \le i,j \le p^n - 1} w(i, j)d^{(i,j+\xi_{i,j}+\sigma)}(r, c)$$

$$\overset{(17)}{=} \sum_{0 \le i,j \le p^n - 1} w(i, j) \sum_{k=md_l}^{md_r} [\rho(m, k)d^{(i,j+\xi_{i,j}+\sigma)} \times (r - m, c - k)]$$

$$= \sum_{k=md_l}^{md_r} \rho(m, k) \sum_{0 \le i,j \le p^n - 1} [w(i, j)d^{(i,j+\xi_{i,j}+\sigma)} \times (r - m, c - k)]$$

$$\overset{(20,19)}{=} \sum_{k=md_l}^{md_r} \rho(m, k)\theta^{(\sigma)}(r - m, c - k). \quad \blacksquare$$

4. Orbit Patterns that are Invariant under Coarse-Graining

4.1. *Invariance under* $[\mathcal{T}^{(\sigma)}_{p^n,\Xi}, W]$*-coarse-graining*

Property 3.1, stating that the $[\mathcal{T}^{(\sigma)}_{p^n,\Xi}, W]$-coarse-graining version of an orbit pattern $O_R(S_0)$ is also an orbit pattern satisfying the same rule, allows one to ask the question whether there exists an $O_R(S_0)$ that equals its coarse-grained version. That is, does an $O_R(S_0)$ exist such that

$$[\mathcal{T}^{(\sigma)}_{p^n,\Xi}, W]O_R(S_0) = O_R(S_0)? \tag{21}$$

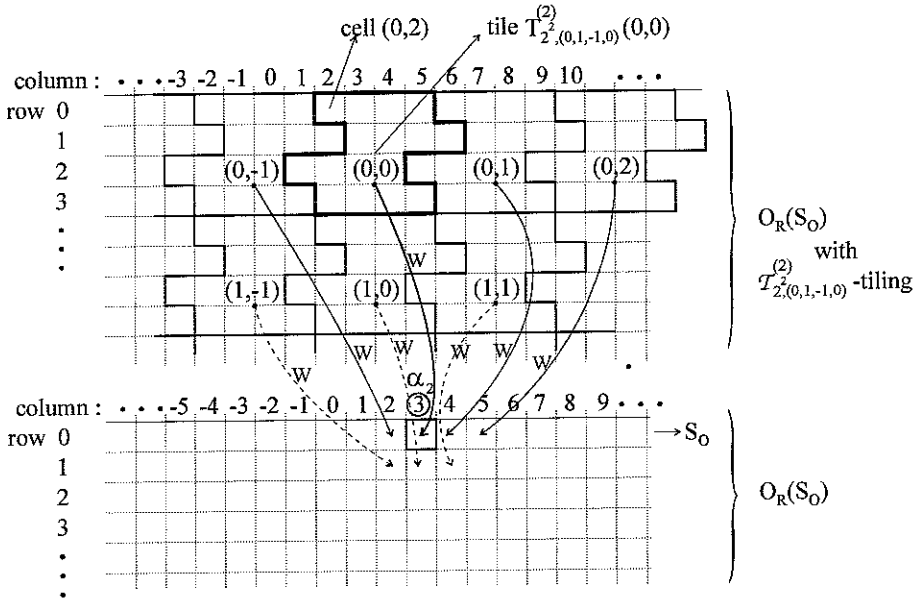

Fig. 6. $[\mathcal{T}^{(\sigma)}_{p^n,\Xi}, W, \alpha_\sigma]$-coarse graining invariance of $O_R(S_0)$ requires an identity between the W-weighted top-row $T^{(\sigma)}_{p^n,\Xi}(0, k)$-tiles and $a(0, k + \alpha_\sigma)$ (here $\sigma = 2$, $\alpha_\sigma = \alpha_2 = 3$).

If so, we say that $O_R(S_0)$ is *invariant* under $[\mathcal{T}^{(\sigma)}_{p^n,\Xi}, W]$-coarse-graining.

It is clear from the fact that both the original and coarse-grained version of $O_R(S_0)$ satisfy the same rule R (Property 3.1), that a necessary and sufficient condition for Eq. (21) to hold is that the top row of tiles covering $O_R(S_0)$ maps into the first row S_0 under the specified coarse-graining. This condition formalizes as

$\forall k \in \mathbb{Z}$:

$$\sum_{0\le i,j\le p^n-1} w(i,\, j)a(i,\, kp^n + \xi_{i,j} + \sigma + j) = a(0,\, k)\,. \tag{22}$$

Invariance modulo a shift

We can introduce a generalization at this place, by observing that from a certain point of view, patterns that are defined on a half-infinite two-dimensional lattice but which are just horizontally shifted versions of each other, are indistinguishable. The shift will only be relevant when considering an absolute coordinate system in the lattice, thereby fixing once and for all the (0, 0)-cell. But as far as the pattern as such is concerned, this shift is irrelevant. For this reason, we will from here on allow such a shift (w.r.t. an absolute reference). Let $S_0 = \langle a(0,\, c)\rangle_{c\in\mathbb{Z}}$ be the initial state of the automaton w.r.t. a given absolute reference, then ${}^{\alpha}S_0$ will denote the horizontally shifted version over α cells, i.e. ${}^{\alpha}S_0 = \langle a(0,\, c+\alpha)\rangle_{c\in\mathbb{Z}}$. The corresponding shifted orbital pattern will be denoted by ${}^{\alpha}O_R(S_0)$, whereby it is clear that ${}^{\alpha}O_R(S_0) = O_R({}^{\alpha}S_0)$. In general, we will call $O_R(S_0)$ coarse-graining invariant under $[\mathcal{T}^{(\sigma)}_{p^n,\Xi}, W, \alpha_\sigma]$ coarse-graining, whenever

$$[\mathcal{T}^{(\sigma)}_{p^n,\Xi}, W, \alpha_\sigma]O_R(S_0) = {}^{\alpha_\sigma}O_R(S_0)\,. \tag{23}$$

The necessary and sufficient condition for Eq. (23) to hold is then given by the generalized version of Eq. (22)

$\forall k \in \mathbb{Z}$:

$$\sum_{0\le i,j\le p^n-1} w(i,\, j)a(i,\, kp^n + \xi_{i,j} + \sigma + j) = a(0,\, k + a_\sigma)\,. \tag{24}$$

The whole idea is illustrated in Fig. 6. Equations (24) will be called the *coarse-graining invariance equations* (CGI-equations) for the $[\mathcal{T}^{(\sigma)}_{p^n,\Xi}, W, \alpha_\sigma]$-coarse-graining invariance problem. In the next section, we will discuss how these equations can be solved when d_l, the minimal degree of the rule polynomial $R(x)$, is restricted to be 0. It will be shown in a later section how the problem with arbitrary d_l can be reduced to this restricted problem.

4.2. *Solution of the CGI-equations for CA-rules with $d_l = 0$*

4.2.1. *The initial-state-reduced CGI-equations*

For convenience, initial-state cell $a(0,\, c)$ will mostly be written as $a(c)$ in what follows.

All $a(i, *)$ elements in Eq. (24) can be expressed in their dependence on the initial-state-cells, using Eq. (10) (with $d_l = 0$):

$$a(i, kp^n + \xi_{i,j} + \sigma + j) = \sum_{s=0}^{id_r} \rho(i, s)a(kp^n + \xi_{i,j} + \sigma + j - s)\,.$$

It follows that the left-hand side of Eq. (24) can be rewritten as

$$\sum_{0\le i,j\le p^n-1} \sum_{s=0}^{id_r} w(i,j)\rho(i,s)a(kp^n + \xi_{i,j} + \sigma + j - s)\,.$$

Let

$$\eta_{\max} \triangleq \max_{i,j}(\xi_{i,j} + j) = \max_{i,j}(\beta_i + \gamma_{i,j}p^n + j)$$

$$\eta_{\min} \triangleq \min_{i,j}(\xi_{i,j} + j) = \min_{i,j}(\beta_i + \gamma_{i,j}p^n + j),$$

then it follows that the column coordinate $kp^n + \xi_{i,j} + \sigma + j - s$ in the double-sum expression above ranges from the maximal value $kp^n + \eta_{\max} + \sigma$ to the minimal value $kp^n + \eta_{\min} + \sigma - (p^n - 1)d_r$, so that this expression can be reformulated as

$$\sum_{t=0}^{(\eta_{\max}-\eta_{\min})+(p^n-1)(d_r)} u(t)a(kp^n + \eta_{\max} + \sigma - t)\,, \tag{25}$$

where $u(t) = \sum_{(i,j,s)\in Q_{t,p^n,\Xi}} w(i,\, j)\rho(i,\, s)$, with $Q_{t,p^n,\Xi} = \{(i,\, j,\, s) | 0 \le i,\, j \le p^n - 1,\, 0 \le s \le id_r,\, \xi_{i,j} + j - s = \eta_{\max} - t\}$.

Replacing the dummy index t by i in Eq. (25), we may conclude that the CGI-equation Eq. (24) can be transformed into:

$\forall k \in \mathbb{Z}$:

$$\sum_{i=i_{\min}}^{i_{\max}} u(i)a(kp^n + \eta_{\max} + \sigma - i) = a(0,\, k + \alpha_\sigma)\,, \tag{26}$$

where $i_{\min}$ and $i_{\max}$ are the minimal and maximal values of i for which $u(i) \neq 0$. Observe that the $u(i)$ only depend on p^n, Ξ, W and *not* on σ, the particular tiling-shift. Equations (26) are the *initial-state-reduced CGI-equations*. Solving these equations will produce an initial state $S_0 = \langle a(c)\rangle_{c\in\mathbb{Z}}$ for which $O_R(S_0)$ is $[T^{(\sigma)}_{p^n,\Xi}, W, \alpha_\sigma]$-coarse-graining invariant. Equations (26) being homogeneous, there is a particular trivial solution: the *null-solution* for which $a(j) = 0$ for all j. It is the *trivial solution* for *any* $[T^{(\sigma)}_{p^n,\Xi}, \alpha_\sigma, W, R]$-*coarse-graining problem*; as such it is not very interesting as it makes all cells in the corresponding orbit 0.

4.2.2. *The standard recursions for the initial-state sequence*

Consider Eq. (26). Rearranging terms and using

$$\begin{aligned} c_r(0) &\triangleq (u(i_{\min}))^{-1} \pmod{p^n} \\ c'_r(i) &\triangleq -(u(i_{\min}))^{-1}u(i) \\ &= (u(i_{\min}))^{-1}\cdot(p-u(i)) \pmod{p^n}, \end{aligned}$$

produces the following equivalent form

$$\begin{aligned} &\forall k\in\mathbb{Z}:\ a(kp^n+\eta_{\max}+\sigma-i_{\min}) \\ &= c_r(0)a(k+\alpha_\sigma)+\sum_{i=i_{\min}+1}^{i_{\max}} c'_r(i)a(kp^n+\eta_{\max}+\sigma-i)\,. \end{aligned} \tag{27}$$

This equation can be written in a simpler form by substituting $kp^n+\eta_{\max}+\sigma-i_{\min}$ by m, $(i-i_{\min})$ by j, $c'_r(j+i_{\min})$ by $c_r(j)$, and finally by replacing the dummy j by i again. Using, in addition, the notations

$$\Phi_r \triangleq \eta_{\max} - i_{\min} \tag{28}$$

$$\begin{aligned} \overline{\mathcal{M}}^{(\sigma)}_r &\triangleq \{kp^n+\Phi_r+\sigma | k\in\mathbb{Z}\} \\ &= \{v | v\equiv(\Phi_r+\sigma) \bmod p^n\} \end{aligned} \tag{29}$$

produces the set of equations

$$\begin{aligned} \forall m\in\overline{\mathcal{M}}^{(\sigma)}_r : a(m) &= c_r(0)a\left(\frac{m-\sigma-\Phi_r}{p^n}+\alpha_\sigma\right) \\ &+ \sum_{i=1}^{i_{\max}-i_{\min}} c_r(i)a(m-i) \end{aligned} \tag{30}$$

Observe that in this equation, the cell state $a(m)$ can be expressed as a function of several $a(j)$'s with $j < m$ when the address of the cell referred to by the first right-hand side term is less than m; i.e. when

$$m > \mu^{(\sigma)}_r \triangleq \frac{\alpha_\sigma p^n-\sigma-\Phi_r}{p^n-1}\,. \tag{31}$$

Under this additional condition, Eq. (30) gives the state of the cell located at $(0, m)$ as a function of states of cells which are all located to the left of this $(0, m)$-cell: the equations become strictly right-propagating recursion equations. With the following restricted subset of $\overline{\mathcal{M}}^{(\sigma)}_r$:

$$\mathcal{M}^{(\sigma)}_r \triangleq \{v | v\in\overline{\mathcal{M}}^{(\sigma)}_r \text{ and } v > \mu^{(\sigma)}_r\}\,, \tag{32}$$

we therefore define the

Standard (strictly) right-propagating recursion

$$\begin{aligned} &\forall m\in\mathcal{M}^{(\sigma)}_r : \\ &a(m) = c_r(0)a\left(\frac{m-\sigma-\Phi_r}{p^n}+\alpha_\sigma\right)+\sum_{i=1}^{i_{\max}-i_{\min}} c_r(i)a(m-i)\,. \end{aligned} \tag{33}$$

In contrast with Eqs. (33), Eqs. (30) will be called the *extended* standard right-propagating equations.

In a similar way, by isolating now the term with $i_{\max}$ in Eq. (26), and by using

$$\Phi_l \triangleq \eta_{\max} - i_{\max} \tag{34}$$

$$\begin{aligned} \overline{\mathcal{M}}^{(\sigma)}_l &\triangleq \{kp^n+\Phi_l+\sigma | k\in\mathbb{Z}\} \\ &= \{v | v\equiv(\Phi_l+\sigma) \bmod p^n\} \\ \mathcal{M}^{(\sigma)}_l &\triangleq \{v | v\in\overline{\mathcal{M}}^{(\sigma)}_l \text{ and } v < \mu^{(\sigma)}_l\} \text{ with} \\ \mu^{(\sigma)}_l &\triangleq \frac{\alpha_\sigma p^n-\sigma-\Phi_l}{p^n-1}\,, \end{aligned} \tag{35}$$

we obtain the

Standard (strictly) left-propagating recursion

$$\begin{aligned} &\forall m\in\mathcal{M}^{(\sigma)}_l : \\ &a(m) = c_l(0)a\left(\frac{m-\sigma-\Phi_l}{p^n}+\alpha_\sigma\right)+\sum_{i=1}^{i_{\max}-i_{\min}} c_l(i)a(m+i)\,. \end{aligned} \tag{36}$$

When extended to all $m\in\overline{\mathcal{M}}^{(\sigma)}_l$, these equations will be referred to as the *extended* standard left-propagating equations.

Remarks

- Observe from the previous developments, that $c_r(0) \neq 0$ and $c_l(0) \neq 0$, while some or all of the $c_r(i)$ and $c_l(i)$ for $i \neq 0$ may be zero.
- Observe that $c_r(i)$, $c_l(i)$ only depend on p^n, Ξ (i.e. β and Γ), W, R and *not* on σ, because they inherit this property from their predecessors, the $u(i)$ coefficients in Eq. (26). For the same reason, $i_{\min}$ and $i_{\max}$ do not depend on σ.

4.2.3. *Finding the solutions*

When the recurrence equations (33) and (36) are provided with the proper initial conditions on $a(j)$, they automatically generate a solution for the initial state sequence $\langle a(c)\rangle_{c\in\mathbb{Z}}$ that produces a coarse-graining invariant orbit pattern. So, we will now investigate how to obtain these initial conditions, by proving the existence of solutions in a constructive way.

We will find that there are an infinite number of solutions. However, when the equations are solved simultaneously for *all* possible shifts $\sigma \in \{0, 1, \ldots p^n - 1\}$, the number of solutions becomes finite. An illustration of the solution procedure for this so-called *complete CGI-problem* will be given in Examples 4.1 and 4.2.

Definition 4.1.

- The *right index range* $IR_r^{(\sigma)}(m)$, $m \in \mathbb{Z}$ of Eq. (33) is the set of all j in the $a(j)$ that appear in the right-hand side of the right-propagating Eq. (33) and for which the corresponding coefficient differs from 0, i.e.

$\forall m \in \mathbb{Z}:$

$$IR_r^{(\sigma)}(m) \triangleq \left\{\frac{m-\Phi_r-\sigma}{p^n} + \alpha_\sigma\right\} \cup \{m-i | i \in \mathcal{I}_r\}, \tag{37}$$

where $\mathcal{I}_r \triangleq \{i | 1 \leq i \leq i_{\max} - i_{\min}, c_r(i) \neq 0\}$.
- Similarly, we consider the *left index range* $IR_l^{(\sigma)}(m)$ of Eq. (36)

$\forall m \in \mathbb{Z}:$

$$IR_l^{(\sigma)}(m) = \left\{\frac{m-\Phi_l-\sigma}{p^n} + \alpha_\sigma\right\} \cup \{m+i | i \in \mathcal{I}_l\}, \tag{38}$$

where $\mathcal{I}_l \triangleq \{i | 1 \leq i \leq i_{\max} - i_{\min}, c_l(i) \neq 0\}$.

- Let $a, b \in \mathbb{Z}$ and $a \leq b$, then $I[a, b]$ denotes the integer interval $\{a, a+1, \ldots b-1, b\}$.

Lemma 4.1.

(A) $\forall m \in \mathbb{Z}:$ $\min IR_r^{(\sigma)}(m+1) > \min IR_r^{(\sigma)}(m)$ (39)

$$\max IR_l^{(\sigma)}(m-1) < \max IR_l^{(\sigma)}(m). \tag{40}$$

(B) *Let* $m \in \mathbb{Z}:$

— *when* $m > \mu_r^{(\sigma)} \triangleq \dfrac{-\Phi_r - \sigma + \alpha_\sigma p^n}{p^n - 1}$,

then $\max IR_r^{(\sigma)}(m) < m$ (41)

— *when* $m < \mu_l^{(\sigma)} \triangleq \dfrac{-\Phi_l - \sigma + \alpha_\sigma p^n}{p^n - 1}$,

then $\min IR_l^{(\sigma)}(m) > m$. (42)

Proof

(A) *Proof of Eqs. (39)-(40).*
Candidates for the minimal elements in $IR_r^{(\sigma)}(m)$ are $g_1(m) = \frac{m-\Phi_r-\sigma}{p^n} + \alpha_\sigma$ and $g_2(m) = m - \max \mathcal{I}_r$. There are two possibilities:
- First possibility: $g_1(m) \leq g_2(m)$. Then $\min IR_r^{(\sigma)}(m) = g_1(m) < g_1(m+1) < g_2(m+1)$. The very last inequality shows that $g_1(m+1) = \min IR_r^{(\sigma)}(m+1)$, and so Eq. (39) is valid.
- Second possibility: $g_2(m) < g_1(m)$. Then either
  1. $\min IR_r^{(\sigma)}(m) = g_2(m) < g_2(m+1) < g_1(m+1)$, meaning that $\min IR_r^{(\sigma)}(m+1) = g_2(m+1)$, and Eq. (39) is satisfied. Or,
  2. $g_2(m+1) > g_1(m+1)$, meaning that $\min IR_r^{(\sigma)}(m+1) = g_1(m+1) > g_1(m) > g_2(m) = \min IR_r^{(\sigma)}(m)$, which also satisfies Eq. (39).

Equation (40) is proven along similar lines, while using the $IR_l^{(\sigma)}(m)$-expressions.

(B) *Proof of Eqs. (41)-(42).*
Candidates for $\max IR_r^{(\sigma)}(m)$ are $g_1(m)$ (see above), and $g_3(m) = m - \min \mathcal{I}_r$. If $\max IR_r^{(\sigma)}(m) = g_3(m)$, then Eq. (41) is automatically satisfied as all elements of $\mathcal{I}_r$ are nonzero

positive. If $\max IR_r^{(\sigma)}(m) = g_1(m)$, then the first inequality in Eq. (41) is necessary for the second inequality to hold. Both possibilities together imply Eq. (41).

Equation (42) is proven along similar lines using the $IR_l^{(\sigma)}(m)$-expressions. ■

Lemma 4.2.

(A) *There exist finite integers* κ *and* λ *such that*

$$IR_r^{(\sigma)}(\lambda) \subset I[\kappa+1,\, \lambda-1] \quad \text{(a)}$$
$$\text{and} \quad IR_l^{(\sigma)}(\kappa) \subset I[\kappa+1,\, \lambda-1] \quad \text{(b)} \qquad (43)$$

(B) *If Eq. (43) holds for* $\kappa = \kappa_0$, $\lambda = \lambda_0$, *then it holds for all* $\kappa = \kappa_0 - s (s \in \mathbb{N})$ *and all* $\lambda = \lambda_0 + t$ $(t \in \mathbb{N})$.

Proof. Equation (43) requires that

$$\begin{aligned} &\text{(a)} \quad \max IR_r^{(\sigma)}(\lambda) < \lambda \\ &\text{(b)} \quad \min IR_r^{(\sigma)}(\lambda) > \kappa \\ &\text{(c)} \quad \min IR_l^{(\sigma)}(\kappa) > \kappa \\ &\text{(d)} \quad \max IR_l^{(\sigma)}(\kappa) < \lambda\,. \end{aligned} \qquad (44)$$

We show that all these conditions can be met simultaneously as a direct consequence of Lemma 4.1. The inequalities (a) and (c) can be satisfied by taking λ sufficiently large and κ sufficiently small, as indicated by Eqs. (41) and (42). Let κ' and λ' be integers for which (a) and (c) are satisfied. If (b) is not satisfied, i.e. if $\min IR_r^{(\sigma)}(\lambda') < \kappa'$, then take a new $\lambda = \lambda' + s$, and by letting s increase, a λ-value will be reached for which $\min IR_r^{(\sigma)}(\lambda) > \kappa'$ by virtue of Eq. (39). The new $\lambda > \lambda'$ keeps satisfying (a). If (d) might still not be satisfied, take $\kappa = \kappa' - s$, and by letting s increase, a κ-value will be obtained for which $\max IR_l^{(\sigma)}(\kappa) > \lambda$.

A further increase of λ and a further decrease of κ will only strengthen the conditions of Eq. (44), and this proves part B. ■

Core interval, seed, seedcode, seed-internal equations, freecells, depcells

Let $\kappa^{(\sigma)} \in \mathcal{M}_l^{(\sigma)}$ and $\lambda^{(\sigma)} \in \mathcal{M}_r^{(\sigma)}$ be such that the interval $I[\kappa^{(\sigma)}+1,\, \lambda^{(\sigma)}-1]$ satisfies Eqs. (43) and has *minimal length*, i.e. the number of elements $(\lambda^{(\sigma)} - \kappa^{(\sigma)} - 1)$ is minimal. Then such an interval will be called a *core interval* (see Fig. 7). The associated array of orbit-lattice cells with top-row addresses $(0, j)$, $j \in I[\kappa^{(\sigma)}+1,\, \lambda^{(\sigma)}-1]$ will be called the *seed*. Any particular configuration of the associated cell-states, i.e. any $\mathcal{S}^{(\sigma)} \triangleq \langle a(j)\rangle_{j \in I[\kappa^{(\sigma)}+1,\, \lambda^{(\sigma)}-1]}$ will be called a *seedcode*. As the seed has $(\lambda^{(\sigma)} - \kappa^{(\sigma)} - 1)$ cells, there are $p^{(\lambda^{(\sigma)} - \kappa^{(\sigma)} - 1)}$ *possible* seedcodes. As the examples will show, the core interval and the associated seed are not necessarily unique.

Lemma 4.2 has an important consequence: it shows the existence of a core interval and associated seed, such that $a(\kappa^{(\sigma)})$ and $a(\lambda^{(\sigma)})$ can be expressed in terms of the cell-states in the seed, through use of the standard left- and right-propagating recursions Eq. (33) and Eq. (36) for $m = \kappa^{(\sigma)}$ and $m = \lambda^{(\sigma)}$, respectively. Further application of the right-propagating equation gives the $a(\lambda^{(\sigma)} + sp^n)$-states $(s \in \mathbb{N})$ in their dependence on $a(j)$, $j \in IR_r^{(\sigma)}(\lambda^{(\sigma)} + sp^n)$, whereby $\lambda^{(\sigma)} + sp^n - 1 \overset{(41)}{\geq} \max IR_r^{(\sigma)}(\lambda^{(\sigma)} + sp^n) \geq \min IR_r^{(\sigma)}(\lambda^{(\sigma)} + sp^n) \overset{(39)}{>} \min IR_r^{(\sigma)}(\lambda^{(\sigma)}) \overset{(44.b)}{\geq} \kappa^{(\sigma)} + 1$. This means that $a(\lambda^{(\sigma)} + sp^n)$ can be written as a linear combination of the states of cells to its left, but which are nevertheless always to the right of the leftmost cell of the seed. It follows that all $a(\lambda^{(\sigma)} + sp^n)$, $s \in \mathbb{N}$ can be generated from knowledge of the seedcode and from knowledge of the cell states $a(\lambda^{(\sigma)} + sp^n - j)$, $s \in \mathbb{N}$, $j \in \{1, 2, \ldots p^n - 1\}$ (as the left- and right-propagation equations only define the $a(\lambda^{(\sigma)} + sp^n)$ states).

In a similar way, it can be shown that all $a(\kappa^{(\sigma)} - sp^n)$, $s \in \mathbb{N}$ can be generated from knowledge of the seedcode and from knowledge of the cell states $a(\kappa^{(\sigma)} - sp^n + j)$, $s \in \mathbb{N}$, $j \in \{1, 2, \ldots p^n - 1\}$, by using the left-propagating recursion.

In conclusion, what we need for generating the complete solution of the standard recursion Eqs. (33) and (36), is a specification of the seedcode and of all $a(z)$, $z \notin \mathcal{M}_r^{(\sigma)} \cup \mathcal{M}_l^{(\sigma)} \cup I[\kappa^{(\sigma)}+1,\, \lambda^{(\sigma)}-1]$. It is clear that these last elements can be assigned an arbitrary value (in $\mathbb{Z}_p$).

The seedcode itself can be considered as an initial condition allowing the recursions to be started properly. Can all seed-cells be given an arbitrary state value (in $\mathbb{Z}_p$)? The answer depends on whether there are equations of the type of Eq. (26) for which *all* $a(j)$ that appear in it are part of the seedcode.

Such an equation will be called *seed-internal* and introduces a dependency among the seedcode elements.

If there are *seed-internal* equations, we should solve the complete set of seed-internal equations. As this set of equations is homogeneous, it always has a solution. In general, it leads to a number of $a(j) \in \mathcal{S}^{(\sigma)}$ that can be chosen freely: the associated cells will be called the (seed)-internal *freecells*. There may be some seedcells which *depend* on the freecell-states: the corresponding cells are called (seed)-internal *depcells*. Any seedcode that satisfies the seed-internal set of equations will be called a *good seedcode*, otherwise it is a *bad seedcode*. Only good seedcodes can be used as a starting point to generate the complete solution of the $[\mathcal{T}^{(\sigma)}_{p^n,\Xi}, W, \alpha_\sigma, R]$-coarse-graining invariant problem. The free cells and dependent cells outside the seeds will be called the (seed)-*external* freecells and (seed)-*external* depcells. If there are no seed-internal equations, all seed-cells are freecells.

The general structure of a solution for the initial CA-state S_0 that generates a $[\mathcal{T}^{(\sigma)}_{p^n,\Xi}, W, \alpha_\sigma]$-coarse-graining invariant orbit $O_R(S_0)$ is given in Fig. 7. With N_f denoting the number of internal freecells, the number of possible solutions N_{sol} is given by

$$N_{\text{sol}} = p^{N_f + \infty\cdot(p^n-1)}. \tag{45}$$

[$\infty\cdot(p^n-1)$ is a symbolic representation of the fact that we have an infinite number of (p^n-1) external freecells, see Fig. 7.]

The solutions to this problem and the resulting structure of the orbital pattern will very much depend on how the freecell-states are assigned. Moreover, the number of degrees of freedom and the related number of solutions are too overwhelming to be very interesting. We will now show the way of how to decrease the number of solutions until it becomes eventually finite.

4.3. *Invariance under* $[\mathcal{T}^{(\sigma_1,\sigma_2,\ldots\sigma_f)}_{p^n,\Xi}, W]$ *coarse-graining (for CA-rules with* $d_l = 0$*)*

In the previous section, we have discussed the solution related to *one* particular σ-shifted tiling $\mathcal{T}^{(\sigma)}_{p^n,\Xi}$ $(0 \le \sigma \le p^n - 1)$. What happens if we select several different shifts of the same basic tiling, e.g. $\mathcal{T}^{(\sigma_1)}_{p^n,\Xi}, \mathcal{T}^{(\sigma_2)}_{p^n,\Xi}, \ldots, \mathcal{T}^{(\sigma_f)}_{p^n,\Xi}$ $(0 \le \sigma_u \le p^n - 1)$, and ask for an orbit $O_R(S_0)$ which is coarse-graining invariant under *all* these tilings (with the same weight matrix W)? That is we require that

$$[\mathcal{T}^{(\sigma_u)}_{p^n,\Xi}, W, \alpha_{\sigma_u}]O_R(S_0) = {}^{\alpha_{\sigma_u}}O_R(S_0) \text{ for } u = 1, 2, \ldots, f. \tag{46}$$

This will be indicated as the $[\mathcal{T}^{(\sigma_1,\sigma_2,\ldots,\sigma_f)}_{p^n,\Xi}, W, (\alpha_{\sigma_1}, \ldots, \alpha_{\sigma_f}), R]$-coarse-graining invariance problem.

The solution to this problem is given by solving the left- and right propagation Eqs. (33) and (36), but now for all $\sigma \in \Omega \triangleq \{\sigma_1, \sigma_2, \ldots, \sigma_f\}$. It means that the $a(j)$ have to satisfy the standard right-propagation equations Eq. (33) for all $m \in \cup_{\sigma\in\Omega}\mathcal{M}^{(\sigma)}_r$. Hereby it is essential to observe that $\mathcal{M}^{(\sigma_i)}_r \cap \mathcal{M}^{(\sigma_j)}_r = \phi$ when $i \neq j$ [cf. Eqs. (29)–(32)], implying that for each additional σ_i, a new set of equations has to be satisfied in which the $a(m)$, $m \in \mathcal{M}^{(\sigma_i)}_r$ appear as dependent variables. Also, the $a(j)$

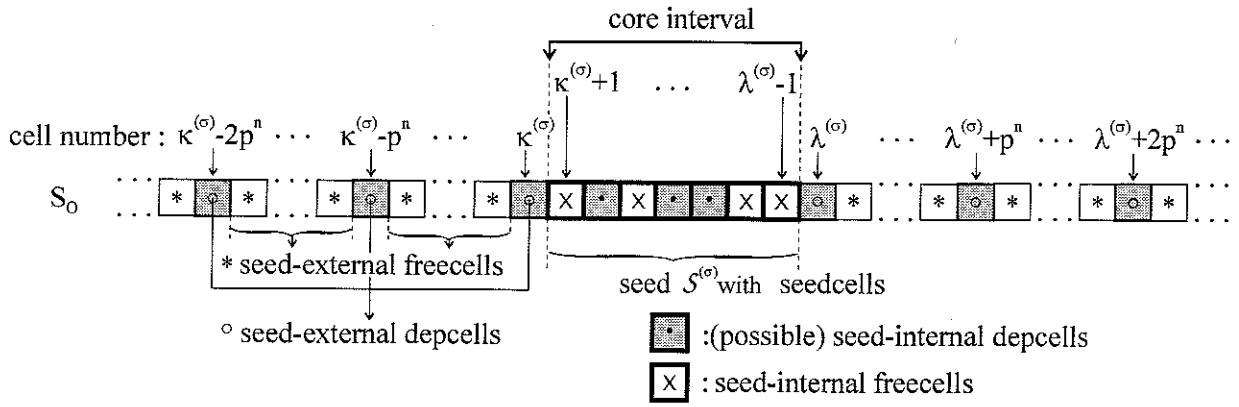

Fig. 7. The generic structure of the initial-state solution of a $[\mathcal{T}^{(\sigma)}_{p^n,\Xi}, W, \alpha_\sigma, R]$-coarse graining problem.

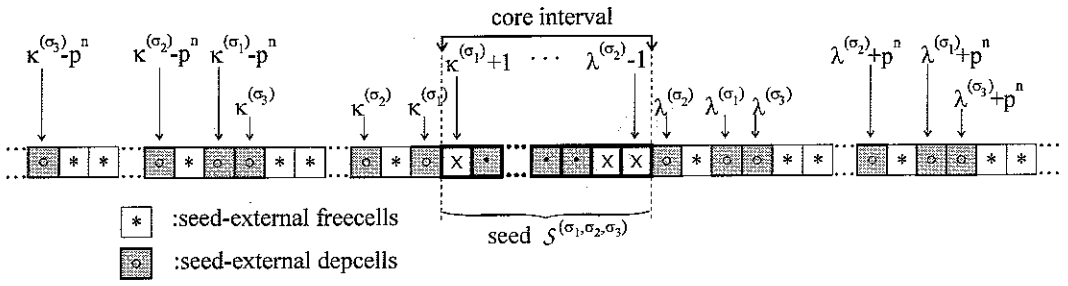

(a)

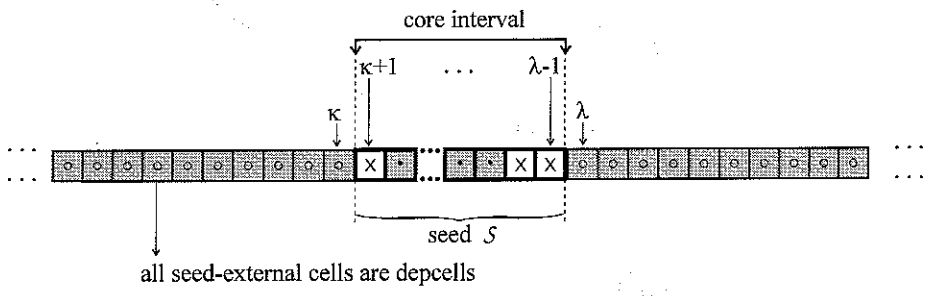

(b)

Fig. 8. (a) Structure of the coarse-graining invariant initial state solution for $\Omega = \{\sigma_1, \sigma_2, \sigma_3\}$, $(3 < p^n - 1)$. (b) Structure of the coarse-graining invariant initial state solution for the *complete* CGI-problem ($\Omega = \{0, 1, \ldots, p^n - 1\}$).

have to satisfy the standard left-propagating equations [Eq. (36)] for all $m \in \cup_{\sigma\in\Omega}\mathcal{M}_l^{(\sigma)}$.

Just as in the case of a single σ, the solutions can be obtained from these left- and right propagating equations by starting them with a proper seed and seedcode. These can be obtained through the construction of a core interval, by just extending the procedure for the single-σ case. We summarize the steps:

Step 1. Define

$$IR_r^{(\Omega)}(m) \triangleq \cup_{\sigma\in\Omega} IR_r^{(\sigma)}(m) \quad \text{(a)}$$

$$IR_l^{(\Omega)}(m) \triangleq \cup_{\sigma\in\Omega} IR_l^{(\sigma)}(m)\,. \quad \text{(b)}$$

Step 2. Find a *minimal length* interval $I[\kappa + 1, \lambda - 1]$ such that it simultaneously satisfies:

$$\begin{aligned} &\text{(a)}\ \max IR_r^{(\Omega)}(\lambda) < \lambda \\ &\text{(b)}\ \min IR_r^{(\Omega)}(\lambda) > \kappa \\ &\text{(c)}\ \min IR_l^{(\Omega)}(\kappa) > \kappa \\ &\text{(d)}\ \max IR_l^{(\Omega)}(\kappa) < \lambda\,. \end{aligned} \tag{47}$$

This is possible because the equations in Lemmas 4.1 and 4.2 can be extended to the situation where σ is replaced by Ω.

Step 3. Find a core interval $I[\kappa^{(\Omega)} + 1, \lambda^{(\Omega)} - 1]$ with $\kappa^{(\Omega)} \in \mathcal{M}_l^{(\Omega)} \triangleq \cup_{\sigma\in\Omega}\mathcal{M}_l^{(\sigma)}$, $\lambda^{(\Omega)} \in \mathcal{M}_r^{(\Omega)} \triangleq \cup_{\sigma\in\Omega}\mathcal{M}_r^{(\sigma)}$, and of *minimal length* $(\lambda^{(\Omega)} - \kappa^{(\Omega)} - 1)$ (this can be done by possibly enlarging the minimal length interval found in Step 2). The seed is defined as the string of cells confined in this core interval, i.e. the cells located at $(0, j)$, $j \in I[\kappa^{(\Omega)} + 1, \lambda^{(\Omega)} - 1]$.

Step 4. Determine the set of seed-internal equations of the type of Eq. (26), and solve it in order to determine the freecells and the depcells of the seed and to find good seedcodes.

The solution for the initial state sequence now has a structure as illustrated in Fig. 8(a) With N_f being again the number of seed-internal freecells, the number of solutions is now $p^{N_f + \infty\cdot(p^n - \text{card}\,\Omega)}$.

As long as the orbit pattern $O_R(S_0)$ is *not* subjected to coarse-graining invariance for *all possible*

tiling-shifts σ, i.e. as long as $\Omega \neq \{0, 1, \ldots, p^n - 1\}$, we find an infinite number of solutions because card $\Omega \neq p^n$. However, the most interesting situation occurs when $[\mathcal{T}^{(\sigma)}_{p^n,\Xi}, W, \alpha_\sigma]$-coarse-graining invariance is required for *all possible* tiling-shifts (i.e. $\Omega = \{0, 1, \ldots p^n - 1\}$), because then card $\Omega = p^n$, whereby the number of solutions becomes finite ($= p^{N_f}$). In this *complete* CGI-case, the core interval coincides with a minimal length interval as found in Step 2 in the procedure above, and all cells outside the seed are now depcells [see Fig. 9(b)].

This complete CGI-case is also the most interesting one from a "physical" point of view, as it places all shifted tilings on the same level without any preference: they all induce a coarse-graining for which invariance is requested. A particular complete CGI-problem will be denoted by $[\mathcal{T}_{p^n,\Xi}, W, \alpha, R]$-CGI-problem, whereby $\alpha \triangleq (\alpha_0, \alpha_1, \ldots \alpha_{p^n-1})$ is the *pattern-shift vector*. α is a fixed parameter for a given problem, together with the tile size $p^n(\times p^n)$, the global tile-configuration matrix Ξ with elements $\xi_{i,j} = \beta_i + \gamma_{i,j}$, the $p^n \times p^n$ weight matrix W and the automaton rule R. Possible solutions depend on all these control parameters, which form an unexhaustible source of diverse coarse-graining invariant orbit patterns. In the sections to come, we will analyze some properties of the solutions of the complete CGI-problem. Before giving an illustrative example of the solution procedure that we have been discussing, we display, by way of summary and for further reference, the

Complete CGI-equations

— First version: initial-state-reduced equations

$\forall k \in \mathbb{Z}$ & $\forall \sigma \in \mathcal{Z}_{p^n}$:[2]

$$\sum_{i=i_{\min}}^{i_{\max}} u(i)a(kp^n + \eta_{\max} + \sigma - i) = a(k + \alpha_\sigma)\,. \tag{48}$$

This set splits in p^n disjoint subsets, each subset being associated with the particular tiling shift σ.

— Second version: the extended standard right-propagating equations

$\forall m \in \mathbb{Z}$:

$$a(m) = c_r(0)a\left(\left\lfloor \frac{m - \Phi_r}{p^n} \right\rfloor + \alpha_{(m-\Phi_r) \bmod p^n}\right) + \sum_{i=1}^{\Delta} c_r(i)a(m - i)\,, \tag{49}$$

$$\text{with } \Delta \triangleq i_{\max} - i_{\min}\,. \tag{50}$$

Again, this set of equations partitions in p^n subsets for the different $\sigma \in \mathcal{Z}_{p^n}$. A given m belongs to the σ-subset $\overline{\mathcal{M}}^{(\sigma)}_r$ [Eq. (30)], with

$$\sigma = (m - \Phi_r) \bmod p^n\,, \tag{51}$$

where Φ_r is given by Eq. (28).
In fact, Eq. (51) was used in deriving Eq. (49) from Eq. (30); it guarantees that $\frac{m-\sigma-\Phi_r}{p^n}$ which appears in Eq. (30) is an integer for all m.

— Third version: the extended standard left-propagating equations

$\forall m \in \mathbb{Z}$:

$$a(m) = c_l(0)a\left(\left\lfloor \frac{m - \Phi_l}{p^n} \right\rfloor + \alpha_{(m-\Phi_l) \bmod p^n}\right) + \sum_{i=1}^{\Delta} c_l(i)a(m + i) \tag{52}$$

A given m belongs to the σ-subset $\overline{\mathcal{M}}^{(\sigma)}_l$ [Eq. (35)], with

$$\sigma = (m - \Phi_l) \bmod p^n\,, \tag{53}$$

where Φ_l is given by Eq. (34).

Example 4.1. This is an example featuring a unique core-interval, and seed-internal equations. Consider a binary automaton with rule $R(x) = 1 + x^2$ in $\mathbb{Z}_2[x]$. So all equations have to be taken modulo 2. We will find all possible solutions for a particular complete $[\mathcal{T}_{p^n,\beta}, W, \alpha, R]$-CGI problem.

(A) General expressions for the coarse-graining invariance equations with

$p^n = 2^2, \beta = (0, \beta_1, \beta_2, \beta_3), \Gamma = [0], \alpha = (\alpha_1, \alpha_2, \alpha_3, \alpha_4)$

and $W = \begin{bmatrix} 1 & 1 & 1 & 1 \\ 1 & 1 & 1 & 1 \\ 1 & 1 & 1 & 1 \\ 1 & 1 & 1 & 1 \end{bmatrix}$ (i.e. the coarse-graining makes the sum modulo 2 of all cell-states in the tiles).

[2] $\mathcal{Z}_l \triangleq \{0, 1, \ldots l - 1\}$. We usually use $\mathbb{Z}_l$ instead of $\mathcal{Z}_l$ when we want to indicate implicitly that these elements can be subjected to addition and multiplication modulo l.

For convenience, the cell-states of the top row in the orbit pattern (i.e. the initial cell-states) will be denoted by a_k (instead of the $a(k)$ used in the general analysis). In the same way, b_k, c_k, d_k will denote the kth-cell state on rows 1, 2, 3 respectively.

An orbit pattern $O_R(S_0)$ is $[T_{2^2,\beta}, W \equiv 1, \alpha, R]$-coarse-graining invariant when Eq. (24) is satisfied for all $\sigma \in \mathcal{Z}_4 = \{0, 1, 2, 3\}$. This requirement produces the following set of equations:

$$\forall k \in \mathbb{Z} \;\&\; \forall \sigma \in \mathcal{Z}_4 : \begin{array}{l} a_{4k+\sigma} + a_{4k+1+\sigma} + a_{4k+2+\sigma} + a_{4k+3+\sigma} \\ + b_{4k+\beta_1+\sigma} + b_{4k+1+\beta_1+\sigma} + b_{4k+2+\beta_1+\sigma} + b_{4k+3+\beta_1+\sigma} \\ + c_{4k+\beta_2+\sigma} + c_{4k+1+\beta_2+\sigma} + c_{4k+2+\beta_2+\sigma} + c_{4k+3+\beta_2+\sigma} \\ + d_{4k+\beta_3+\sigma} + d_{4k+1+\beta_3+\sigma} + d_{4k+2+\beta_3+\sigma} + d_{4k+3+\beta_3+\sigma} = a_{k+\alpha_\sigma} . \end{array} \tag{54}$$

Recall that the left-hand side represents the sum of all cell-states covered by the tile $T^{(\sigma)}_{2^2,\beta}(0,k)$. Now use the CA's local rule:

$$\begin{aligned} b_k &= a_k + a_{k-2} \\ c_k &= b_k + b_{k-2} \\ d_k &= c_k + c_{k-2} \end{aligned}$$

to express all terms in Eq. (54) as a function of the a_k. This ultimately produces the set of initial-state reduced coarse-graining invariant equations [cf. Eq. (26)]:

$$\forall k \in \mathbb{Z} \;\&\; \forall \sigma \in \mathcal{Z}_4 : \begin{array}{l} a_{4k+\sigma} + a_{4k+1+\sigma} + a_{4k+2+\sigma} + a_{4k+3+\sigma} \\ + a_{4k+\beta_1-2+\sigma} + a_{4k+\beta_1-1+\sigma} + a_{4k+\beta_1+2+\sigma} + a_{4k+\beta_1+3+\sigma} \\ + a_{4k+\beta_2-4+\sigma} + a_{4k+\beta_2-3+\sigma} + a_{4k+\beta_2-2+\sigma} + a_{4k+\beta_2-1+\sigma} \\ + a_{4k+\beta_2+\sigma} + a_{4k+\beta_2+1+\sigma} + a_{4k+\beta_2+2+\sigma} + a_{4k+\beta_2+3+\sigma} \\ + a_{4k+\beta_3-6+\sigma} + a_{4k+\beta_3-5+\sigma} + a_{4k+\beta_3+2+\sigma} + a_{4k+\beta_3+3+\sigma} = a_{k+\alpha_\sigma} . \end{array} \tag{55}$$

(B) We will now apply this to the specific case with $\alpha = (-6, -2, 2, 6)$ and $\beta = (0, 1, 2, 3)$ [which corresponds to the tile configuration of Fig. 4(c)]. This transforms Eq. (55) into the following specific set of initial-state-reduced CGI-equations.

$$\forall k \in \mathbb{Z} : \begin{cases} a_{4k+6} + a_{4k+3} + a_{4k} + a_{4k-3} = a_{k-6} & (\sigma = 0) \\ a_{4k+7} + a_{4k+4} + a_{4k+1} + a_{4k-2} = a_{k-2} & (\sigma = 1) \\ a_{4k+8} + a_{4k+5} + a_{4k+2} + a_{4k-1} = a_{k+2} & (\sigma = 2) \\ a_{4k+9} + a_{4k+6} + a_{4k+3} + a_{4k} = a_{k+6} & (\sigma = 3) \end{cases} \tag{56}$$

Rearranging the terms in these equations gives the (nonstandard extended) *right-propagating equations* [cf. Eq. (27)].

$$\forall k \in \mathbb{Z} : \begin{cases} a_{4k+6} = a_{k-6} + a_{4k+3} + a_{4k} + a_{4k-3} & (\sigma = 0) \\ a_{4k+7} = a_{k-2} + a_{4k+4} + a_{4k+1} + a_{4k-2} & (\sigma = 1) \\ a_{4k+8} = a_{k+2} + a_{4k+5} + a_{4k+2} + a_{4k-1} & (\sigma = 2) \\ a_{4k+9} = a_{k+6} + a_{4k+6} + a_{4k+3} + a_{4k} & (\sigma = 3) \end{cases}$$

The *standard form* of these equations [corresponding to Eq. (30) and Eq. (49)] is given by replacing the indices in the left side term by m, producing respectively (with an additional rearrangement of the equations):

$$\begin{cases} \text{for } m \bmod 4 = 0 : a_m = a_{\frac{m}{4}} + a_{m-3} + a_{m-6} + a_{m-9} & (\sigma = 2) \\ \text{for } m \bmod 4 = 1 : a_m = a_{\frac{m+15}{4}} + a_{m-3} + a_{m-6} + a_{m-9} & (\sigma = 3) \\ \text{for } m \bmod 4 = 2 : a_m = a_{\frac{m-30}{4}} + a_{m-3} + a_{m-6} + a_{m-9} & (\sigma = 0) \\ \text{for } m \bmod 4 = 3 : a_m = a_{\frac{m-15}{4}} + a_{m-3} + a_{m-6} + a_{m-9} & (\sigma = 1) \end{cases} \tag{57}$$

In a similar way, Eqs. (56) can be written in extended *left-propagating form* [corresponding to Eq. (30)]:

$$\begin{cases} a_{4k-3} = a_{k-6} + a_{4k} \quad + a_{4k+3} + a_{4k+6} & (\sigma = 0) \\ a_{4k-2} = a_{k-2} + a_{4k+1} + a_{4k+4} + a_{4k+7} & (\sigma = 1) \\ a_{4k-1} = a_{k+2} + a_{4k+2} + a_{4k+5} + a_{4k+8} & (\sigma = 2) \\ a_{4k} \quad = a_{k+6} + a_{4k+3} + a_{4k+6} + a_{4k+9} & (\sigma = 3) \end{cases}$$

or, in the standard form [corresponding to Eq. (36) and Eq. (52)]:

$$\begin{cases} \text{for } m \bmod 4 = 0 : a_m = a_{\frac{m+24}{4}} + a_{m+3} + a_{m+6} + a_{m+9} & (\sigma = 3) \\ \text{for } m \bmod 4 = 1 : a_m = a_{\frac{m-21}{4}} + a_{m+3} + a_{m+6} + a_{m+9} & (\sigma = 0) \\ \text{for } m \bmod 4 = 2 : a_m = a_{\frac{m-6}{4}} + a_{m+3} + a_{m+6} + a_{m+9} & (\sigma = 1) \\ \text{for } m \bmod 4 = 3 : a_m = a_{\frac{m+9}{4}} + a_{m+3} + a_{m+6} + a_{m+9} & (\sigma = 2) \end{cases} \tag{58}$$

(C) The core interval $I[\kappa + 1, \lambda - 1]$ must satisfy Eqs. (47), which become here

$$\text{(a)} \quad \max\left\{\frac{\lambda}{4}, \frac{\lambda+15}{4}, \frac{\lambda-30}{4}, \frac{\lambda-15}{4}, \lambda-3, \lambda-6, \lambda-9\right\} < \lambda$$

$$\text{(b)} \quad \min\left\{\frac{\lambda}{4}, \frac{\lambda+15}{4}, \frac{\lambda-30}{4}, \frac{\lambda-15}{4}, \lambda-3, \lambda-6, \lambda-9\right\} > \kappa$$

$$\text{(c)} \quad \min\left\{\frac{\kappa+24}{4}, \frac{\kappa-21}{4}, \frac{\kappa-6}{4}, \frac{\kappa+9}{4}, \kappa+3, \kappa+6, \kappa+9\right\} > \kappa$$

$$\text{(d)} \quad \max\left\{\frac{\kappa+24}{4}, \frac{\kappa-21}{4}, \frac{\kappa-6}{4}, \frac{\kappa+9}{4}, \kappa+3, \kappa+6, \kappa+9\right\} < \lambda$$

Working things out, we obtain the equivalent conditions

(a) $\lambda \geq 6$

(b) if $\lambda \leq 2$ then $\lambda - 9 > \kappa$
if $\lambda \geq 2$ then $\lambda > 4\kappa + 30$

(c) $\kappa \leq -8$

(d) if $\kappa \geq -4$ then $\kappa + 9 < \lambda$
if $\kappa \leq -4$ then $\kappa < 4\lambda - 24$

Inspection shows that $\kappa = -8$ and $\lambda = 6$ is the solution that satisfies all conditions, and so $\langle a_k \rangle_{k \in I[-7,5]}$ forms a seedcode. Observe that in this example, the core interval and the corresponding seed are unique. The seed contains 13 cells.

(D) Inspection shows that there are four seed-internal equations, i.e. equations for which the variables all refer to seedcells:

$$\begin{aligned} a_5 + a_2 + a_{-1} + a_{-4} &= a_5 \quad [\text{Eq. (56) case } \sigma = 3,\ k = -1] \\ a_1 + a_1 + a_{-2} + a_{-5} &= a_4 \quad [\text{Eq. (56) case } \sigma = 2,\ k = -1] \\ a_{-3} + a_0 + a_{-3} + a_{-6} &= a_3 \quad [\text{Eq. (56) case } \sigma = 1,\ k = -1] \\ a_{-7} + a_{-1} + a_{-4} + a_{-7} &= a_2 \quad [\text{Eq. (56) case } \sigma = 0,\ k = -1]\,. \end{aligned}$$

Simplified (recall that all equations are in $\mathbb{Z}_2$), we obtain the following set of three homogeneous equations (the first and fourth equations above are identical):

$$\begin{aligned} a_2 + a_{-1} + a_{-4} &= 0 \\ a_4 + a_{-2} + a_{-5} &= 0 \\ a_3 + a_0 + a_{-6} &= 0\,. \end{aligned}$$

In these equations, a_{-1}, a_2, a_{-2}, a_4, a_0 and a_3 can be considered as free variables, while the dependent variables are a_{-6}, a_{-5} and a_{-4}, as given by

$$\begin{aligned} a_{-4} &= a_2 + a_{-1} \\ a_{-5} &= a_4 + a_{-2} \\ a_{-6} &= a_3 + a_0\,. \end{aligned}$$

All other variables in the seedcode are also free. We conclude: a good seedcode for the CGI-problem in this example, is given by

$$\langle a_{-7},\, a_3 + a_0,\, a_4 + a_{-2},\, a_2 + a_{-1},\, a_{-3},\, a_{-2},\, a_{-1},\, a_0,\, a_1,\, a_2,\, a_3,\, a_4,\, a_5 \rangle\,,$$

where all variables that appear in it can be chosen freely.

There are 10 degrees of freedom, and so $2^{10} = 1024$ different orbit patterns can be generated that are invariant under the given complete coarse-graining problem. The complete initial state for these orbit patterns is obtained by applying the right-propagating recursion Eq. (57) when $m \geq 6$, and the left-propagating recursion Eq. (58) when $m \leq -8$, hereby using a good seedcode as an initial condition. Two solution patterns for this specific problem are given in Figs. 9(a) and 9(b). Additional solutions are given in Figs. 12 and 17(a). A quick look at them already reveals the diversity of solutions.

Example 4.2. This is an example in which there are five possible core intervals and seeds, and for which all cells are freecells (i.e. there are no seed-internal equations). It concerns the CGI-problem with $p^n = 3^1$, $R(x) = 1 + 2x + x^2 \in \mathbb{Z}_3[x]$, $W = \begin{bmatrix} 0 & 0 & 1 \\ 0 & 2 & 0 \\ 1 & 0 & 0 \end{bmatrix}$, $\alpha = (2,\, 1,\, 0)$, $\Gamma = [0]$. It will be referred to again in Sec. 6.

The CGI-equations are:

$$\forall k \in \mathbb{Z} \text{ and } \sigma = 1,\, 2,\, 3 : a_{3k+\sigma+2} + 2b_{3k+\sigma+1} + c_{3k+\sigma} = a_k + \alpha_\sigma\,.$$

Application of the CA-rule gives (arithmetic modulo 3!):

$$\begin{aligned} 2b_{3k+\sigma+1} &= 2a_{3k+\sigma+1} + a_{3k+\sigma} + 2a_{3k+\sigma-1} \\ c_{3k+\sigma} &= b_{3k+\sigma} + 2b_{3k+\sigma-1} + b_{3k+\sigma-2} \\ &= a_{3k+\sigma} + a_{3k+\sigma-1} + a_{3k+\sigma-3} + a_{3k+\sigma-4}\,, \end{aligned}$$

and this leads to the initial-state-reduced CGI-equations:

$$\forall k \in \mathbb{Z} : \begin{cases} a_{3k-4} + a_{3k-3} + 2a_{3k} \quad + 2a_{3k+1} + a_{3k+2} = a_{k+2} & (\sigma = 0) \\ a_{3k-3} + a_{3k-2} + 2a_{3k+1} + 2a_{3k+2} + a_{3k+3} = a_{k+1} & (\sigma = 1) \\ a_{3k-2} + a_{3k-1} + 2a_{3k+2} + 2a_{3k+3} + a_{3k+4} = a_k & (\sigma = 2) \end{cases}$$

The corresponding standard left-propagating CGI-equations are

$$\begin{cases} \text{for } m \bmod 3 = 0 : a_m = a_{\frac{m+6}{3}} + 2a_{m+1} \quad + a_{m+4} + a_{m+5} + 2a_{m+6} & (\sigma = 1) \\ \text{for } m \bmod 3 = 1 : a_m = a_{\frac{m+2}{3}} + 2a_{m+1} \quad + a_{m+4} + a_{m+5} + 2a_{m+6} & (\sigma = 2) \\ \text{for } m \bmod 3 = 2 : a_m = a_{\frac{m+10}{3}} + 2a_{m+1}v + a_{m+4} + a_{m+5} + 2a_{m+6} & (\sigma = 0) \end{cases}$$

The standard right-propagating CGI-equations are

$$\begin{cases} \text{for } m \bmod 3 = 0 : a_m = a_{\frac{m}{3}} + a_{m-1} \quad + a_{m-2} + 2a_{m-5} + 2a_{m-6} & (\sigma = 1) \\ \text{for } m \bmod 3 = 1 : a_m = a_{\frac{m-4}{3}} + a_{m-1} + a_{m-2} + 2a_{m-5} + 2a_{m-6} & (\sigma = 2) \\ \text{for } m \bmod 3 = 2 : a_m = a_{\frac{m+4}{3}} + a_{m-1} + a_{m-2} + 2a_{m-5} + 2a_{m-6} & (\sigma = 0) \end{cases}$$

A core interval is a minimal length interval $I[\kappa + 1, \lambda - 1]$ such that

$$\text{(a)} \quad \max\left\{\frac{\lambda-4}{3}, \frac{\lambda}{3}, \frac{\lambda+4}{3}, \lambda-1, \lambda-2, \lambda-5, \lambda-6\right\} < \lambda$$

$$\text{(b)} \quad \min\left\{\frac{\lambda-4}{3}, \frac{\lambda}{3}, \frac{\lambda+4}{3}, \lambda-1, \lambda-2, \lambda-5, \lambda-6\right\} > \kappa$$

$$\text{(c)} \quad \min\left\{\frac{\kappa+2}{3}, \frac{\kappa+6}{3}, \frac{\kappa+10}{3}, \kappa+1, \kappa+4, \kappa+5, \kappa+6\right\} > \kappa$$

$$\text{(d)} \quad \max\left\{\frac{\kappa+2}{3}, \frac{\kappa+6}{3}, \frac{\kappa+10}{3}, \kappa+1, \kappa+4, \kappa+5, \kappa+6\right\} < \lambda .$$

Working things out and keeping in mind that $\kappa, \lambda \in \mathbb{Z}$ transforms these conditions into

$$\begin{aligned} &\text{(a)} \quad \lambda \geq 3 \\ &\text{(b)} \quad \text{if } \lambda \leq 7 \text{ then } \kappa < \lambda - 6 \\ &\qquad \text{if } \lambda \geq 7 \text{ then } \kappa < \frac{\lambda-4}{3} \\ &\text{(c)} \quad \kappa \leq 0 \\ &\text{(d)} \quad \text{if } \kappa \geq -4 \text{ then } \lambda < \kappa + 6 \\ &\qquad \text{if } \kappa \geq -4 \text{ then } \lambda < \frac{\kappa+10}{3} . \end{aligned}$$

There are *five* (κ, λ)-pairs for which $(\lambda - \kappa)$ is minimal and that satisfy the conditions above, namely $(\kappa, \lambda) = (0, 7), (-1, 6), (-2, 5), (-3, 4), (-4, 3)$. The corresponding core intervals are $I[1, 6]$, $I[0, 5]$, $I[-1, 4]$, $I[-2, 3], I[-3, 2]$. Any of these can be selected for specifying the seed, e.g. $I[-2, 3]$ gives the seed $\langle a_{-2}, a_{-1}, a_0, a_1, a_2, a_3\rangle$. Table 1 shows the left and right-propagating equations in the neighborhood of this seed. Inspection shows that there are *no* seed-internal equations, i.e. there are no equations whose variables uniquely refer to seed-internal cells (this is the case whatever core interval or seed is selected). So all seedcells are freecells. Their number is 6 and so there are $3^6 = 729$ solutions to this CGI-problem. The seedcode is a ternary number of 6 digits which correspond to the seedcell-states: $a_{-2}a_{-1}a_0a_1a_2a_3$. The complete CGI-initial-state sequence $\langle a_k\rangle_{k\in\mathbb{Z}}$ can be obtained from $\langle a_{-2}, a_{-1}, a_0, a_1, a_2, a_3\rangle$ by applying the standard right-propagating equations for $k \geq 4$ and the left-propagating equations for $k \leq -3$.

Remarks. All our observations corroborate the conjecture that the existence of seed-internal equations, and so of depcells, implies the existence of a unique core interval.

Table 1. The standard left- and right-propagating CGI-equations in the neighborhood of the selected seed $\langle a_{-2}, a_{-1}, a_0, a_1, a_2, a_3\rangle$ for the $[\mathcal{T}_{3^1,\Xi=[0]}, \alpha = (2, 1, 0), W = \begin{bmatrix} 0 & 0 & 1 \\ 0 & 2 & 0 \\ 1 & 0 & 0 \end{bmatrix}, R(x) = 1 + 2x + x^2 \in \mathbb{Z}_3[x]]$-CGI problem of Example 4.2. The *-sign indicates the *strictly* left-propagating and right-propagating equations respectively. Z_l, L_f, Z_r, M_f are relevant parameters for the periodicity problem (Sec. 6.2).

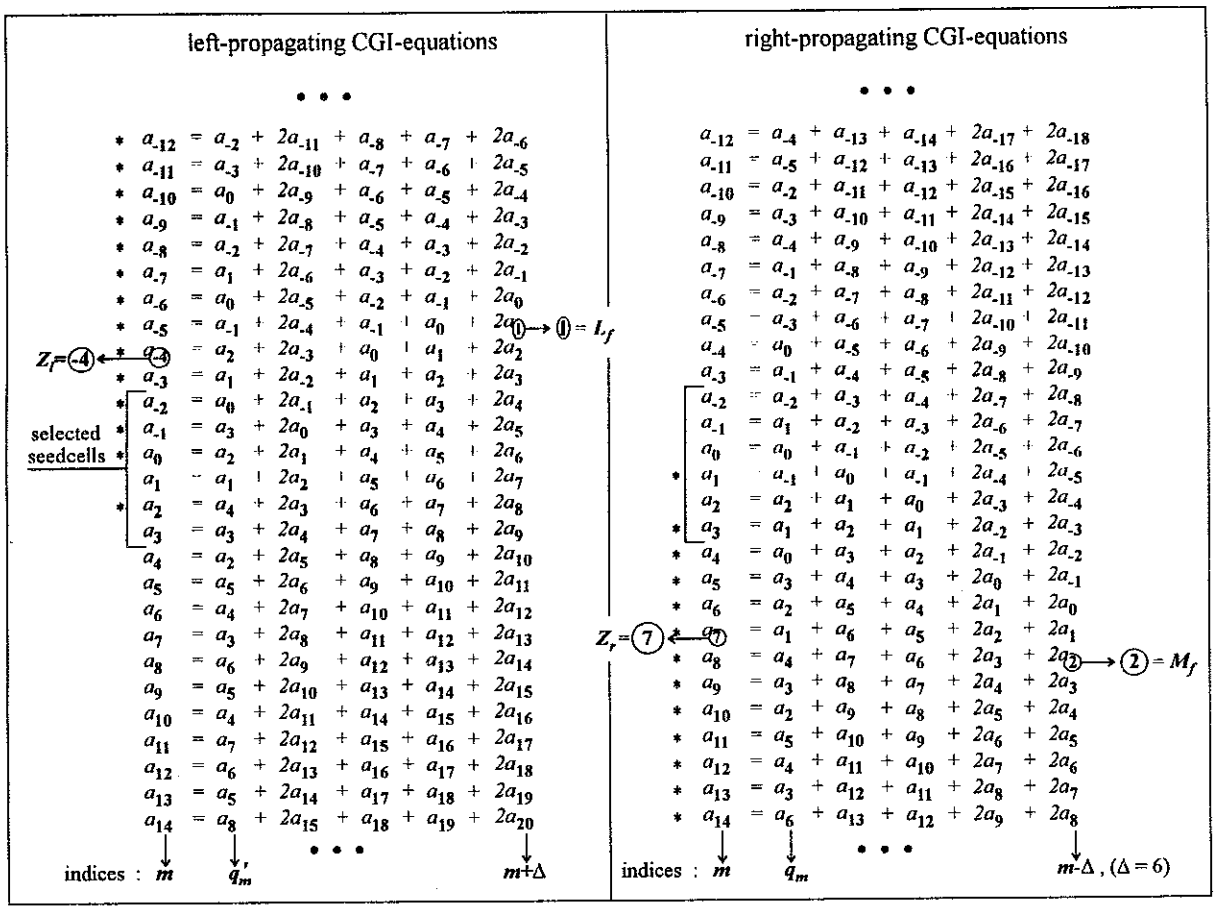

4.4. *Orbit representations in skew coordinates and solutions of the $[\mathcal{T}_{p^n,\Xi}, W, \alpha, R]$-CGI problem for CA-rules with $d_l \neq 0$*

Consider Figs. 9(a) and 9(c). They both represent the same CGI-orbit pattern for the rule $R(x) = 1 + x^2 \in \mathbb{Z}_2[x]$, but in different coordinate systems. Figure 9(a) uses the orthogonal coordinate system presented in Fig. 10(a), while Fig. 9(c) uses a skew coordinate system, where the cells belonging to a given column are placed along a skew line as shown in Fig. 10(b). Observe that this representation also deforms the geometrical shape of the tile-configuration under consideration. We prefer the second representation, not only because of its esthetically more appealing *symmetry*, but also because it shows more of the interesting nonperiodic region that appears in it. Figures 9(b) and 9(d) are related in the same way.

The skew-coordinate case can also be interpreted as the operation which shifts each row over 1 cell to the left with respect to the row above it. In the original orthogonal coordinate system, this shift corresponds to a multiplication of the original CA-rule $R(x)$ with x^{-1}, so that the second representation also corresponds to a CGI-pattern (in rectangular coordinates) of the rule $R'(x) = x^{-1}R(x) = x^{-1} + x$, with tile-configuration vector $\beta' = (0, \beta_1 - 1, \beta_2 - 2, \beta_3 - 3) = (0, 0, 0, 0)$. We state the following generalization of this equivalency-property, which allows us to reduce a CGI-problem for a rule with $d_l \neq 0$ to one with a rule for which $d_l = 0$.

Definition 4.2. An s_d-skew coordinate system for the representation of CA orbit patterns is obtained from the orthogonal coordinate system by shifting

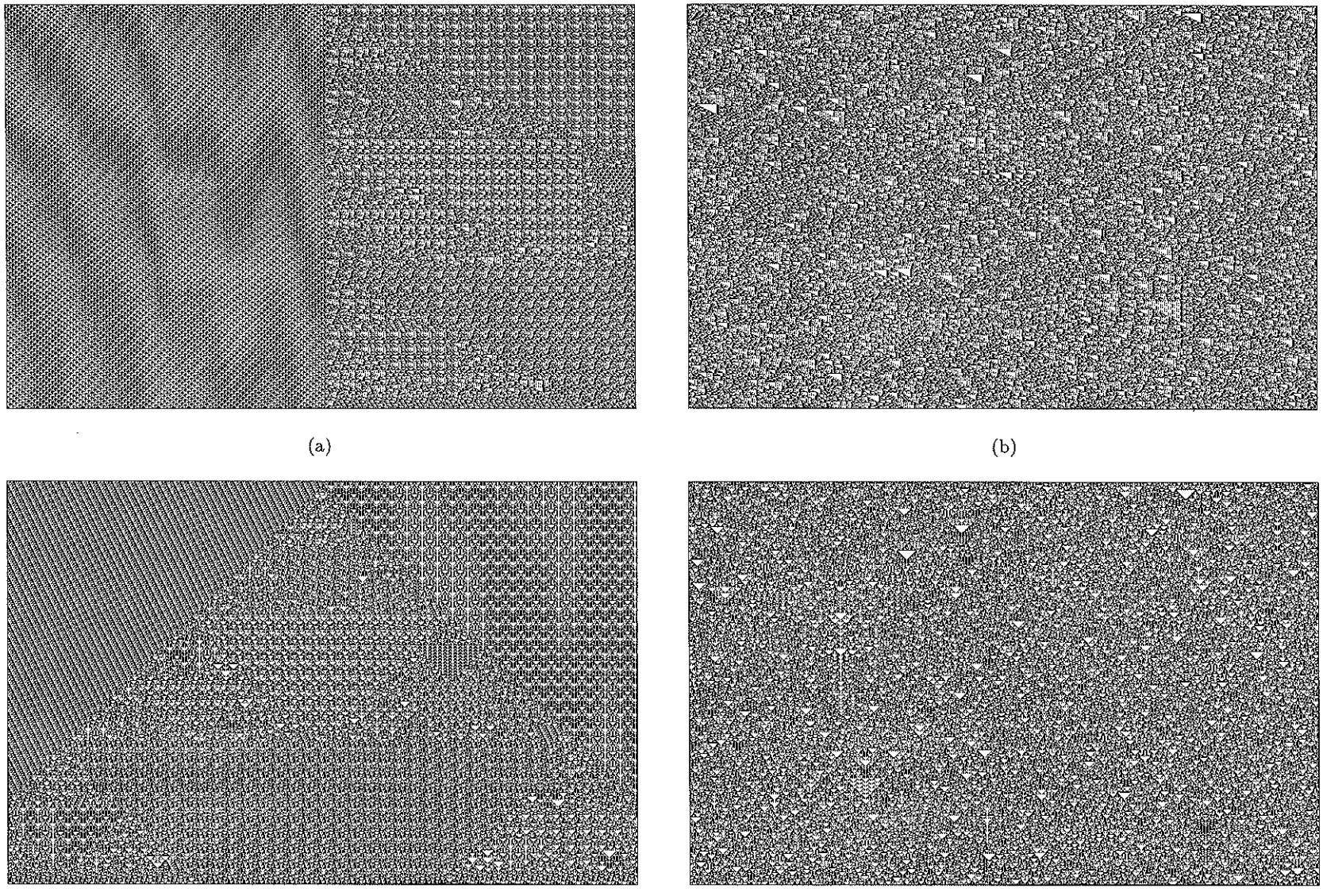

Fig. 9. A few solution patterns for the $[\mathcal{T}_{p^n,\beta}, W, \alpha, R]$-coarse graining invariant problem with $p^n = 2^2$, $\beta = (0, 1, 2, 3)$, $\Gamma = [0]$, $W = [1]$, $\alpha = (-6, -2, 2, 6)$, $R(x) = 1 + x^2 \in \mathbb{Z}_2[x]$. (a) Solution #189 with seedcode $\langle a_{-7} \ldots a_{-5} \rangle = \langle \underline{00110}\underline{10111101} \rangle$ (the freecell-related digits are underlined). (b) Solution #999 with seedcode $\langle \underline{1001}\underline{111100111} \rangle$. (c) Solution (a) represented in 1-skew coordinates. (d) Solution (b) represented in 1-skew coordinates. The patterns (c) and (d) are also representations in orthogonal coordinates of the CGI-problem with p^n, Γ, α, W as above, but with $\beta = (0, 0, 0, 0)$ and $R(x) = x^{-1} + x$ (Display size: 398×621 pixels).

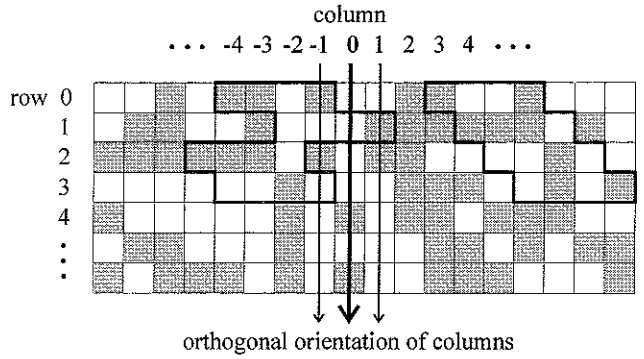

(a)

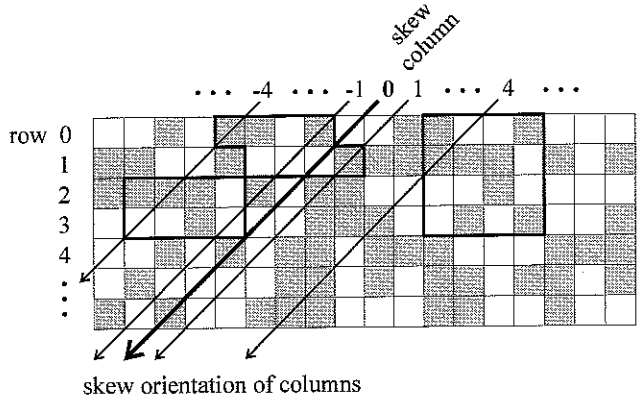

(b)

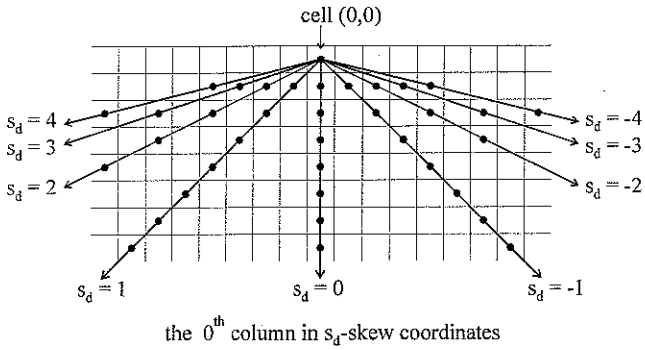

(c)

Fig. 10. Orbit patterns in orthogonal and skew coordinates. (a) Rule $R(x) = 1 + x^2$, tile configuration vector $\beta = (0, \beta_1, \beta_2, \beta_3) = (0, 2, -1, 0)$ and $(0, 1, 2, 3)$ in an orthogonal coordinate system. (b) Same rule and tile configuration vectors as under (a), but now in a 1-skew coordinate system. This pattern is identical to the one corresponding to the rule $R'(x) = x^{-1} + x$ and tile configuration vector $\beta' = (0, \beta_1 - 1, \beta_2 - 2, \beta_3 - 3) = (0, 1, -3, -3)$ and $(0, 0, 0, 0)$ in orthogonal coordinates. (c) Column orientations for s_d-skew coordinate systems.

each row over s_d cells to the left with respect to the previous row [$s_d = 0$ corresponds to the orthogonal coordinate system: when $s_d < 0$, the shift is actually to the right, see Fig. 10(c)]. The shift at row k is then ks_d.

Theorem 4.1. *The solutions to the* $[\mathcal{T}_{p^n,(\beta',\Gamma)}, W, \alpha, R'(x)]$ *CGI-problem where* $R'(x) = \sum_{k=d_l}^{d_r} q(k)x^k$ *and* $\beta' = (0, \beta'_1, \beta'_2, \ldots, \beta'_{p^n-1})$, *when represented in an* s_d*-skew coordinate system, correspond to the solutions of the* $[\mathcal{T}_{p^n,(\beta',\Gamma)}, W, \alpha, R(x)]$ *CGI-problem where* $R(x) = x^{-d_l}R'(x)$ *and* $\beta = (0, \beta'_1 - d_l, \beta'_2 - 2d_l, \ldots, \beta'_{p^n-1} - (p^n - 1)d_l)$, *when represented in a* $(s_d - d_l)$*-skew coordinate system.*

Example 4.3. Let $R'(x) = x^{-3} + x^{-2} + x$ in $\mathbb{Z}_2[x]$ under 2^2-tiling configuration vector $\beta' = (0, 0, 0, 0)$, to be represented in the orthogonal coordinates (i.e. $d_l = -3$, $s_d = 0$). This is equivalent with the rule $R(x) = 1 + x + x^4$ under the 2^2-tiling vector $\beta = (0, 3, 6, 9)$ displayed in 3-skew coordinates. However, if we display the latter solutions in 2-skew coordinates, this corresponds to representing the $R'(x)$-related solutions in (-1)-skew coordinates.

4.5. *The group structure of the solutions*

Hitherto, we have shown that solutions of the $[\mathcal{T}_{p^n,\Xi}, W, \alpha, R]$-CGI problem are orbit patterns $O_R(S_0)$ for which the initial state $S_0 = \langle a(0, j)\rangle_{j\in\mathbb{Z}}$ is completely determined by the seed with a corresponding good seedcode $S_{cd} = \langle a(0, j)\rangle_{j\in I[\kappa+1,\lambda-1]}$ which can be considered as an ordered string of digits in $\mathbb{Z}_p$. The seed may contain depcells and freecells: their particular configuration is the seed-configuration. When writing down a particular seedcode, the freecell-related digits will be underlined. For a given CGI-problem, the seed-configuration is fixed by the choices made during the solution-procedure, and as the depcells in the seed are completely determined by the freecells, we only need to give the freecell-code S_{fcd}, i.e. the seedcode in which

the non-underlined depcell-digits are deleted. For example, when

$$S_{cd} = \underline{1}2\underline{1}\underline{0}10\underline{2}\underline{0}\underline{1}, \text{ then}$$
$$S_{fcd} = 110201.$$

With N_f the number of freecells (this is also the number of digits in the freecell-code), the number of solutions to the given CGI-problem is p^{N_f}. It is clear that the set of freecell-codes is the set $(\mathbb{Z}_p)^{N_f}$ of N_f-tuples of p-ary digits. We will attribute a number n to each freecell-code, to its corresponding initial-state sequence S_0, and to the corresponding CGI orbit pattern: n is the number for which S_{fcd} is the p-ary representation. That is, when $S_{fcd} = s_{N_f-1}, \ldots, s_1 s_0$, then

$$n(S_{fcd}) = \sum_{i=0}^{N_f-1} s_i p^i, \text{ and } n(S_{fcd})$$
$$\in \mathcal{Z}_{p^{N_f}} \triangleq \{0, 1, \ldots, p^{N_f} - 1\}. \quad (59)$$

The freecell-code, the initial sequence and the orbit pattern corresponding to the number $n \in \mathcal{Z}_{p^{N_f}}$ will be denoted by $S_{fcd}(n)$, $S_0(n)$ and $OP(n)$, respectively.

Definition 4.3. For a given CGI-problem,

$\mathcal{S}_{fcd} = (\mathbb{Z}_p)^{N_f} = \{S_{fcd}(n) | n \in \mathcal{Z}_{p^{N_f}}\}$ is the set of all freecell-codes,

$\mathcal{S}_0 \triangleq \{S_0(n) | n \in \mathcal{Z}_{p^{N_f}}\}$ is the set of all initial-state sequences leading to CGI-solutions,

$\mathcal{S}_{OP} \triangleq \{OP(n) | n \in \mathcal{Z}_{p^{N_f}}\}$ is the set of all CGI-orbit patterns.

We will now define an additive operation in these sets.

Definition 4.4.

— Let $n_1, n_2 \in \mathcal{Z}_{p^N}$, then $n_3 = n_1 \boxplus_p n_2 \in \mathcal{Z}_{p^N}$ is the number whose p-ary representation is obtained from the *digitwise addition* modulo p of the digits in the p-ary representation of n_1 and n_2. That is, when $n_1 = \sum_{i=0}^{N-1} a_i p^i$ and $n_2 = \sum_{i=0}^{N-1} b_i p^i$ ($a_i, b_i \in \mathbb{Z}_p$), then

$$n_3 = n_1 \boxplus_p n_2 \triangleq \sum_{i=0}^{N-1} (a_i +_p b_i) p^i,$$

where $+_p$ denotes addition modulo p in $\mathbb{Z}_p$. This definition establishes an *isomorphism* between $\langle \mathcal{Z}_{p^N}, \boxplus_p \rangle$ and $\langle \mathbb{Z}_p^N, \boxplus_p \rangle$, where $\boxplus_p$ in reference to $\mathbb{Z}_p^N$ obviously denotes componentwise modulo p addition.

— Let $S_0(n_1)$ and $S_0(n_2)$ be two initial-state sequence solutions for a given CGI-problem ($n_1 = n_2$ is allowed), then $S_0(n_1) \boxplus_p S_0(n_2)$ is the initial-state sequence obtained by *cellwise* addition modulo p of $S_0(n_1)$ and $S_0(n_2)$.

— Let $OP(n_1)$ and $OP(n_2)$ be two orbit-patterns, then $OP(n_1) \boxplus_p OP(N_2)$ is the pattern obtained by *cellwise* addition modulo p of these patterns.

Theorem 4.2. *$\langle \mathcal{S}_0, \boxplus_p \rangle$, $\langle \mathcal{S}_{OP}, \boxplus_p \rangle$, $\langle \mathcal{Z}_{p^{N_f}}, \boxplus_p \rangle$ are isomorphic. That is, when $S_0(n_1), S_0(n_2) \in \mathcal{S}_0$, then $S_0(n_1) \boxplus_p S_0(n_2) = S_0(n_1 \boxplus_p n_2) \in \mathcal{S}_0$, and when $OP(n_1), OP(n_2) \in \mathcal{S}_{OP}$, then $OP(n_1) \boxplus_p OP(n_2) = OP(n_1 \boxplus_p n_2) \in \mathcal{S}_{OP}$.*

Proof. $S_0(n)$ is completely determined by n: the state of the free seedcells are obtained from the p-ary representation of n, the state of the seed-internal depcells are obtained from the seed-internal equations, and the state of the seed-external depcells are obtained from applying the left- and right-propagation equations. As all these equations are linear homogeneous (in $\mathbb{Z}_p$), it means that $S_0(n_1 \boxplus_p n_2) = S_0(n_1) \boxplus_p S_0(n_2)$, establishing the isomorphism between $\langle \mathcal{Z}_{p^{N_f}}, \boxplus_p \rangle$ and $\langle \mathcal{S}_0, \boxplus_p \rangle$. The isomorphism with $\langle \mathcal{S}_{OP}, \boxplus_p \rangle$ follows because of the linearity of the CA, implying that $S_0(n_1) \boxplus_p S_0(n_2)$ corresponds with $OP(n_1) \boxplus_p OP(n_2)$ and $S_0(n_1 \boxplus_p n_2)$ corresponds with $OP(n_1 \boxplus_p n_2)$. As $S_0(n_1) \boxplus_p S_0(n_2) = S_0(n_1 \boxplus_p n_2)$, it follows that $OP(n_1) \boxplus_p OP(n_2) = OP(n_1 \boxplus_p n_2)$. ■

It was already mentioned above that, by definition, $\langle \mathcal{Z}_{p^N}, \boxplus_p \rangle$ and $\langle \mathbb{Z}_p^N, \boxplus_p \rangle$ were isomorphic. Observing that $\langle \mathbb{Z}_p^N, \boxplus_p \rangle$ is actually the finite Abelian group which is usually represented by $\mathbb{Z}_p^N$ only, and which is the direct product of N copies of the cyclic group $\mathbb{Z}_p$ (see e.g. [Armstrong, 1988]), we can state:

Theorem 4.3. *For a given CGI-problem,* $\langle \mathcal{S}_0, \boxplus_p \rangle$, $\langle \mathcal{S}_{OP}, \boxplus_p \rangle$ *and* $\langle \mathcal{Z}_{p^{Nf}}, \boxplus_p \rangle$ *form an Abelian group which is isomorphic to* $\mathbb{Z}_p^{N_f}$.

Remarks. This means that all orbit-pattern solutions $OP(n) \in \mathcal{S}_{OP}$ form an Abelian group under cellwise modulo p addition. In this solution domain:

- the neutral element is $OP(0)$, i.e. the orbit whose cells are all in the 0-state.
- every element $OP(n)$ with $n = \sum_{i=0}^{N-1} a_i p^i$ has a symmetric element $OP(\bar{n})$ with $\bar{n} = \sum_{i=0}^{N-1} \bar{a}_i p^i$, where $\bar{a}_i = (p - a_i) \bmod p$.

We will now establish a recursive procedure to generate the group-table of $\langle \mathcal{Z}_{p^n}, \boxplus_p \rangle$ starting from the group-table of the cyclic group $\mathbb{Z}_p$ (under addition modulo p):

$\boxplus_p$	0	1	2	...	$(p-2)$	$(p-1)$
0	0	1	2	...	$(p-2)$	$(p-1)$
1	1	2	3	...	$(p-1)$	0
2	2	3	4	...	0	1
3	3	4	5	...	1	2
⋮	⋮	⋮	⋮		⋮	⋮
$(p-1)$	$(p-1)$	0	1	...	$(p-3)$	$(p-2)$

The matrix of inner elements in this table will be represented by T_p. Its element on row a and column b is $T_p(a, b) = a +_p b$ for $a, b \in \mathcal{Z}_p$.

Theorem 4.4. *The group* $\langle \mathcal{Z}_{p^N}, \boxplus_p \rangle$ *of solution numbers of a CGI-problem with* N *freecells has a group-table with matrix* T_{p^N} *(row and column-order:* $0, 1, 2, \ldots, p^N - 1$*) which can be obtained by the recursive matrix substitution scheme*

$$\forall n \geq 2 : T_{p^n} = p^{n-1} T_p \oplus T_{p^{n-1}}\,,^3 \qquad (60)$$

where, by definition:

$$T_{p^n}(a, b) \triangleq a \boxplus_p b \text{ for } a, b \in \mathcal{Z}_{p^n}\,. \qquad (61)$$

(Observe that at each step, the size of the T_{p^n}*-matrix increases by a factor* p*.)*

Proof. when A is a $s \times s$ matrix and B a $t \times t$ matrix, then $C = A \oplus B$ is a matrix of size $(s \times t) \times (s \times t)$, in which element $A(a, b)$ and $B(c, d)$ combine into the element

$$C(at + c, bt + d) = A(a, b) + B(c, d),$$
$$(0 \leq a, b \leq s - 1, 0 \leq c, d \leq t - 1) \qquad (62)$$

Apply this to $C = p^{n-1} T_p \oplus T_{p^{n-1}}$ to obtain that for $0 \leq a, b \leq p - 1$, $0 \leq c, d \leq p^{n-1} - 1$:

$$\begin{aligned} & C(ap^{n-1} + c, bp^{n-1} + d) \\ & \overset{(62)}{=} p^{n-1} T_p(a, b) + T_{p^{n-1}}(c, d)\,. \\ & \overset{(61)}{=} (a +_p b) p^{n-1} + c \boxplus_p d \\ & = (ap^{n-1} + c) \boxplus_p (bp^{n-1} + d) \\ & \overset{(61)}{=} T_{p^n}(ap^{n-1} + c, bp^{n-1} + c)\,. \quad \blacksquare \end{aligned}$$

Remarks. Because of the established isomorphism, T_{p^n} stands in 1–1 correspondence with the group-table of the elements in $\mathcal{S}_0$ (double-infinite sequences of $\mathbb{Z}_p$-digits), $\mathcal{S}_{OP}$ (orbit patterns), and $\mathbb{Z}_p^N$ (N-strings of $\mathbb{Z}_p$-digits). It is a well-known property of the $\mathbb{Z}_p^N$-group (and all isomorphic groups) that it has subgroups isomorphic to $\mathbb{Z}_p^n$ for all $n \leq N$. The number of subgroups of type $\mathbb{Z}_p^n$ for $\mathbb{Z}_p^N$ is given by

$$\Pi_{i=0}^{n-1} \frac{(p^N - p^i)}{(p^n - p^i)}\,.$$

(see, for example, [Carmichael, 1956], Sec. 28)

As an illustration of this theorem, we show the T_{2^4}-matrix for the group $\langle \mathcal{Z}_{2^4} = \{0, 1, 2, \ldots 15\}, \boxplus_2 \rangle$.

[3] Let A and B denote two matrices with elements $A(i, j)$ and $B(i, j)$, respectively, then $A \oplus B$ is the *bigsum* operation which substitutes each element $A(i, j)$ in A by the matrix $A(i, j) + B$, the latter expression denoting the matrix obtained by adding $A(i, j)$ to all elements of B. ([Barbé, 1992]; this is the additive version of the Kronecker product of two matrices, but it is not what is known as the Kronecker sum [Graham, 1981]).

	0	1	2	3	4	5	6	7	8	9	10	11	12	13	14	15
0	0	1	2	3	4	5	6	7	8	9	10	11	12	13	14	15
1	1	0	3	2	5	4	7	6	9	8	11	10	13	12	15	14
2	2	3	0	1	6	7	4	5	10	11	8	9	14	15	12	13
3	3	2	1	0	7	6	5	4	11	10	9	8	15	14	13	12
4	4	5	6	7	0	1	2	3	12	13	14	15	8	9	10	11
5	5	4	7	6	1	0	3	2	13	12	15	14	9	8	11	10
6	6	7	4	5	2	3	0	1	14	15	12	13	10	11	8	9
7	7	6	5	4	3	2	1	0	15	14	13	12	11	10	9	8
8	8	9	10	11	12	13	14	15	0	1	2	3	4	5	6	7
9	9	8	11	10	13	12	15	14	1	0	3	2	5	4	7	6
10	10	11	8	9	14	15	12	13	2	3	0	1	6	7	4	5
11	11	10	9	8	15	14	13	12	3	2	1	0	7	6	5	4
12	12	13	14	15	8	9	10	11	4	5	6	7	0	1	2	3
13	13	12	15	14	9	8	11	10	5	4	7	6	1	0	3	2
14	14	15	12	13	10	11	8	9	6	7	4	5	2	3	0	1
15	15	14	13	12	11	10	9	8	7	6	5	4	3	2	1	0

There are 15 subgroups of type $\mathbb{Z}_2$ and of type $\mathbb{Z}_2^3$, and 35 subgroups of type $\mathbb{Z}_2^2$ (Klein group). An example of a $\mathbb{Z}_2^3$-type subgroup is formed by the elements $\{0, 3, 4, 7, 8, 11, 12, 15\}$, a type $\mathbb{Z}_2^2$-subgroup is formed by $\{0, 2, 9, 11\}$.

5. Morphology of CGI-Orbit Patterns

We have solved $[\mathcal{T}_{p^n,\Xi}, W, \alpha, R]$-coarse-graining invariant problems for a large number of situations, thereby producing orbit patterns of a potentially unlimited diversity. However, all these patterns can seemingly be classified into a limited number of categories, several representatives of which are shown in Figs. 12 to 20. Unfortunately, the size of the display window is rather very restricted. Because of this, and also for computational comfort, we had to limit ourselves to rather modest values of both p^n and the degree of the CA-rule, but we assume that the nature of the patterns shown here is also typical for larger values of p^n and $\deg R(x)$. Moreover, it is assumed (and corroborated by experience) that the nature of the patterns outside the window shown, is the trivial continuation of the characteristics that manifest itself inside the display window.

In discussing the structural properties of the patterns, we will sometimes refer to the (v, h)-*shift identity pattern* $SIP_{v,h}$, $(v, h \in \mathbb{N})$. This correlates a given pattern with a shifted version of itself, thereby highlighting the pixels which are identical in both the original and shifted pattern. That is when an original pattern P has value $P(r, c)$ at the (r, c)th pixel $(r \in \mathbb{N}, c \in \mathbb{Z})$, then $SIP^P_{v,h}$ is the pattern such that $SIP^P_{v,h}(r, c) = 0$ iff $P(r, c) = P(r + v, c + h)$, otherwise $SIP^P_{v,h}(r, c) = 1$. When $P(r, c)$ is only known over the finite window $(0 \leq r \leq r_u, c_l \leq c \leq c_u)$ in which it is displayed, $SIP^P_{v,h}(i, j)$ is only known over the smaller window $(0 \leq i \leq r_u - v, c_l \leq j \leq c_u - h)$. Figure 11 shows how this window is formed as the overlap region between the original P-displaying window D^P and its (v, h)-shifted version $D^P_{v,h}$ (v=vertical shift, h = horizontal shift). In this overlap region, a pixel is white whenever its value in D^P is identical to its value in $D^P_{v,h}$, otherwise it is black. The $SIP^P_{v,h}$-pattern is a generalization of the shift-add operation for purely binary patterns that was introduced in [Barbé *et al.*, 1995].

Now follows a categorization of CGI-invariant patterns. It is based primarily on the visual characteristics observed in several CGI-solution patterns

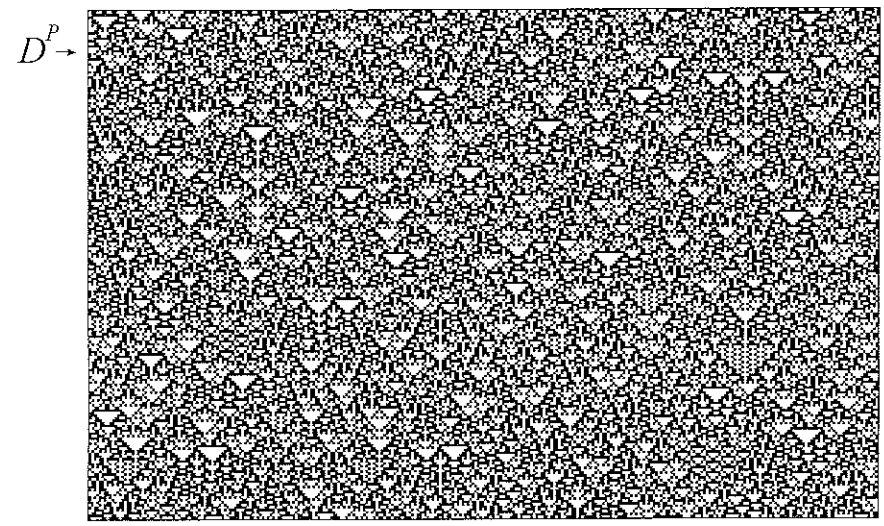

(a)

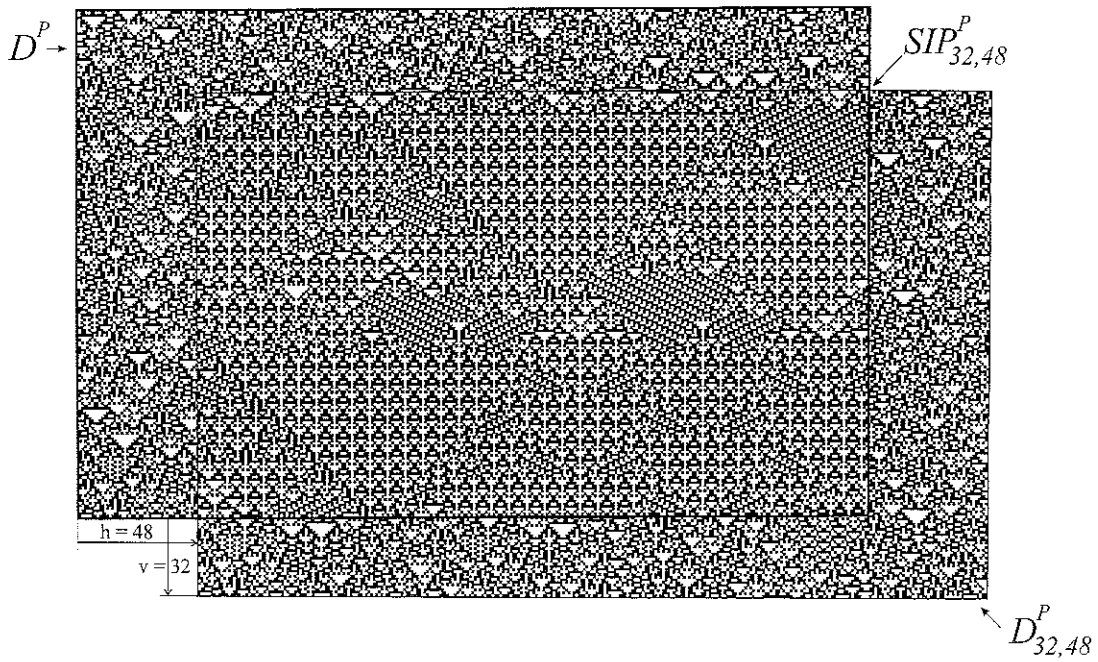

(b)

Fig. 11. (a) The finite display D^P of an orbit pattern P (a solution of the $[\mathcal{T}_{2^2,\beta=(0,1,2,3)}, \alpha = (0, 2, 4, 6), W = [1], R(x) = 1 + x^2]$-CGI problem in 1-skew coordinates. Displayed is $\{a(r, c) | 0 \leq r \leq 198, -155 + r \leq c \leq 155 + r\}$). (b) The overlap region between D^P and $D^P_{v,h}$ determines the displayable part of the (v, h)-shift identity correlation of pattern P (i.e. $SIP^P_{v,h}$). A white pixel in this domain corresponds with a $P(r, c)$ pixel for which $P(r, c) = P(r + v, c + h)$, otherwise the pixel is black.

and their SIPs. These solutions are related to CGI-problems which are listed in the Appendix.

The *U*-class of uniform patterns

These are the patterns displaying rather uniform structural characteristics.

Category U_P: Full P-periodic patterns. Examples are shown in Fig. 12, giving the eight full-periodic patterns that appear as solutions of Problem 1. The problem has actually 64 full-periodic solutions: they are all similar to one of the eight patterns shown (up to some vertical and horizontal shift or to a

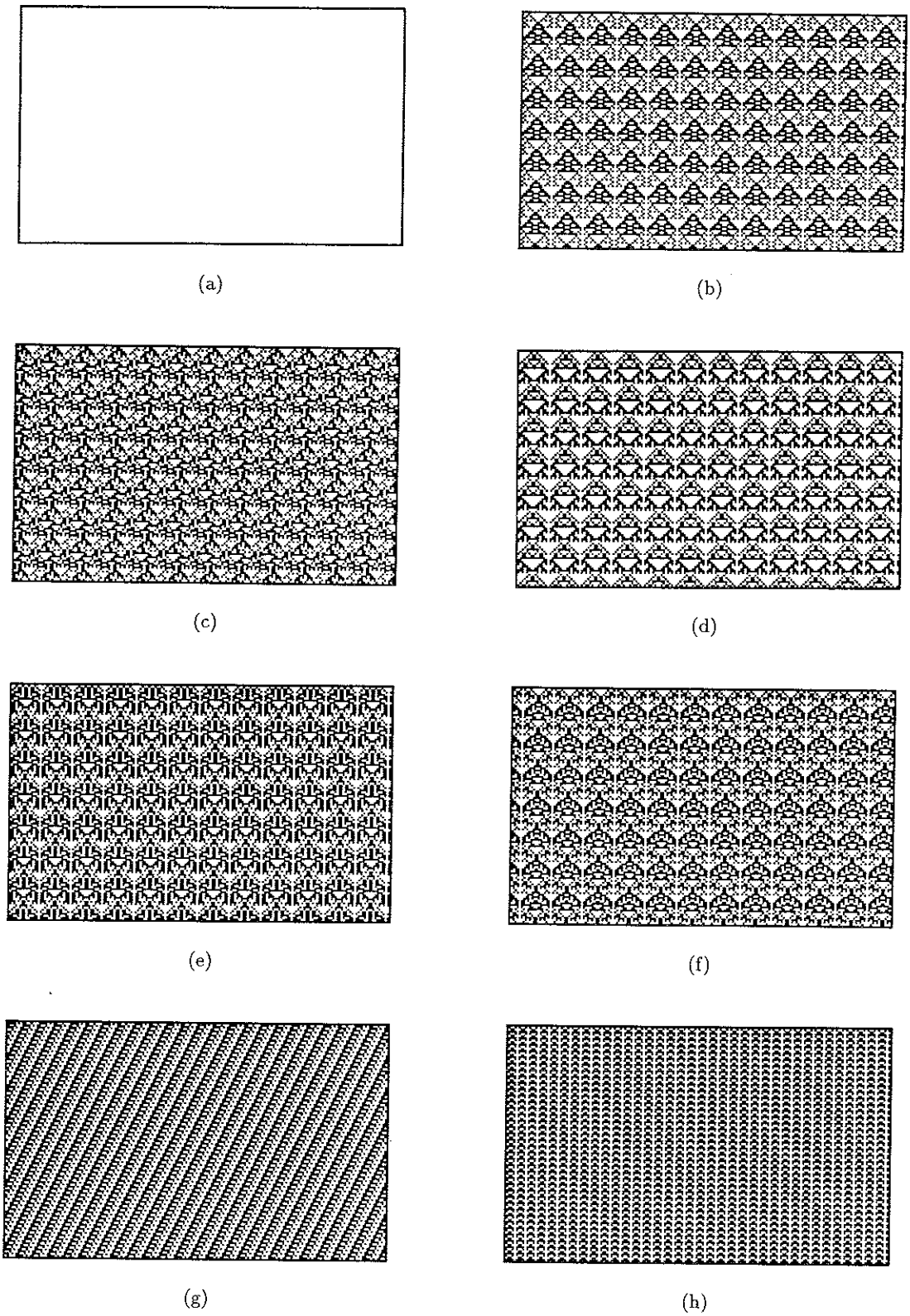

Fig. 12. The eight full-periodic textures that may appear in the 64 different full-periodic CGI solutions of Problem 1. Displayed is $\{a(r, c) | 0 \leq r \leq 100, -80+r \leq c \leq 80+r\}$, in 1-skew coordinates. The seed is $\langle a_{-7} \ldots a_5 \rangle$ and the seedcodes for the solutions above are (a) $\langle 000\underline{\underline{000}}000000\rangle$, (b) $\langle 0001\underline{\underline{000}}001000\rangle$, (c) $\langle 0001\underline{\underline{000}}101100\rangle$, (d) $\langle 1000\underline{\underline{000}}000001\rangle$, (e) $\langle 100\underline{\underline{100}}0001001\rangle$, (f) $\langle 100\underline{\underline{000}}0010\underline{\underline{01}}\rangle$, (g) $\langle 1001\underline{\underline{000}}111101\rangle$, (h) $\langle 1010\underline{\underline{010}}100101\rangle$. Underlined digits refer to the seed-freecells, the double-underlined ones to the freecells which remain freecells under the conditions for full periodicity (Sec. 6).

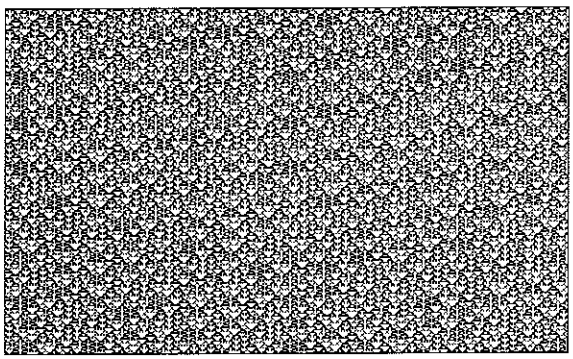

(a)

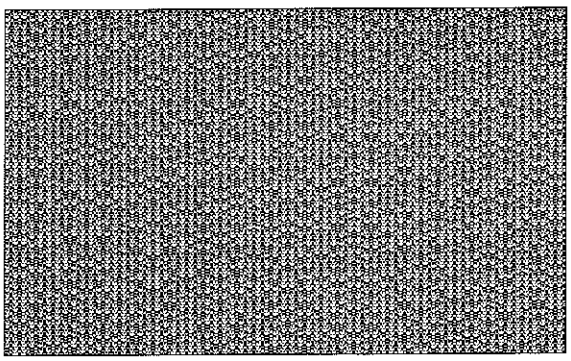

(b)

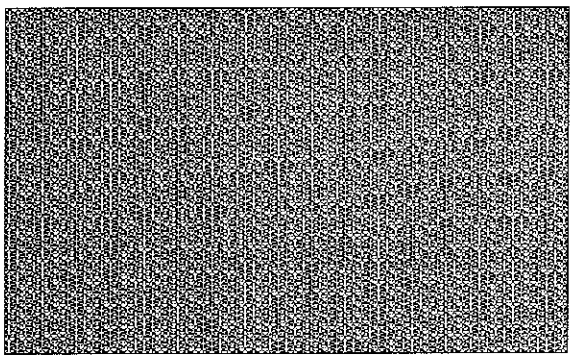

(c)

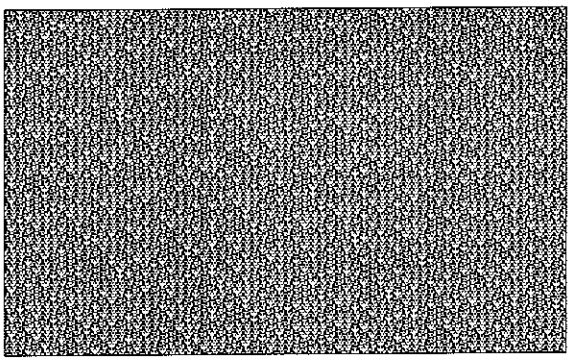

(d)

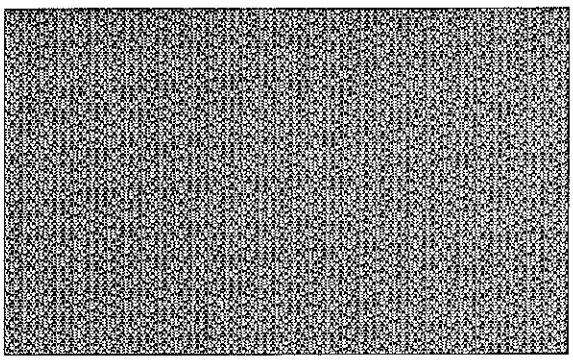

(e)

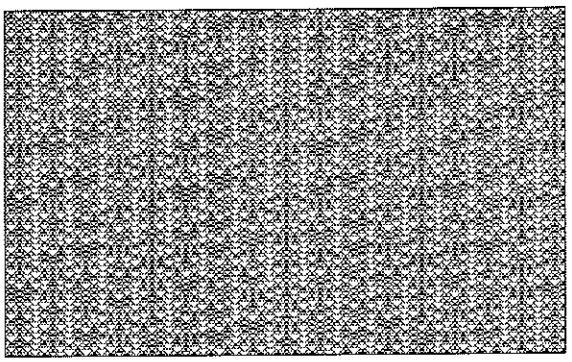

(f)

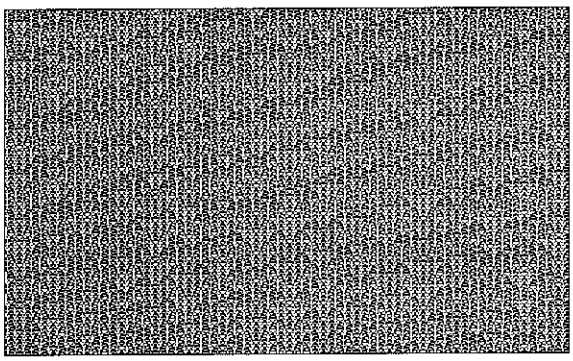

(g)

Fig. 13. Quasiperiodic solutions for Problem 3, with selected seed $\langle a_{-2}a_{-1}a_0a_1a_2a_3\rangle$, all cells of which are freecells. These patterns have seedcode (a) $\langle\underline{000001}\rangle$; (b) $\langle\underline{000101}\rangle$; (c) $\langle\underline{001000}\rangle$; (d) $\langle\underline{001100}\rangle$; (e) $\langle\underline{010111}\rangle$; (f) $\langle\underline{101010}\rangle$; (g) $\langle\underline{101100}\rangle$ (displayed is $\{a(r,c)|0 \leq r \leq 235, -200+r \leq c \leq 200+r\}$ in 1-skew coordinates).

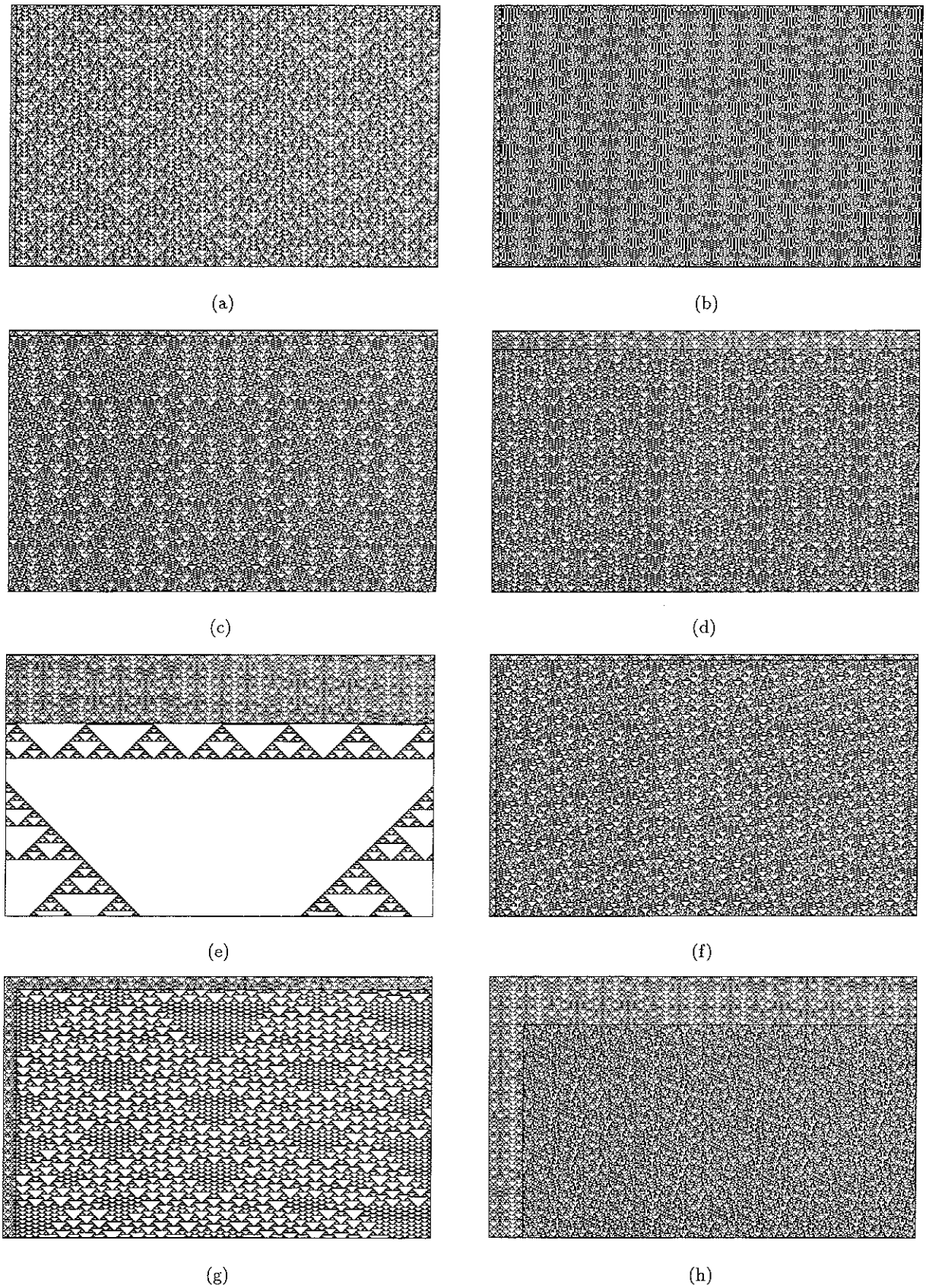

Fig. 14. Shift-identity patterns ($SIP_{v,h}$) for the solution of Fig. 13(f). (a) $(v, h) = (0, 5)$; (b) $(v, h) = (0, 6)$; (c) $(v, h) = (5, 0)$; (d) $(v, h) = (17, 0)$; (e) $(v, h) = (64, 0)$; (f) $(v, h) = (5, 6)$; (g) $(v, h) = (12, 12)$; (h) $(v, h) = (45, 32)$.

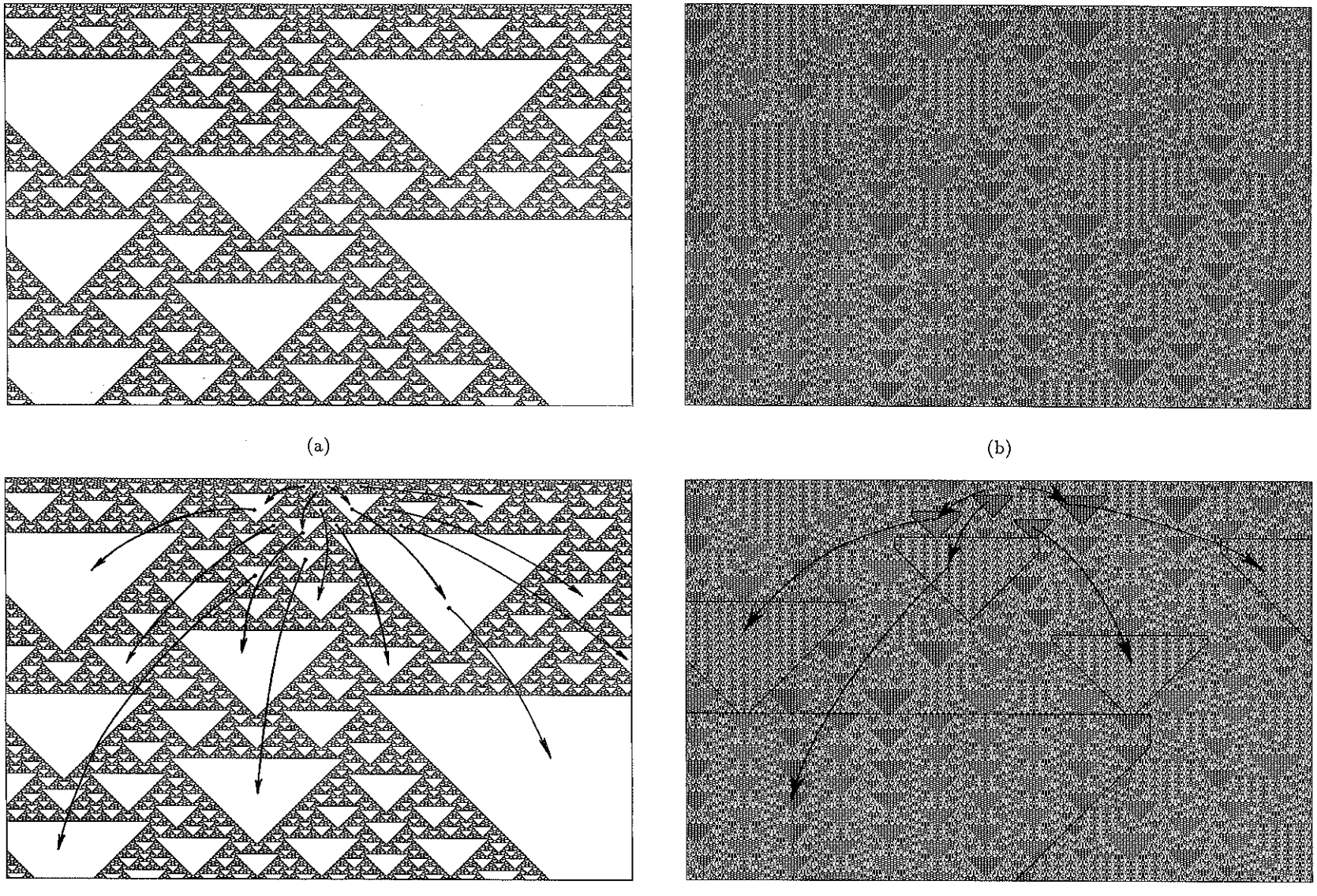

Fig. 15. Visually self-similar solutions. (a) Solution with seedcode $\langle a_0 \dots a_3 \rangle = \langle \underline{1001} \rangle$ for Problem 2. (b) Solution with seedcode $\langle \underline{0101} \rangle$ for Problem 2. (c) Self-similarity of the first kind in (a). (d) Self-similarity of the second kind in (b). (e) Solution with seedcode $\langle a_{-2} \dots a_2 \rangle = \langle \underline{00001} \rangle$ for Problem 6. (f) Solution with seedcode $\langle a_{-2} \dots a_3 \rangle = \langle \underline{100001} \rangle$ for Problem 7. (g) Self-similarity of the third kind in (e). (h) Self-similarity of the third kind in (f). (displayed is $\{a(r, c) | 0 \leq r \leq 397, -310 + r \leq c \leq 310 + r\}$, in 1-skew coordinates).

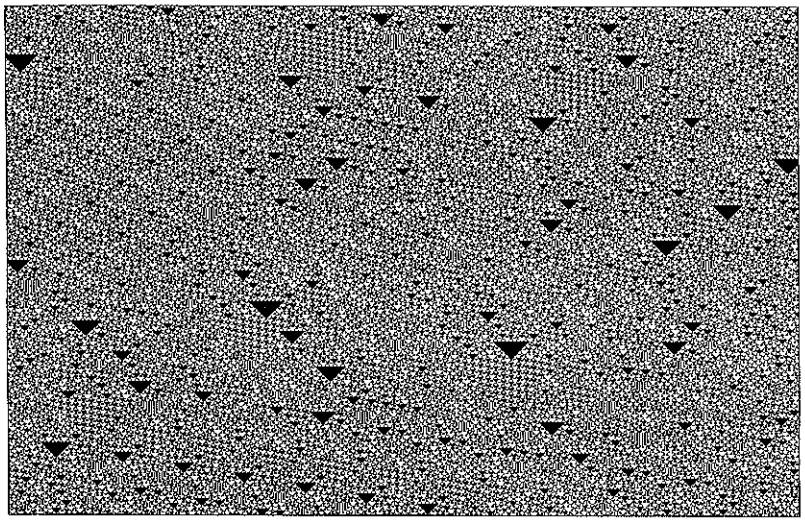

(e)

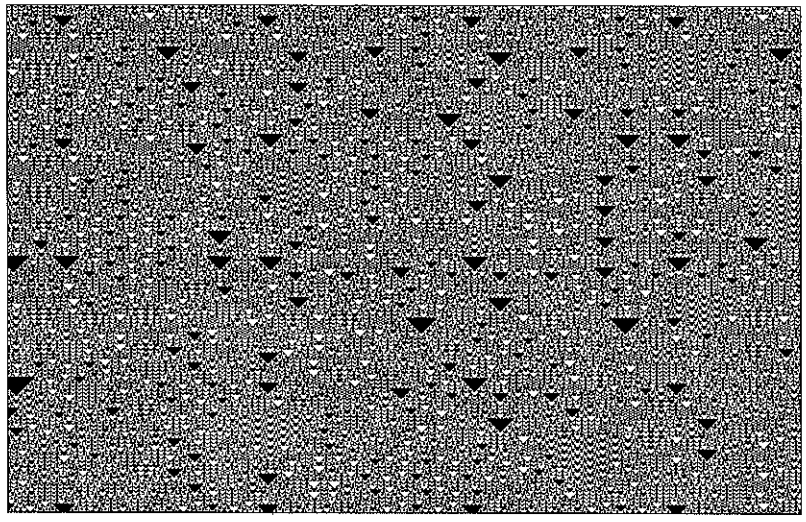

(f)

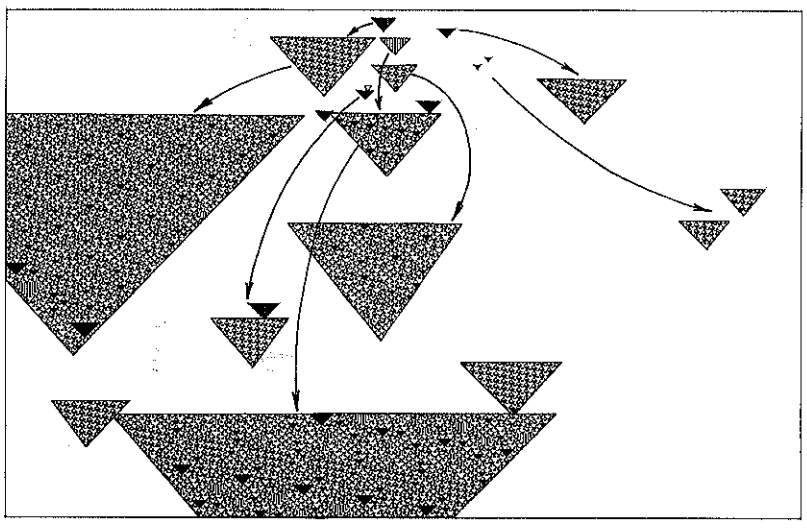

(g)

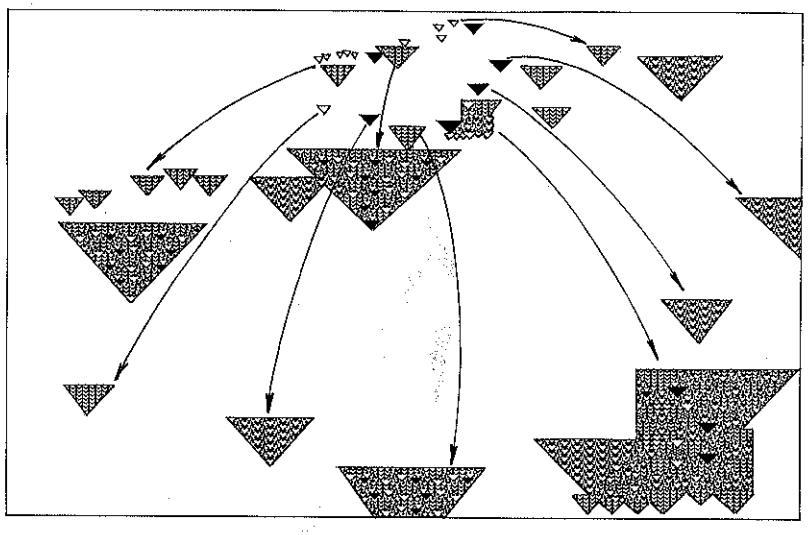

(h)

Fig. 15. (*Continued*)

left–right mirroring). From the 64 full-periodic solutions, there are 60 solutions with (minimal) period $P = 15$, 3 solutions with period $P = 5$, and one solution with period $P = 1$ (the trivial 0-solution). The period P concerns the period of the initial-state sequence (i.e. the top row).

Category U_{QP}: Quasiperiodic patterns. Figures 13(a)–13(g) show solutions $\#1, 5, 8, 12, 23, 42, 44$ from Problem 3. Apart from solutions $0, 3, 60$ and 63, which are simultaneously biperiodic *and* self-similar complex of the first kind (see further for these categories), the remaining 60 solutions all show a texture which is similar to one of the patterns shown. The appearance of these patterns is indeed almost periodic: different local structures are repeated all over the pattern in a regular but nonperiodic way. At *all* (v, h)-shifts, the corresponding $SIP_{v,h}$-patterns clearly exhibit structure too (at least for the display-restricted (v, h)-values). Figures 14(a) to 14(h) show a few possible $SIP_{v,h}$-patterns for the solution displayed in Fig. 13(f).

Except for the trivial 0-pattern and a Sierpinsky-like pattern, quasi periodic patterns

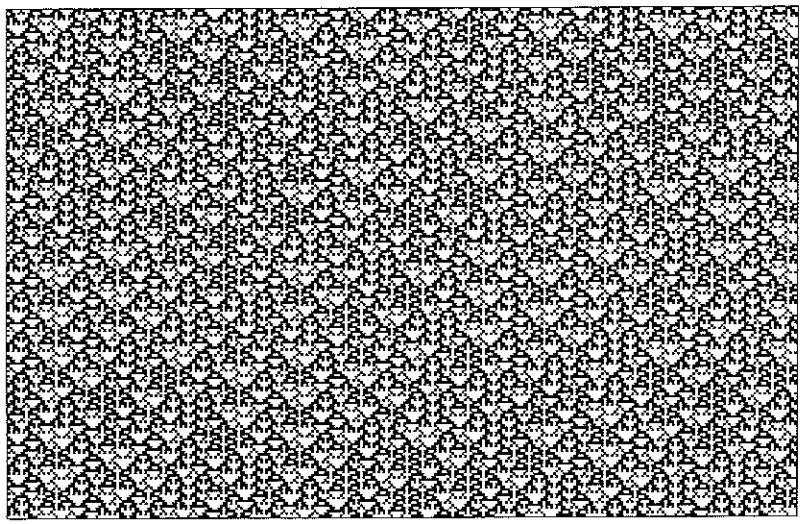

(a)

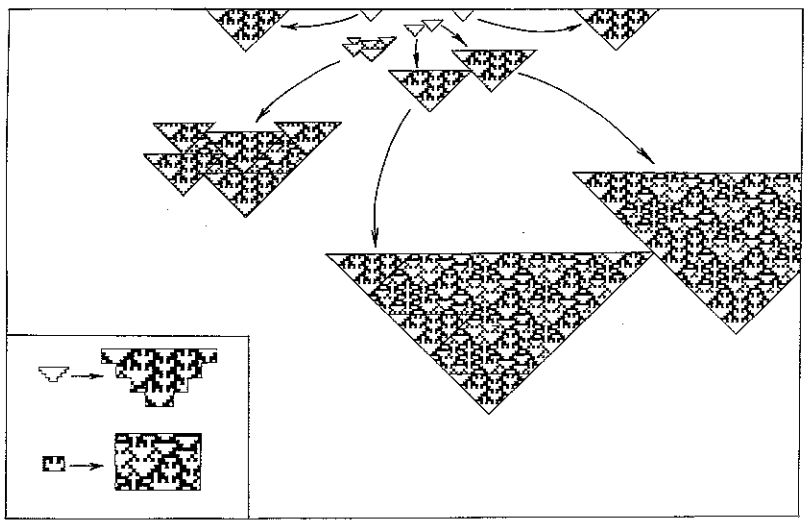

(b)

Fig. 16. A quasi-periodic pattern is also self-similar (a) Enlarged part of Fig. 13(a). (b) Its self-similar structure uncovered (insert: the main underlying substitutions).

were the only ones that appeared as solutions for the $[\mathcal{T}_{2^1,\beta=(0,0)}, \alpha = (0, 0), W = \begin{bmatrix} 1 & 1 \\ 1 & 1 \end{bmatrix}, R(x) = \sum_{i=-d_l}^{dr} q(i)x^i, (d_l, d_r, > 0)]$-CGI problem that was studied in [Barbé *et al.*, 1995]. (That paper also deals with correlation and Fourier analysis of such patterns, and proves 2-automaticity of the corresponding initial state sequence.)

Category U_S: (Visually) Self-similar patterns. The 15 nontrivial (i.e. nonzero) solutions of Problem 2 can be divided into two categories containing similar patterns. One contains the solutions 3, 9, 10 and the other contains the solutions 1, 2, 4, 5, 6, 7, 8, 11, 12, 13, 14, 15. Figure 15(a) shows solution #9 from the first category, and Fig. 15(b) shows solution #5 from the second category. A visual examination of Fig. 15(a) shows that the pattern repeats itself on every 4-tuple scale (4 being the coarse-grain size of the problem), as illustrated in Fig. 15(c). Therefore this kind of pattern is qualified as displaying a (visual) *self-similarity of the first kind.* As shown in Fig. 15(d), pattern 15(b) also shows a visual self-similarity, although it is less trivial: at each increment of scale, there is an alternation between two possible local structures that fill the larger triangular domains. This will be called *self-similarity of the second kind.* Figures 15(e) and 15(f) are solutions of Problems 6 and 7, respectively. Despite their high degree of visual complexity, a careful examination uncovers a self-similar structure. This is illustrated in Figs. 15(g) and 15(h): at each increment of scale, there is a substitution of local patterns which is more complex than in the first examples. This feature will be called *self-similarity of the third kind.*

This self-similarity in the examples is visually detectable because triangular structures of growing (p^n-tupling) size appear at p^n-tupling distance of the seedcells. In the examples, these triangles are filled with periodic patterns, and they are detectable because these periodic patterns contrast with the pattern outside the triangular domains.

Figure 16(a) shows an enlarged part of Fig. 13(a). After some puzzling, one can detect that this pattern is also self-similar (here of the second kind), as illustrated in Fig. 16(b). Observe the complexity of the underlying substitution. Self-similarity in the quasi-periodic case may be generic, but it is not a visual self-similarity.

Category U_{QR}: Quasirandom patterns. Figure 17(a) shows solution #478 for Problem 1 (there are 896 solutions of this kind). It is visually difficult to distinguish its structure from a pattern obtained with the same CA-rule from a *random* initial-state sequence, an example of which is shown in Fig. 17(b). This last pattern is not coarse-graining invariant. However, there is a subtle hidden difference between the nature of the patterns 17(a) and 17(b): the $SIP_{v,h}$-patterns of Fig. 17(a) show definitely a more organized structure than the original pattern for *some* discrete values of (v, h), and remain more or less randomlike (like the original pattern) for other values of (v, h). On the other hand, the $SIP_{v,h}$-patterns of the randomly generated Fig. 17(b) remain randomlike for all (v, h)-shifts. Figures 17(c)–17(k) show several shift identity patterns of the pattern in Fig. 17(a). Several are clearly quasi-periodic. For this particular problem, we found more or less structured patterns of the type of Fig. 17(i) and 17(j) for some (v, h) where both v and h are a sum of certain powers of 2. Patterns like in Fig. 17(c) appear for some (v, h) where both v and h are a multiple of 15 (and it happens that 15 is a possible period in the periodic solutions of Problem 1). For the other values of (v, h), and these form a majority, the $SIP_{v,h}$ look more like Fig. 17(k). Observe that some of the structured SIP's are *left–right symmetric* [Figs. 17(c), (d), (f), (g)], although this is *not* the case for the original pattern (this hidden symmetry has been detected in several quasi-random patterns, but it does not seem to be generic).

The name *quasi-random* is given to this kind of solution just because the pattern itself and most of its $SIP_{v,h}$'s are very similar to a pattern that is generated from a random top row. However, for certain (v, h), the $SIP_{v,h}$ displays a structure which may be surprisingly structured. In general, quasi-random patterns are those for which the $SIP_{v,h}$ shows a non-randomlike structure only for a set of values $(v, h) = (kV_P, lP)(k, l \in \mathbb{N}, P$ is the possible maximal strict period of periodic solutions of the CGI-problem (see Sec. 6); V_P is another integer which is the vertical period of solutions with horizontal period P). There *may* also appear structure in $SIP_{v,h}$ for which both v and h are *particular* sums of powers of p (for some problems, the 0th power of p may be included). The size of the (v, h)-set for which the extra structure in $SIP_{v,h}^P$ emerges is problem/solution dependent and may vary widely.

We have observed that quasi-random solutions may appear in CGI-problems for which there are also possibly periodic solutions.

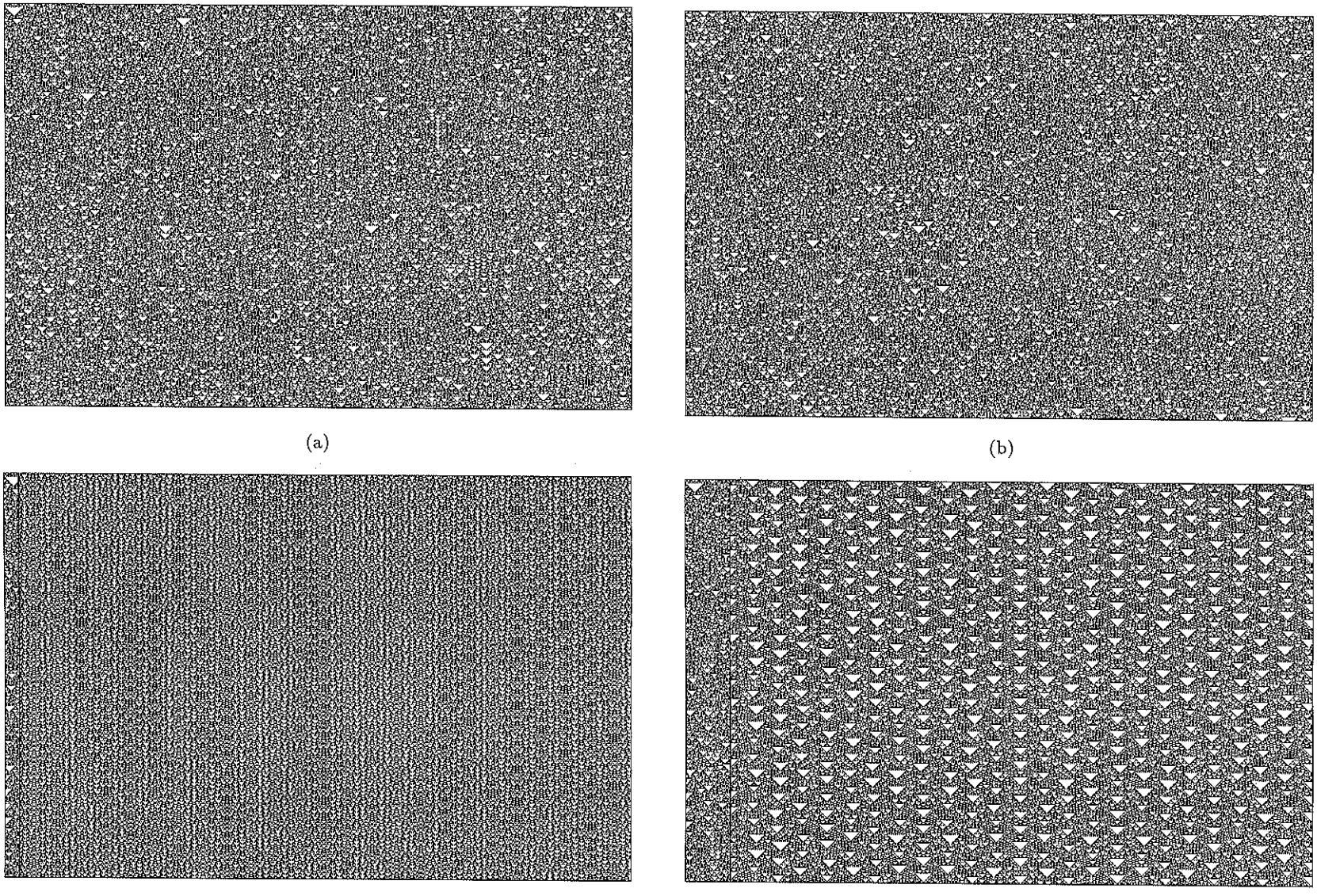

(a) (b) (c) (d)

Fig. 17. (a) a quasi-random solution for CGI-problem 1. (seedcode $\langle a_{-5} \ldots a_7 \rangle = \langle \underline{0}1001\underline{11011110} \rangle$) (b) an orbit generated from a random top row for the CA with the same rule as under (a). This orbit is not CGI invariant. (c) to (k): the shift identity patterns $SIP_{v,h}$ of the pattern under (a), for (c) $(v, h) = (0, 15)$, (d) $(v, h) = (0, 45)$, (e) $(v, h) = (45, 30)$, (f) $(v, h) = (60, 0)$, (g) $(v, h) = (30, 30)$, (h) $(v, h) = (64, 0)$, (i) $(v, h) = (30, 54)$, (j) $(v, h) = (48, 144)$, (k) $(v, h) = (77, 83)$. (l) the symmetric quasi-random solution with symmetric seedcode $\langle \underline{1}1101\underline{00010111} \rangle$. (displayed is $\{a(r, c) | 0 \leq r \leq 397, -310 + r \leq c \leq 310 + r\}$, in 1-skew coordinates).

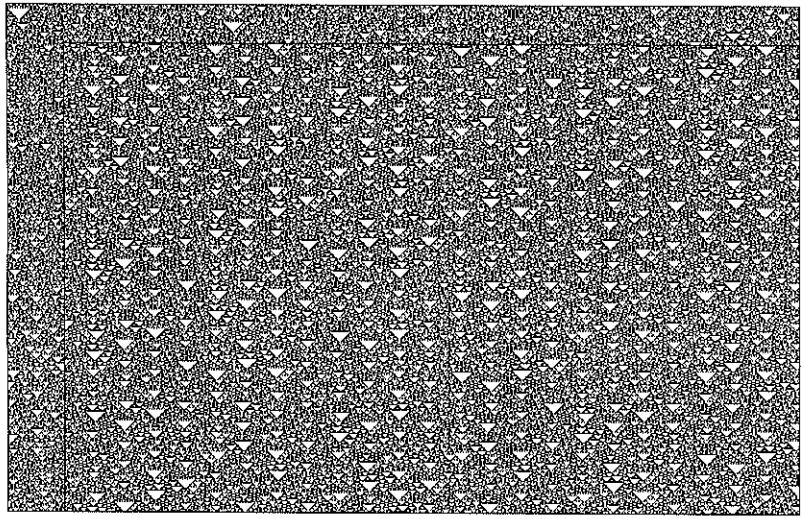

(e)

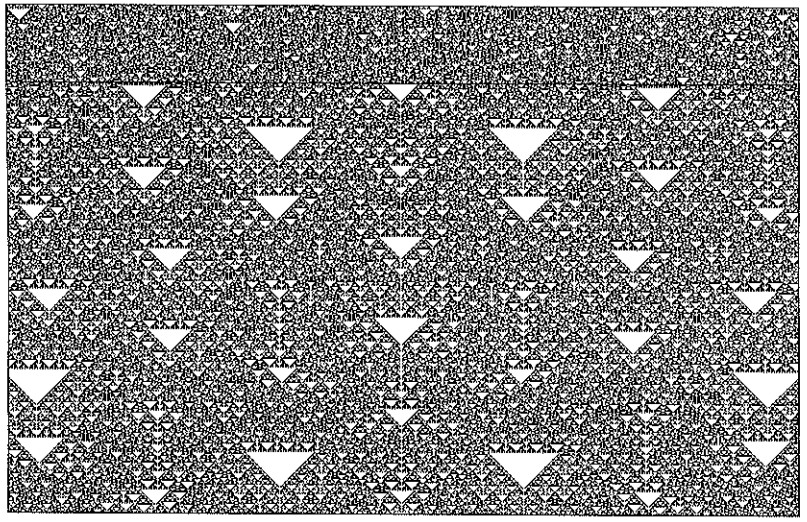

(f)

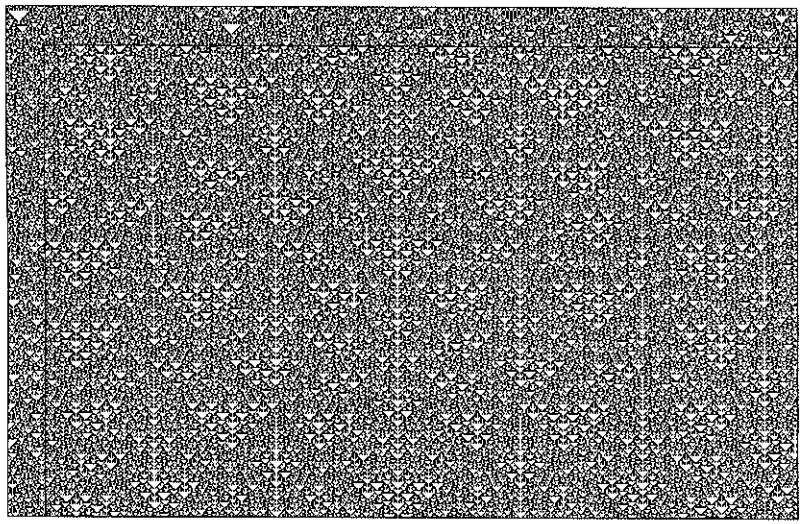

(g)

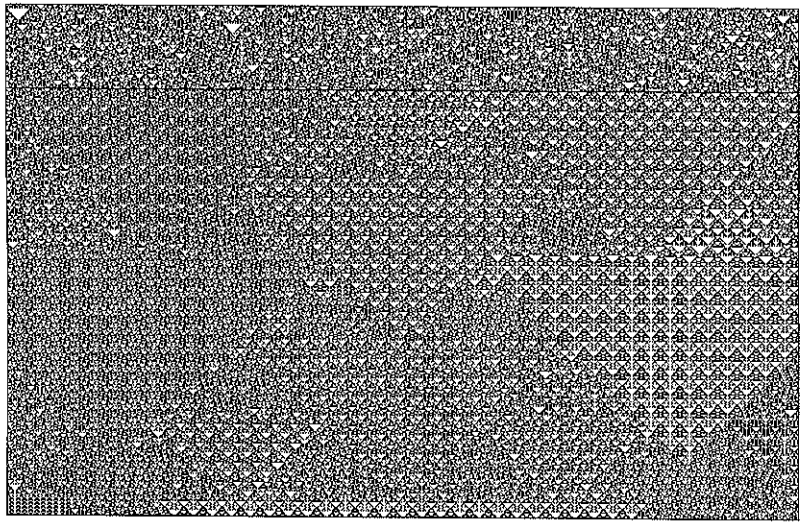

(h)

Fig. 17. (*Continued*)

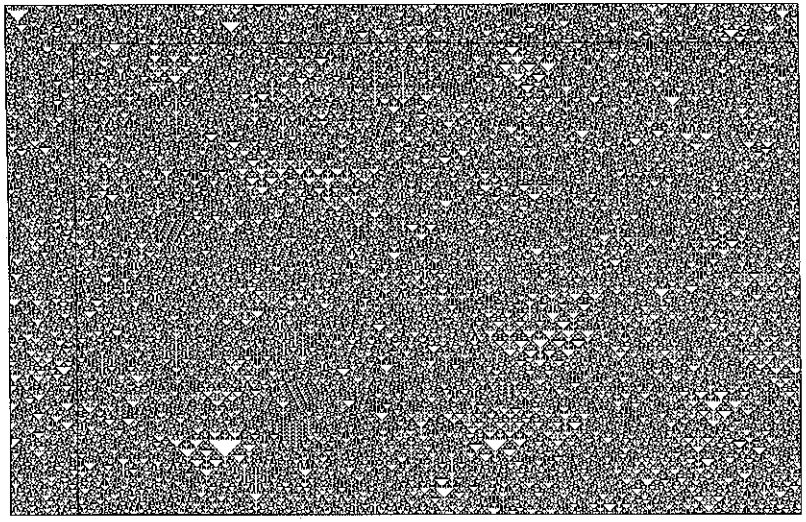

(i)

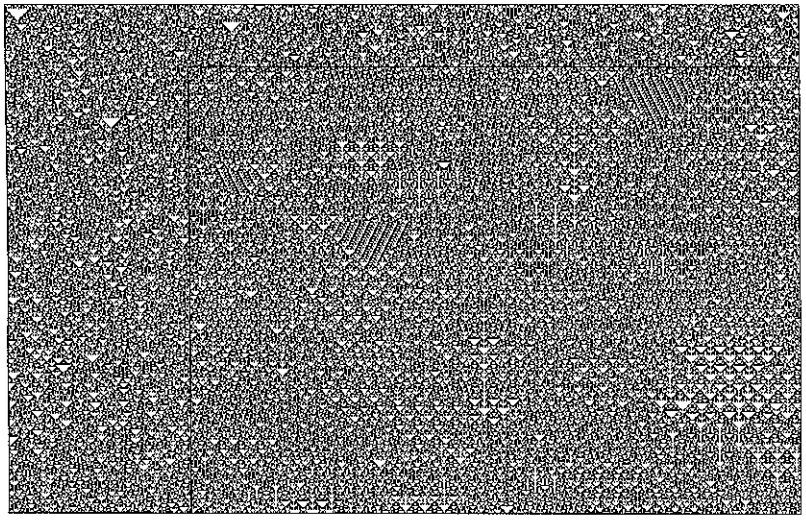

(j)

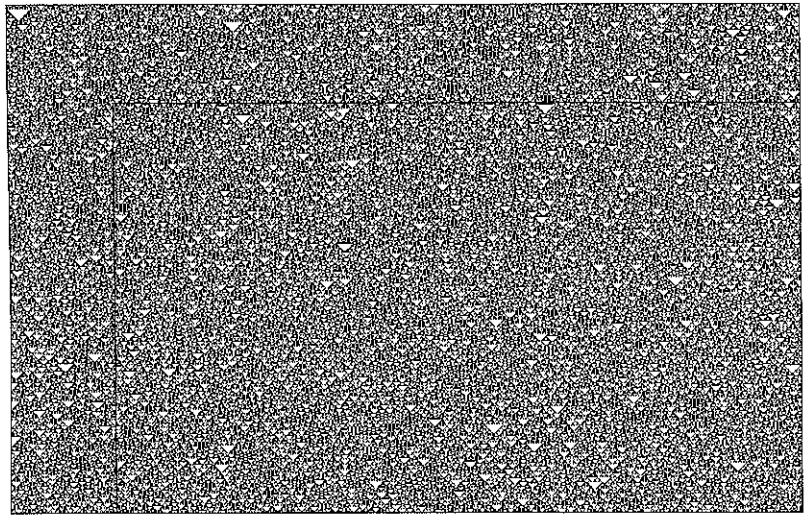

(k)

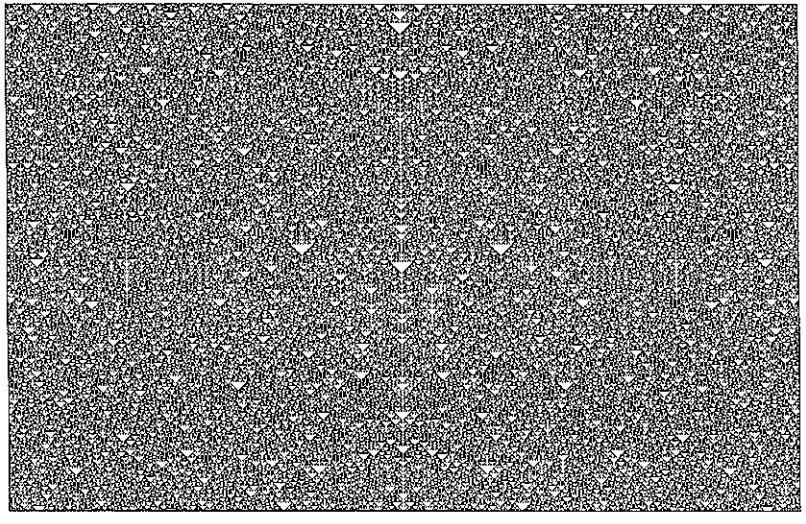

(l)

Fig. 17. (*Continued*)

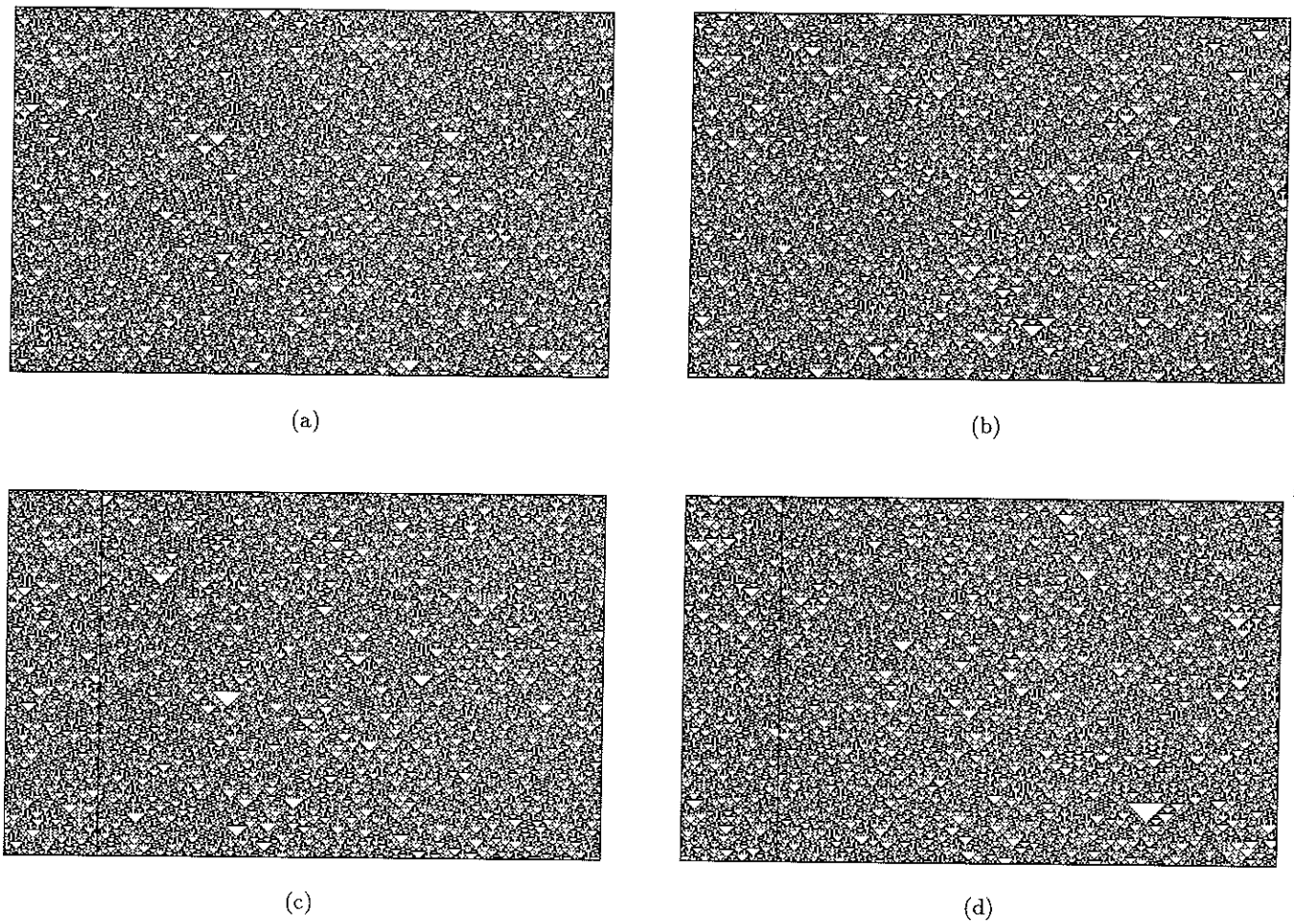

Fig. 18. (a) solution with seedcode $\langle a_{-5} \dots a_5 \rangle = \langle \underline{00000100000} \rangle$ for Problem 5. (b) an orbit with a random top row. (c) $SIP_{0,63}$ for pattern (a). (d) $SIP_{0,65}$ for pattern (b). (displayed is $\{a(r,c) | 0 \leq r \leq 245, -200 + r \leq c \leq 200 + r\}$, in 1-skew coordinates).

Category U_R: Randomlike patterns. Figure 18(a) shows solution #32 of Problem 5. *Any* of its $SIP_{v,h}$-patterns have a similar appearance: two examples for $(v,h) = (0,63)$ and $(0,65)$ are shown in Figs. 18(c) and 18(d). For comparison, Fig. 18(b) shows the orbit obtained with the same CA-rule from a random top row. The many solutions that we've been looking at for Problem 5 (which has 2048 solutions) were all of this type (and so we are tempted to conjecture that all 2047 nonzero solutions are of this type). From the results of the next section (Sec. 6), we know for sure that there are no solutions which involve periodic behavior.

The categories U_P, U_{QP}, U_S, U_{QR} and U_R were presented in order of increasing visual intricacy. However, there seems to be patterns that clearly do not belong to one of them: they have a structure which is somewhere in between U_{QP} and U_S, and will be put in an intermediate category U_C.

Category U_C: Complex patterns. These are patterns which somehow bridge the quasi-periodic patterns and the quasi-random patterns, with a possible weak visual self-similarity. Actually, Fig. 15(f) already displays such a rather weak visual self-similarity. Two additional examples are given in Fig. 19 (solution #33 of Problem 23, and solution #44 of Problem 18). The SIP's of a complex pattern are either complex too, or randomlike (the occurrence of the latter seems to be typical for this category).

The *S*-class of split patterns

These are the patterns which show different characteristics at the left- and right-sides, like in Figs. 20–21. This split is caused by a discontinuity which occurs in the initial-state sequence at (or close to) the seed which is located in the middle of the top row in the display window. It is as if the

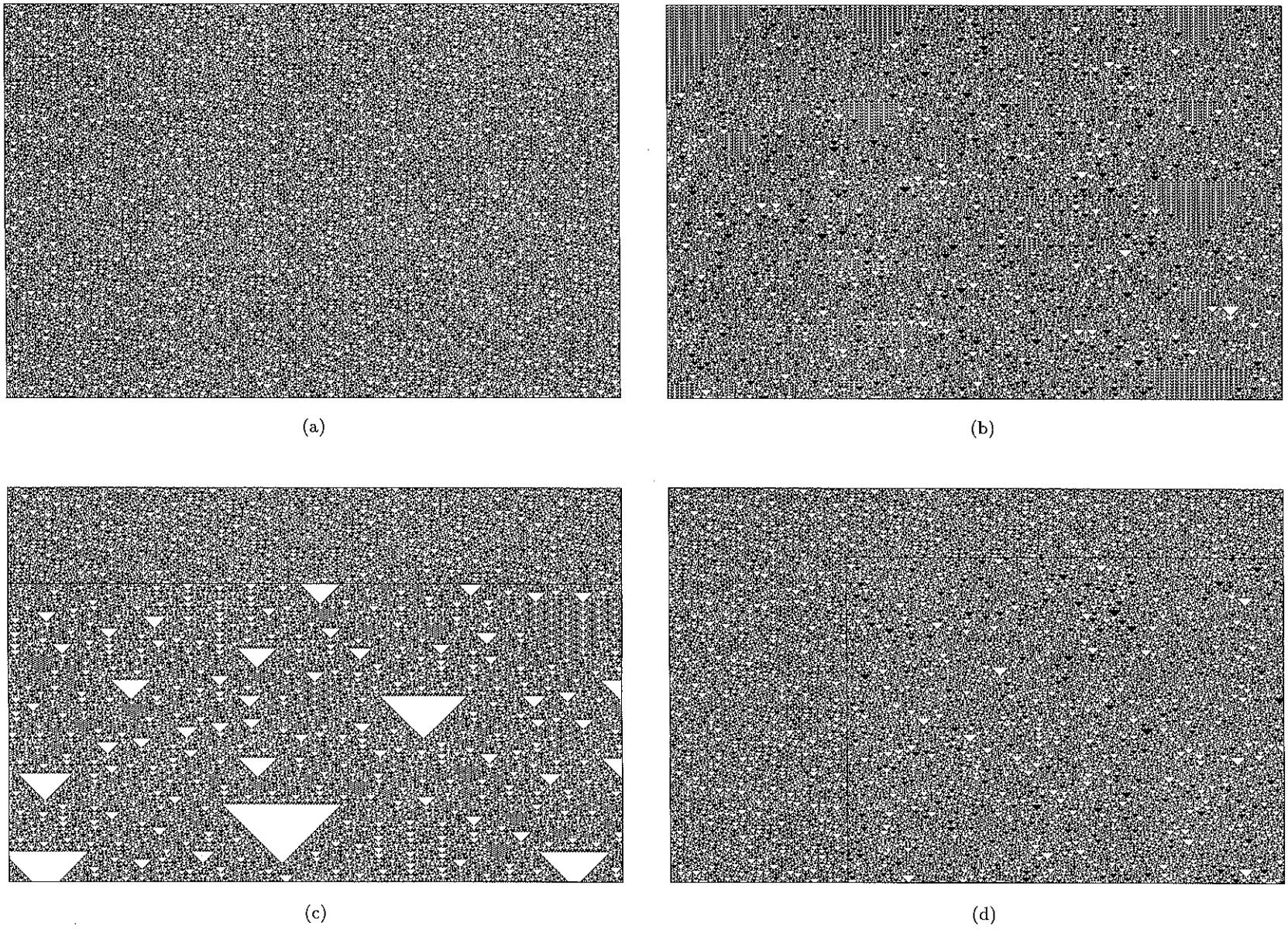

Fig. 19. Complex patterns. (a) solution #33 of Problem 23 (almost quasi-periodic), (b) solution #12 of Problem 18 (partially visually self-similar), (c) $SIP_{96,0}$ of pattern (a), (d) randomlike $SIP_{69,180}$ of pattern (a).

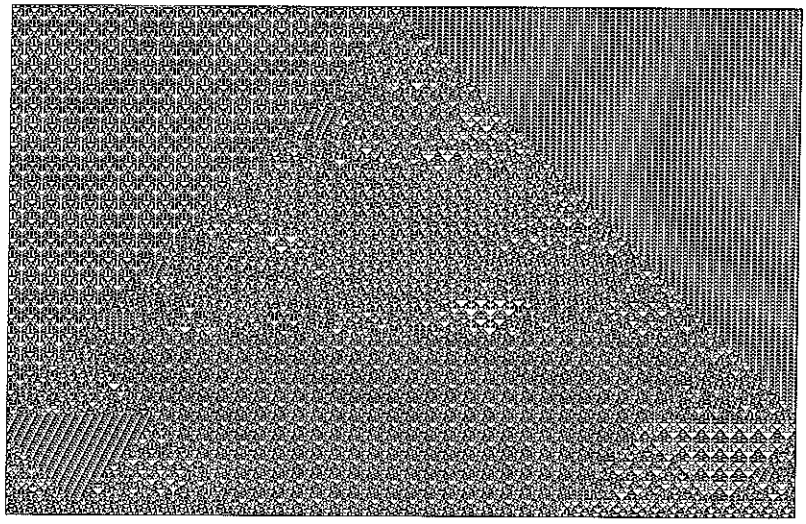

(a)

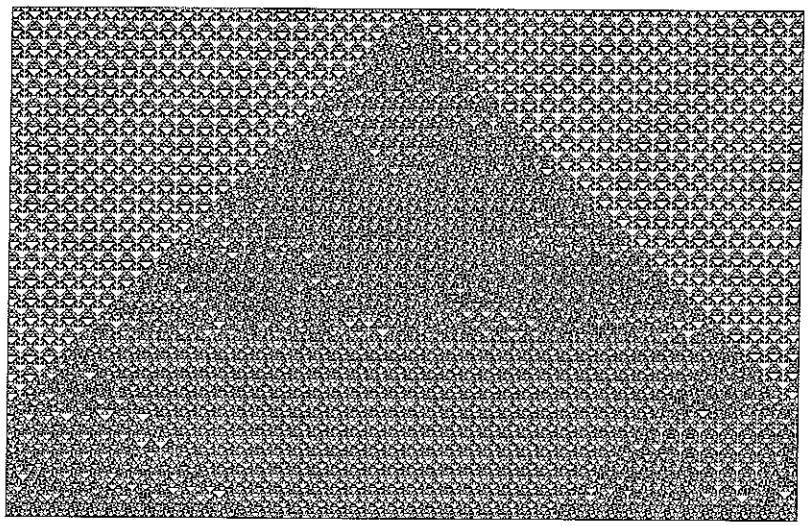

(b)

Fig. 20. Two biperiodic solutions for Problem 1. (displayed is $\{a(r, c)|0 \leq r \leq 397, -310 + r \leq c \leq 310 + r\}$, 1-skew coordinates) (a) $(15, 5)$-biperiodic solution with seedcode $\langle a_{-7} \ldots a_5 \rangle = \langle \underline{\underline{0}}011\underline{\underline{1}}10111\underline{\underline{1}}101 \rangle$. This is also a $(15, 15)$-biperiodic solution, but 5 is the *minimal* period for the right-periodic part. (b) $(15, 15)$-biperiodic solution with seedcode $\langle \underline{\underline{1}}011\underline{\underline{0}}10101\underline{\underline{1}}00 \rangle$. (double-underlined digits refer to freecells under, respectively, $(15, 5)$- and $(15, 15)$-biperiodicity conditions (Sec. 6)).

left- and right-propagating equations lock in on different types of solutions, or at least on "phase-shifted" versions of the same type of solutions). The types of solutions in both the left- and right-part may be similar to the ones appearing in the U-class. The discontinuity induces an interference pattern between the left-side and right-side solutions. Here are a few examples.

Category $S_{P,P}$: (P_l, P_r)-biperiodic patterns. Two examples are given in Fig. 20. They are the solutions #445 and #648 of Problem 1, with (left-period, right-period) $= (P_l, P_r) = (15, 5)$ and $(P_l, P_r) = (15, 15)$, respectively. Figure 9(c) already showed another example of this category. These solutions show an interference pattern originating from the seed. They are reminiscent of the

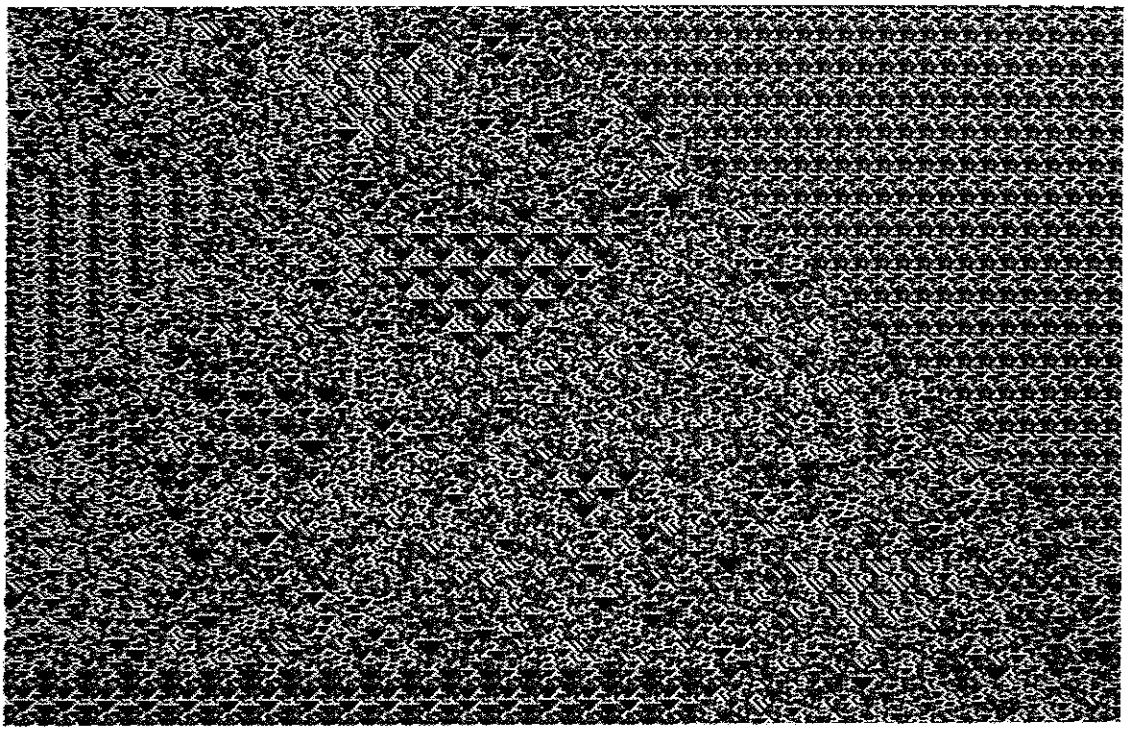

(a)

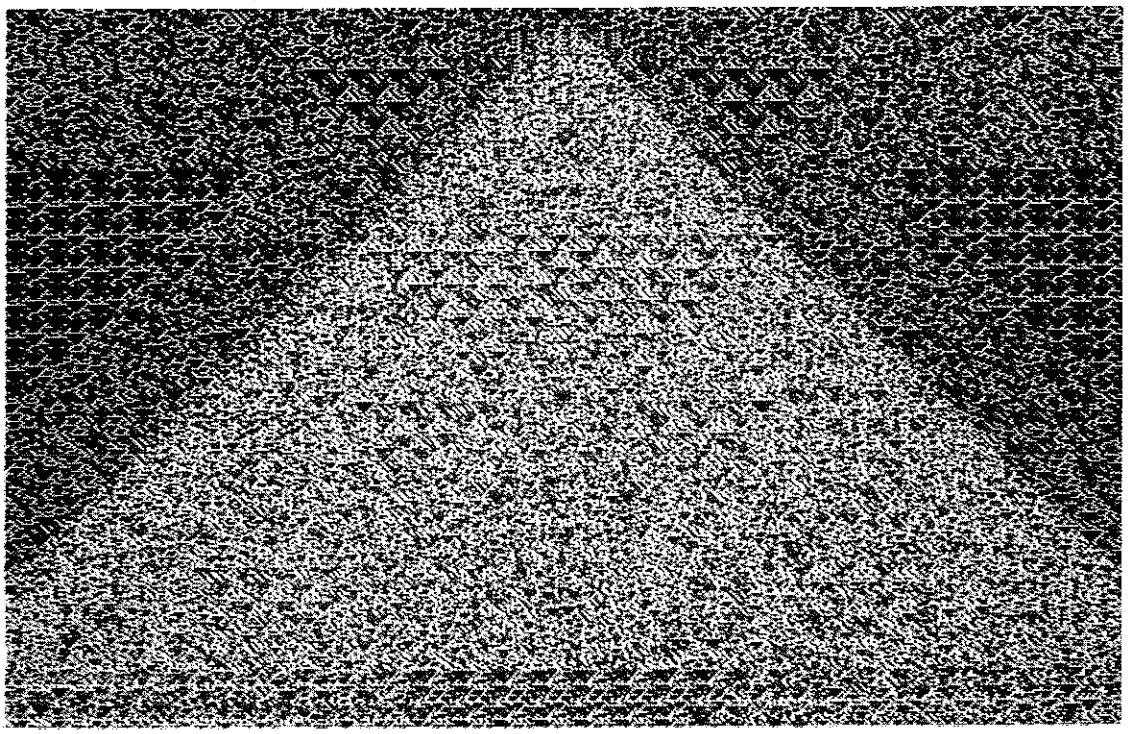

(b)

Fig. 21. (a) and (b) Solutions for Problem 4: (a) Left-self-similar, right-periodic solution with seedcode $\langle a_{-8} \ldots a_9 \rangle = \langle \underline{0}212220222121\underline{22202} \rangle$. (b) Bi-self-similar solution with seedcode $\langle \underline{2}20202020202\underline{0}20\underline{200} \rangle$. (c), (d) Solutions for Problem 19: (c) Bi-complex solution with seedcode $\langle \underline{1}20\underline{2}0\underline{00} \rangle$; (d) Bi-complex solution with seedcode $\langle \underline{20}2\underline{2}0\underline{11} \rangle$. (displayed is $\{a(r, c) | 0 \leq r \leq 350, -280 + r \leq c \leq 280 + r\}$ in 1-skew coordinates).

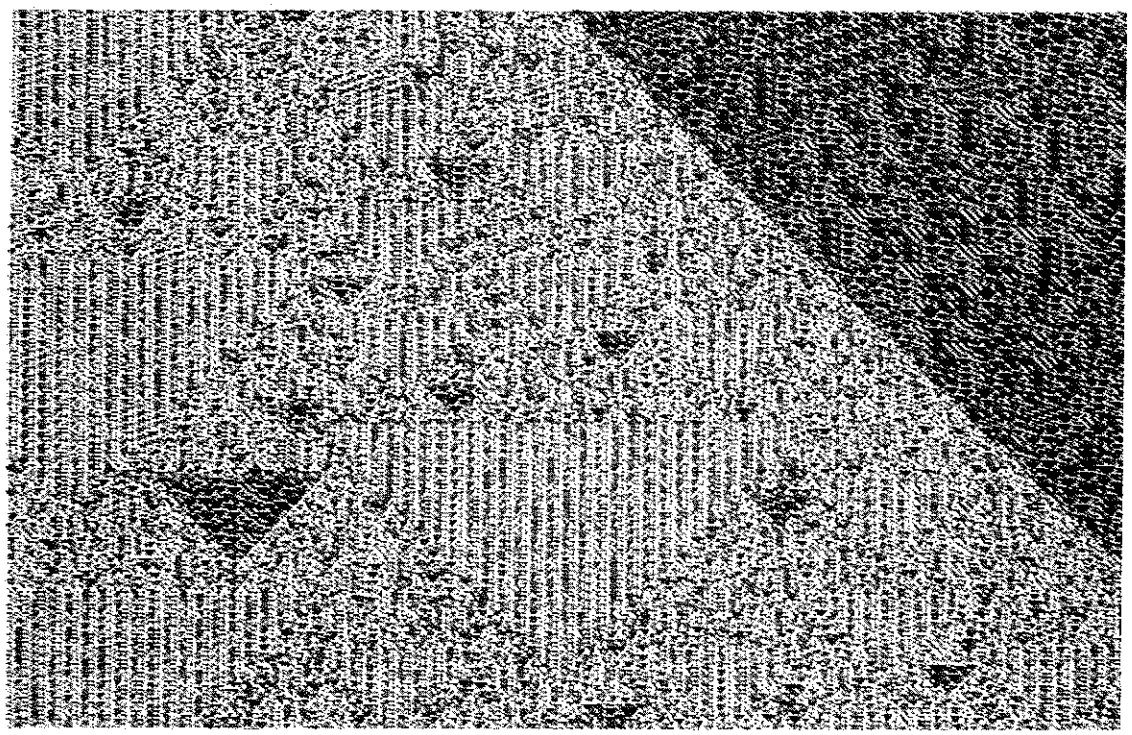

(c)

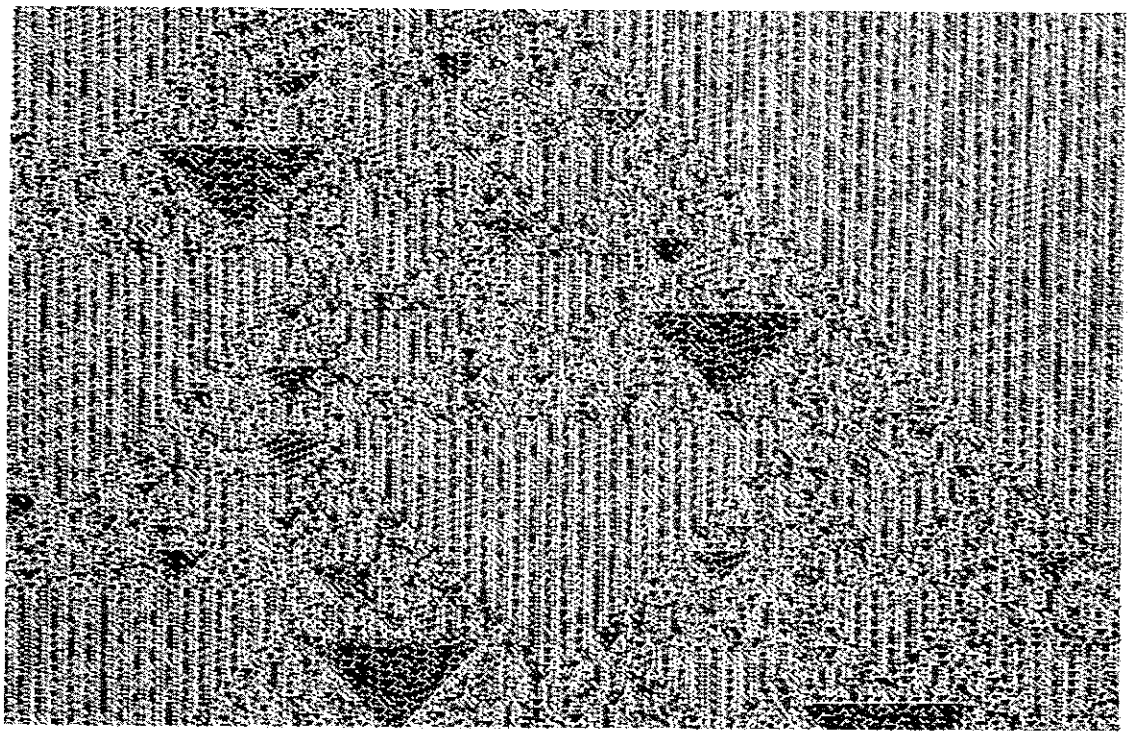

(d)

Fig. 21. (*Continued*)

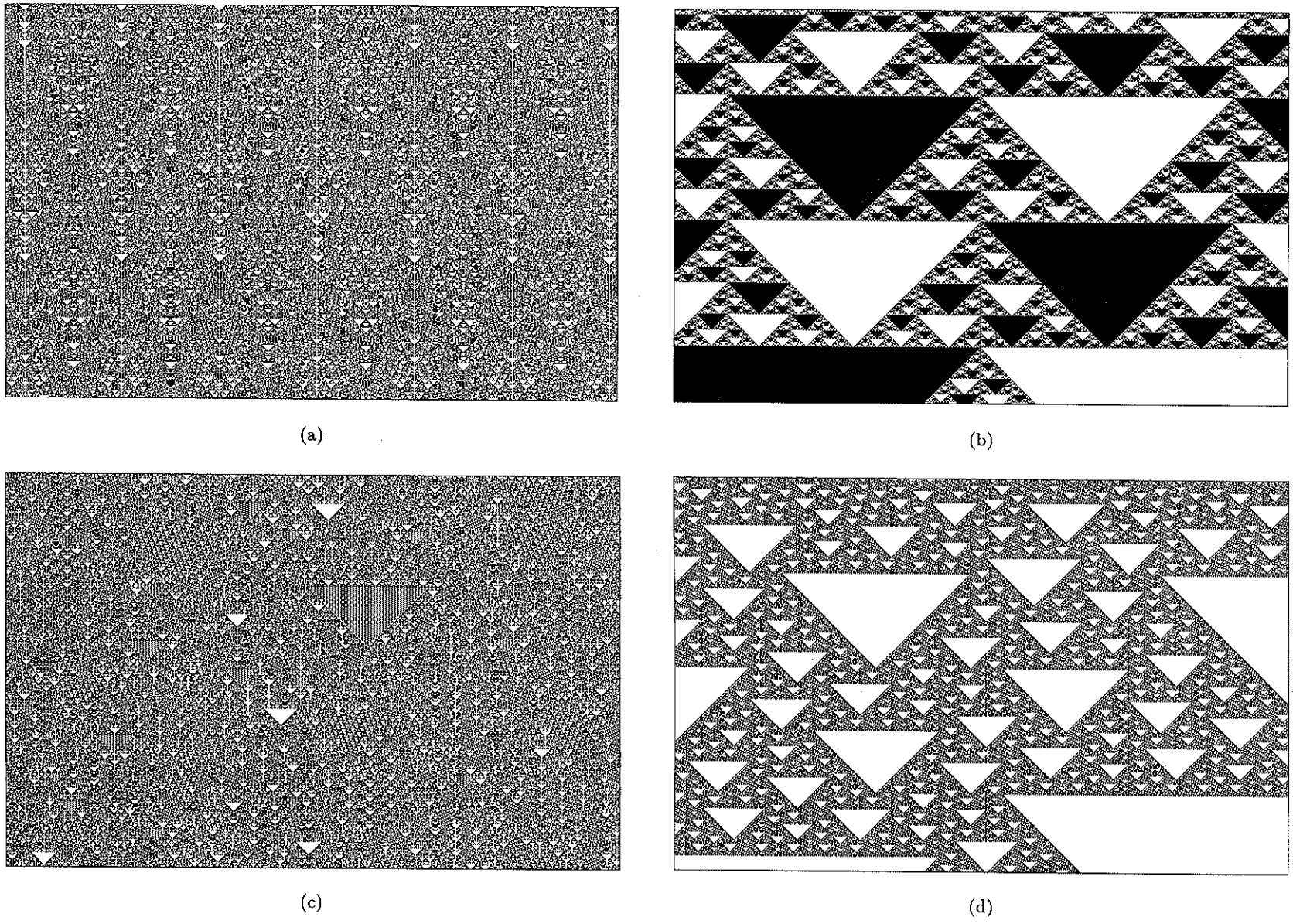

Fig. 22. An additional set of CGI-solutions (a) periodic solution #125 of Problem 8 (period=99), (b) self-similar solution #1 of Problem 10, (c) complex solution #77 of Problem 9, d) self-similar solution #55 of Problem 11, (e) quasi-random (complex ?) solution #6 of Problem 13; (f) $SIP_{28,0}$ of pattern (e), (g) solution with seedcode $(111000)^{10}$ of Problem 12, (h) solution with seedcode $(11000)^{12}$ of Problem 12. [(a), (b), (c), (d): 1-skew coordinates; (e), (f): 2-skew coordinates; (g), (h): 3-skew coordinates].

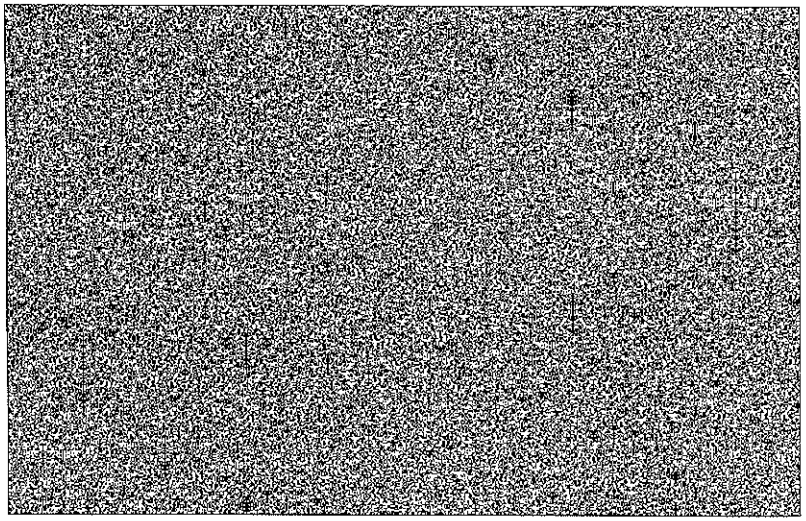

(e)

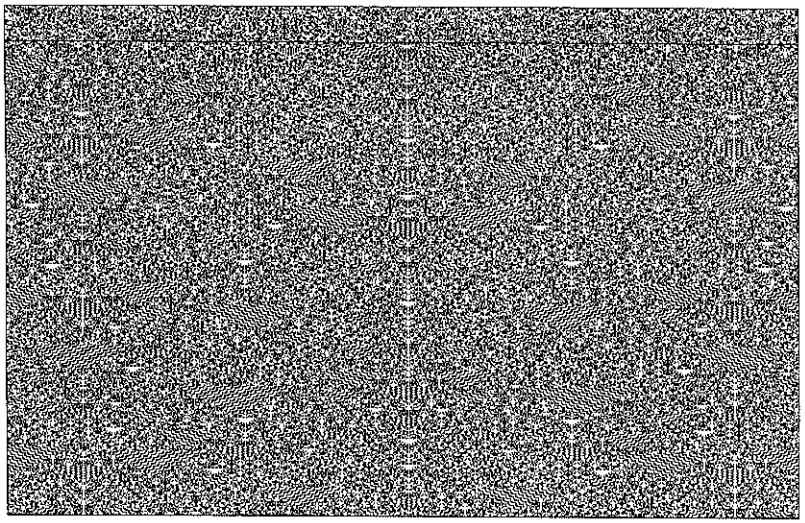

(f)

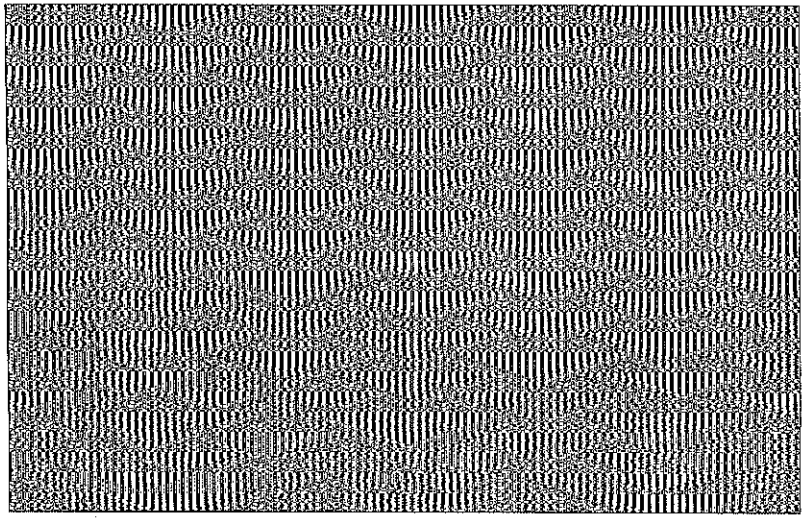

(g)

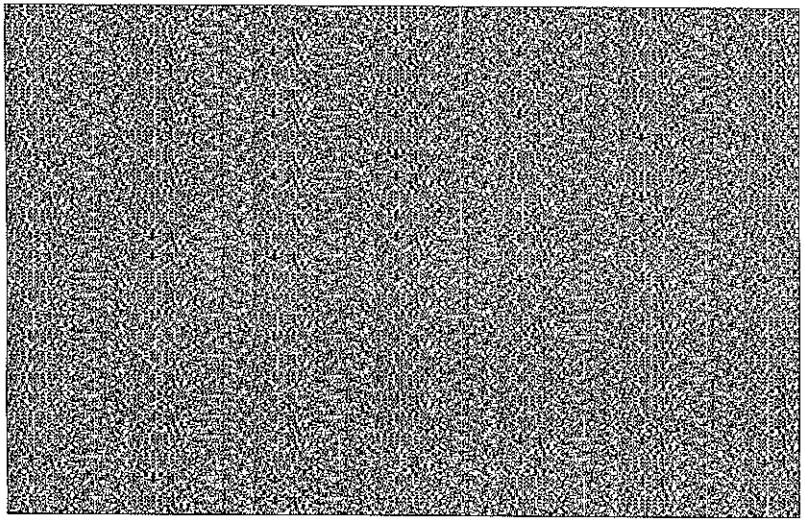

(h)

Fig. 22. (*Continued*)

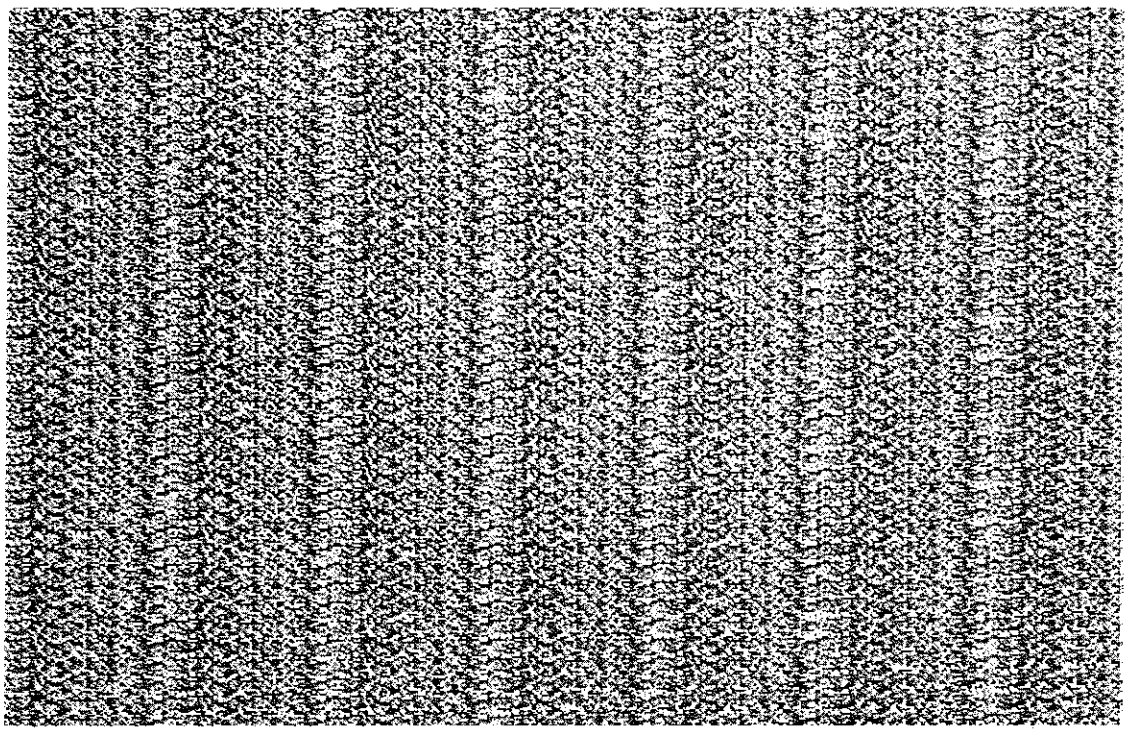

(a)

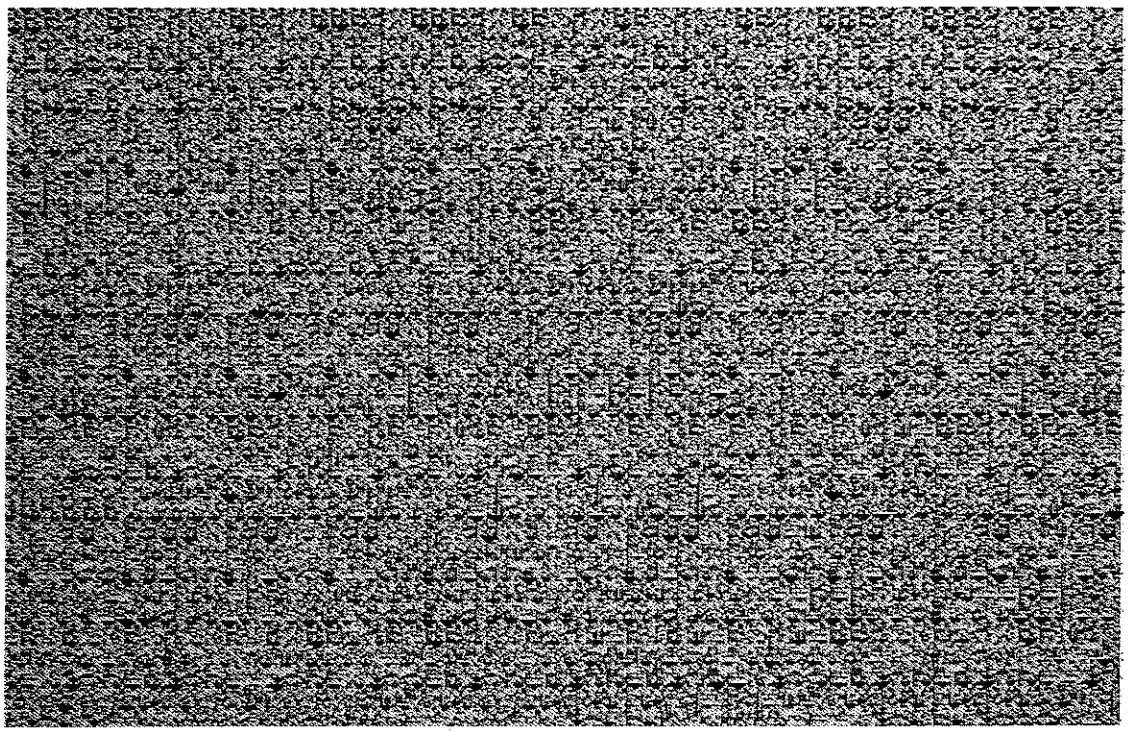

(b)

Fig. 23. An additional set of CGI-solutions for automata with more than 2 states. (a) quasi-periodic solution with seedcode $\langle 102^2 1^2 20^2 102101^2 02^3 01^2 0^3 2^2 1^3 0\rangle$ of Problem 14 ($p^n = 3^2$). (b) quasi-periodic solution #779 of Problem 15 ($p^n = 5^1$). (c) biperiodic solution #226580692 of Problem 16 ($p^n = 5^1$). (d) periodic solution with seedcode $\langle 10510^3 403460^2 1202045040^7 3412\rangle$ of Problem 17 ($p^n = 7^1$). (e) solution #55 of Problem 19 ($p^n = 3^1$, L-self-similar- R-periodic). (f) complex solution #12 of Problem 20 ($p^n = 3^1$). (g) solution #123 of Problem 21 ($p^n = 5^1$, self-similar first kind). (h) solution with seedcode $\langle 1^6 2^4 1^5 2\rangle$ of Problem 22 ($p^n = 5^1$, self-similar first kind).

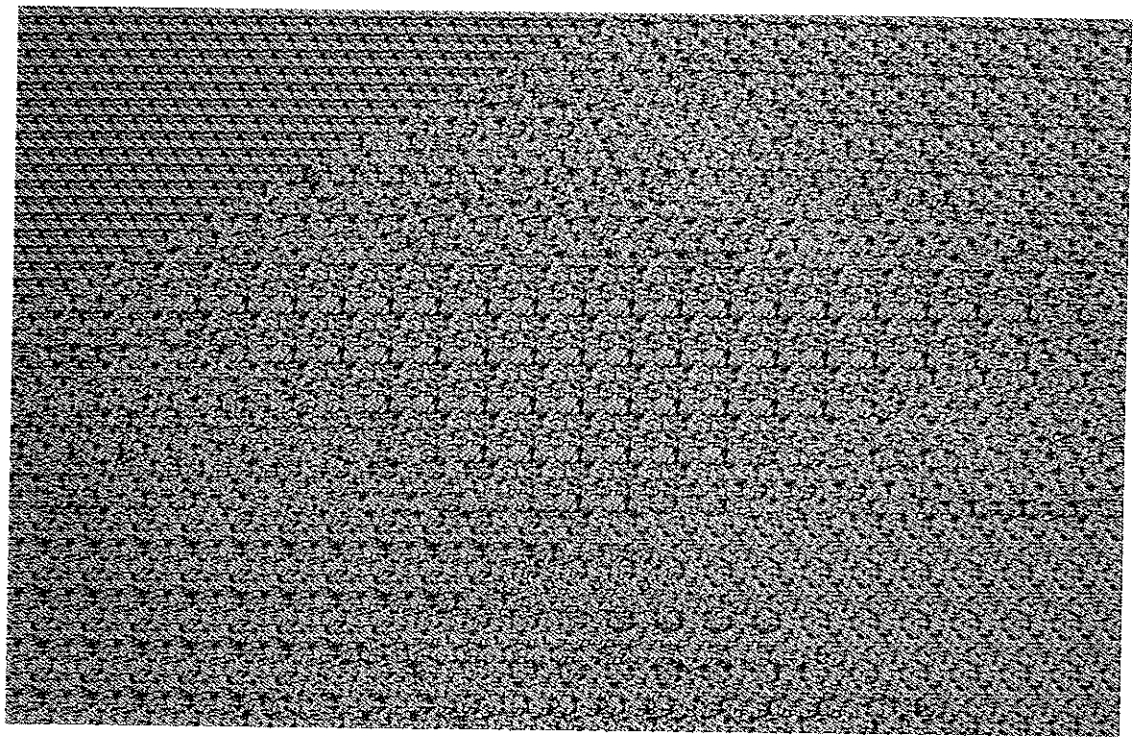

(c)

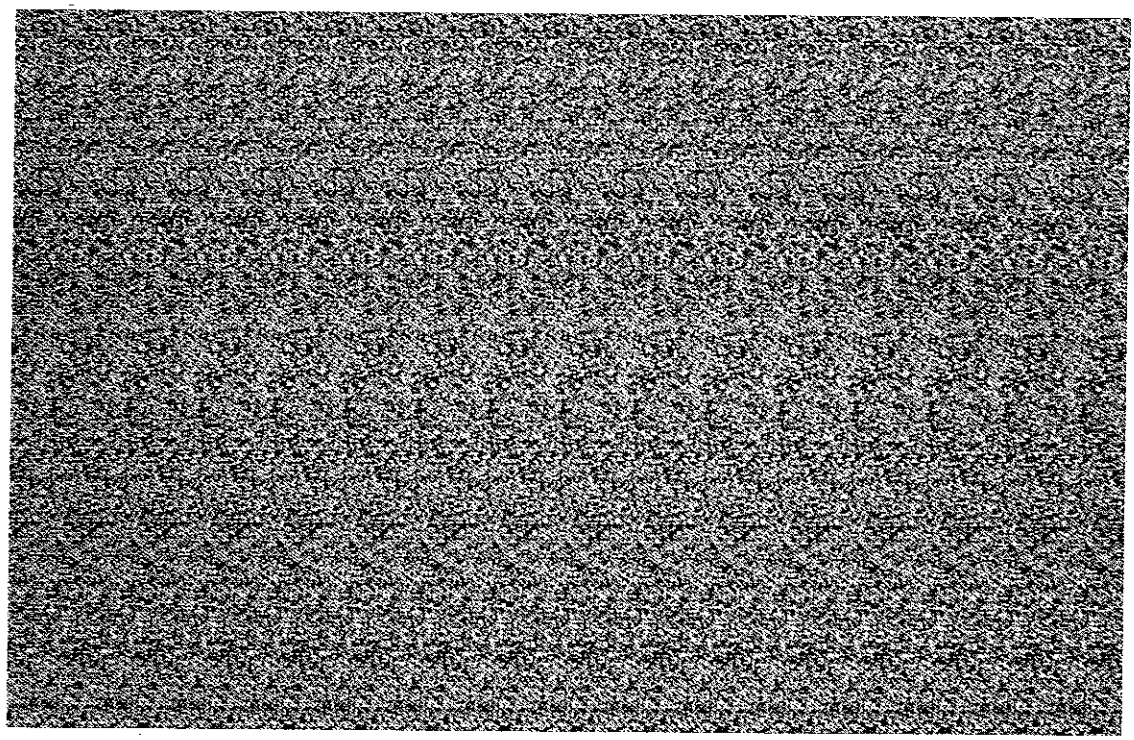

(d)

Fig. 23. (*Continued*)

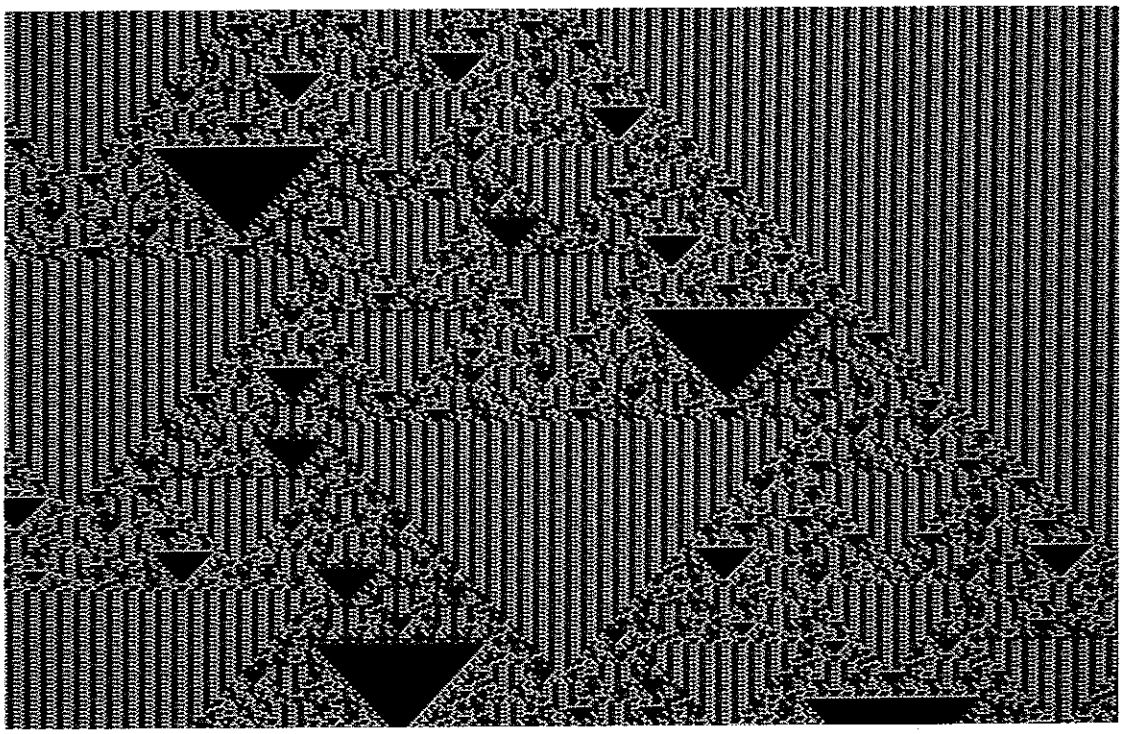

(e)

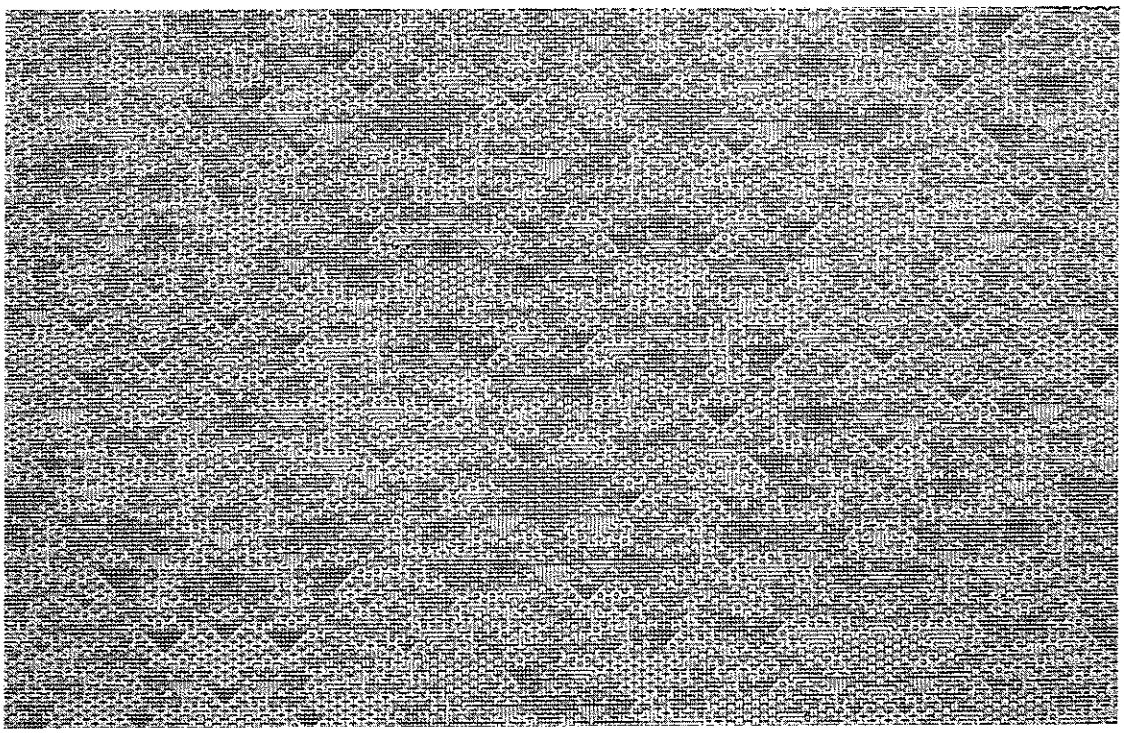

(f)

Fig. 23. (*Continued*)

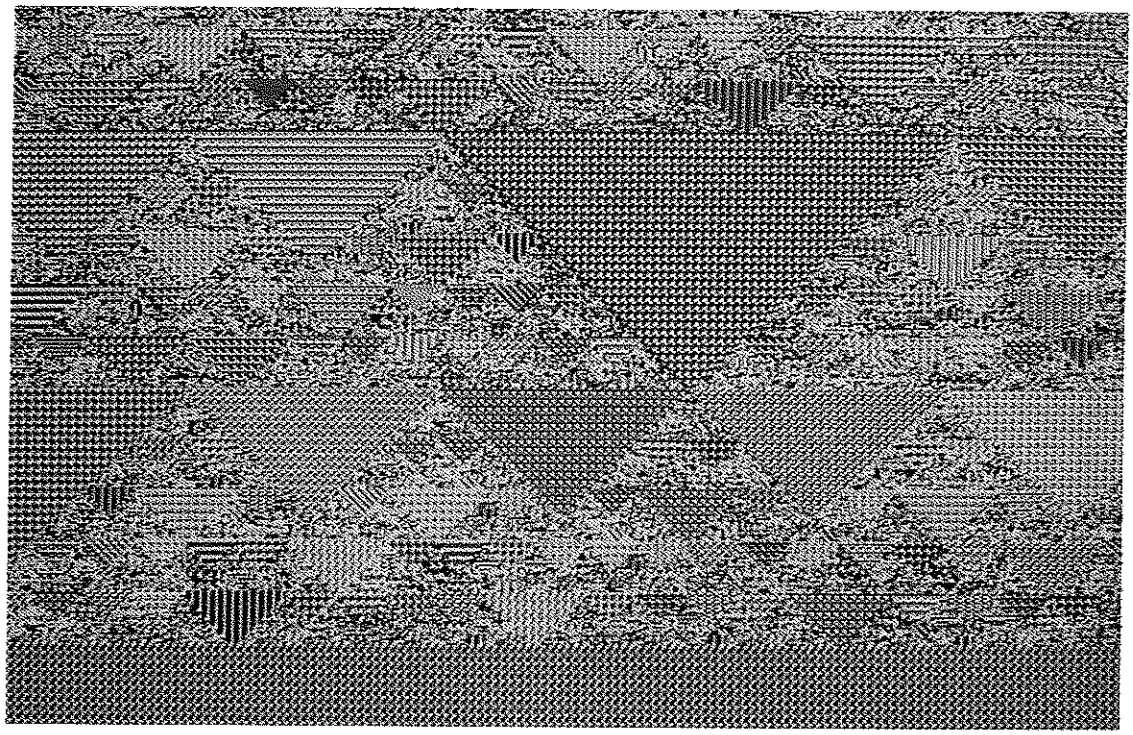

(g)

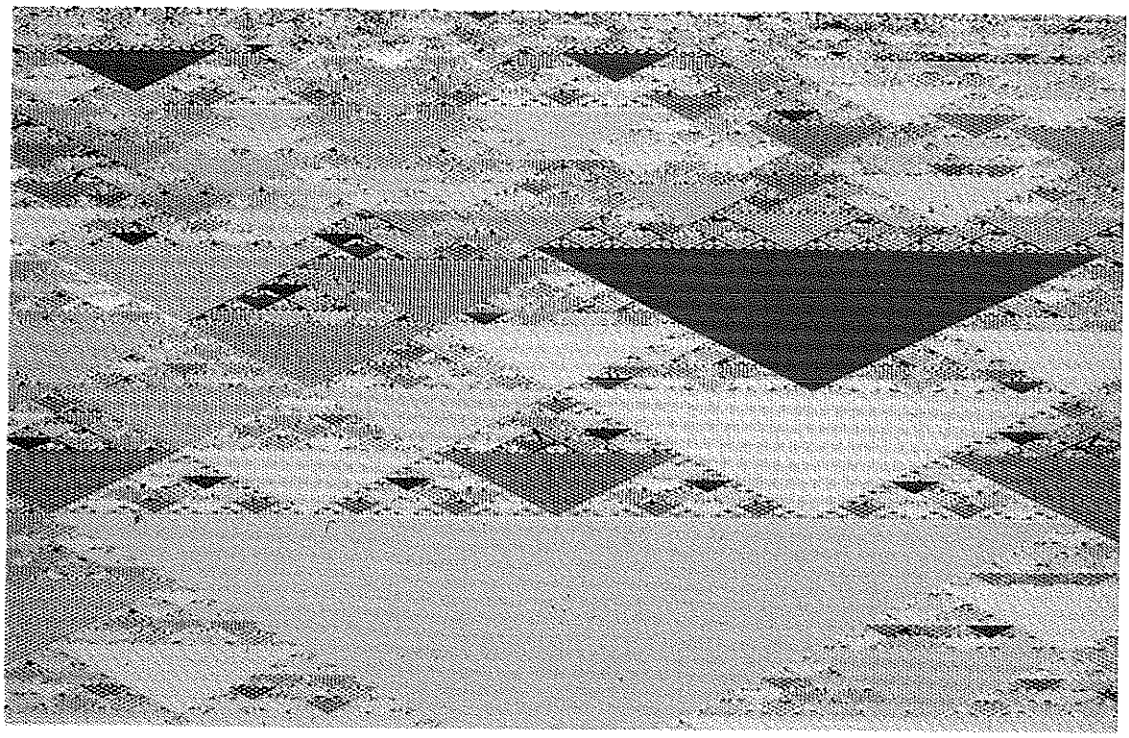

(h)

Fig. 23. (*Continued*)

kind of periodic patterns which appeared in [Barbé, 1988] (in connection with the CA-rule $R(x) = 1+x$; periodicity was enforced there as such).

Category $S_{P,S}$: Periodic-self-similar complex patterns. Figure 21(a) shows solution #236 of Problem 4. For obvious reasons, it is called left-self-similar, right-periodic (from the $3^6 = 729$ solutions of this problem, there are 81 full-periodic solutions whose periods are divisors of 20. 162 solutions are left-self-similar, right-periodic; as many are left-periodic, right-self-similar).

Category $S_{S,S}$: Bi-self-similar patterns. Figure 21(b) shows solution #345 of Problem 4. The middle triangular section clearly shows the interference between two different left- and right-self-similar patterns.

Category $S_{C,C}$: Bi-complex patterns. Examples are given in Figs. 21(c) and 21(d) (solution #45 and #76 of problem 19). Both figures are also weakly visually self-similar.

Category $S_{QR,QR}$: Bi-quasi-random patterns. An example is found in Fig. 17(l), where a *left–right symmetry* appears (actually, all left–right symmetric seed configurations for this problem produce symmetric patterns).

The previous examples dealt exclusively with cases where the tile configuration matrix $\Gamma = [0]$, and mostly with binary patterns. Figure 22 shows an additional selection of binary patterns, including some cases for which $\Gamma \neq [0]$. Figure 22(e) has a complexity which is very close to quasi-randomness: if one looks carefully, a few small local structures can be detected that are left-right symmetric. Although this pattern is not globally left-right symmetric, some SIP's are [as illustrated in Fig. 22(f)]. Figure 22(g) seems to be quasi-periodic at first sight, but when the display size is sufficiently increased, it can be seen that this pattern is actually visually self-similar (second kind). It is an example where categorization on a visual basis starts to become difficult because of a too restricted display size: what we observe is just local behavior. Here this is a consequence of the relatively large coarse-graining size (2^4) and large CA-rule degree (6). Figure 23 shows a selection of CGI-solutions for $\mathbb{Z}_p$-automata with $p > 2$. An idea of how the problem parameters may affect the number and type of CGI-solutions is given in the Problem-table from the Appendix. It would be nice to be able to derive all the solution-characteristics from the problem parameters. We are already able to do so for the number of solutions (this follows from the number of freecells in the seeds). In the next section, we will succeed in determining all solutions that have some periodic feature.

6. Periodic Solutions

In the previous section, we have seen that in many cases, some of the solutions are full-periodic, half-periodic to the left or to the right, or biperiodic. In this section, we will derive conditions for possible periodicity, and we will show also how the seedcodes which correspond to these periodic solutions can be obtained.

Definition 6.1. $S_0 = \langle a(k)\rangle_{k\in\mathbb{Z}}$ is a CGI-initial state sequence with minimal period P, when P is the minimal (positive) integer for which

$$a(m + cP) = a(m) \text{ for all } m,\ c \in \mathbb{Z}\,. \tag{63}$$

The corresponding orbit pattern will also be said to have period P or to be P-periodic.

6.1. *The search for possible periods*

The main result of this section is given by Theorem 6.1, which provides a necessary condition for P to be a possible period of a CGI-solution. We will proceed towards it through a series of Lemmas.

With

$$q_m \triangleq \frac{m-\sigma-\Phi_r}{p^n} + \alpha_\sigma \overset{(51)}{=} \left\lfloor \frac{m-\Phi_r}{p^n} \right\rfloor + \alpha_{(m-\Phi_r) \bmod p^n}\,, \tag{64}$$

the CGI-equations in their right-propagating form [Eq. (49)] can be rewritten as

$$\forall m \in \mathbb{Z}: \quad a(m) = c_r(0)a(q_m) + c_r(1)a(m-1)\ldots + c_r(\Delta)a(m-\Delta)\,. \tag{65}$$

Recall the relationship between σ and m [Eq. (51)], which we rewrite here as

$$\sigma_m = (m - \Phi_r) \bmod p^n\,. \tag{66}$$

Lemma 6.1.

$$\forall m,\ s \in \mathbb{Z} : q_{m+sp^n} = q_m + s\,. \tag{67}$$

Proof. This is a straightforward consequence of Eq. (64). ■

Corollary 6.1. $\forall m_0 \in \mathbb{Z} : \{q_{m_0+sp^n} | s \in \mathbb{Z}\} = \mathbb{Z}$ *and* $\{q_m | m \in \mathbb{Z}\} = \mathbb{Z}$.

Lemma 6.2. *For all* $m \in \mathbb{Z}$:

(a) $q_{m+1} - q_m$
$= \alpha_{\sigma_m+1} - \alpha_{\sigma_m}$ *when* $\sigma_m \in \{0, 1, \ldots p^n - 2\}$,

(b) $q_{m+1} - q_m = \alpha_p - \alpha_{p^n-1} + 1$
when $\sigma_m = p^n - 1$. (68)

Proof. Observe from Eq. (66) that when $\sigma_m \in \{0, 1, \ldots, p^n - 2\}$:

$$\sigma_{m+1} = \sigma_m + 1 \text{ and } \left\lfloor \frac{m+1-\Phi_r}{p^n} \right\rfloor = \left\lfloor \frac{m-\Phi_r}{p^n} \right\rfloor ;$$

when $\sigma_m = p^n - 1$:

$$\sigma_{m+1} = 0 \text{ and } \left\lfloor \frac{m+1-\Phi_r}{p^n} \right\rfloor = \left\lfloor \frac{m-\Phi_r}{p^n} \right\rfloor + 1\,.$$

Obtain Eqs. (68) by applying this to

$$q_{m+1} - q_m \overset{(64)}{=} \left\lfloor \frac{m+1-\Phi_r}{p^n} \right\rfloor - \left\lfloor \frac{m-\Phi_r}{p^n} \right\rfloor + \alpha_{\sigma_{m+1}} - \alpha_{\sigma_m}\,. \quad ■$$

Lemma 6.3. *Suppose that a CGI-problem has a solution with minimal period* P, *then*

(a) $\forall m \in \mathbb{Z} : a(q_m) = a(q_m + P)$
(b) *moreover, when* $\forall m \in \mathbb{Z} : a(q_m) = a(q_{m+\gamma})$ *for some* $\gamma \in \mathbb{N}$, *then* P *divides* γ.

Proof

(a) follows from the periodicity condition Eq. (63) and from the $\mathbb{Z}_p$-equation
$a(m+P) - a(m) \overset{(65)}{=} c_r(0)[a(q_{m+P}) - a(q_m)] + \sum_{i=1}^{\Delta} c_r(i)[a(m+P-i) - a(m-i)]$, (with $c_r(0) \neq 0$).

(b) from the premises, it follows that
$\forall m,\ k,\ s,\ l \in \mathbb{Z} : a(q_m) = a(q_{m+k\gamma})$
$= a(q_{m+sp^n\gamma}) \overset{(67)}{=} a(q_m + s\gamma) \overset{(63)}{=} a(q_m + lP)$.
As $\{q_m | m \in \mathbb{Z}\} = \mathbb{Z}$ (Corollary 6.1), this is equivalent with the condition

$$\forall m,\ s,\ l \in \mathbb{Z} : a(m + s\gamma) = a(m + lP)\,.$$

This means that the sequence $\langle a(m)\rangle_{m\in\mathbb{Z}}$ has two periods: γ and P. As P is by definition the minimal period, P must divide γ. ■

Lemma 6.4. *A necessary condition for* P *to be a possible minimal period of a CGI-problem is that*

$$\forall m \in \mathbb{Z} : P \text{ divides } (q_{m+1} - q_m)p^n - 1\,. \tag{69}$$

Proof. Equation (66) shows that

$$\forall m \in \mathbb{Z} : q_{m+(q_{m+1}-q_m)p^n} = q_{m+1}$$

and as a consequence

$$\forall m \in \mathbb{Z} : a(q_{m+(q_{m+1}-q_m)p^n}) = a(q_{m+1})\,. \tag{70}$$

Applying Lemma 6.3 (b) to this produces condition Eq. (69). ■

Corollary 6.2. *The period of a possible periodic solution of a* $[\mathcal{T}_{p^n,\Xi}, W, \alpha, R]$*-CGI problem cannot be a multiple of* p.

Proof. Suppose $P = kp$ (for some $k \in \mathbb{N}$) is a possible period. Then kp must divide expressions of the form $zp^n - 1$ (for some $z \in \mathbb{Z}$), and so p must divide $zp^n - 1$. As p divides zp^n, it must also divide 1, which it does not; and so there is contradiction. ■

Corollary 6.3. *When* P *is a period for a CGI-solution, then*

$$\forall m \in \mathbb{Z} :\ q_{m+P} = q_m + j_m P \text{ for some } j_m \in \mathbb{Z}\,. \tag{71}$$

Proof. From Lemma 6.4, it follows that $\forall m \in \mathbb{Z}$:

$$P \text{ divides } \sum_{i=1}^{P}[(q_{m+i} - q_{m+i-1})p^n - 1] = (q_{m+P} - q_m)p^n - P\,,$$

or P divides $(q_{m+P} - q_m)p^n$. As $\gcd(p^n, P) = 1$ (consequence of Corollary 6.2), this means that P divides $q_{m+P} - q_m$, yielding Eq. (71). ■

Theorem 6.1. *A necessary condition for* P*-periodicity of a* $[\mathcal{T}_{p^n,\Xi}, W, \alpha, R]$*-CGI solution is that*

$\forall \sigma \in \{0, 1, \ldots, p^n - 2\}$:

$$P \text{ divides } (\alpha_{\sigma+1} - \alpha_\sigma)p^n - 1\,. \tag{72}$$

Proof

(a) First apply Eq. (68a) to the condition of Lemma 6.4 [Eq. (69)] in order to find that for all m such that $\sigma_m \in \{0, 1, \ldots, p^n - 2\}$ the proposition "P divides $(q_{m+1} - q_m)p^n - 1$" in Lemma 6.4 is equivalent to "P divides $(\alpha_{\sigma_m+1} - \alpha_{\sigma_m})p^n - 1$".

(b) Then observe that Eq. (72) also implies that P divides $[-\sum_{\sigma=0}^{p^n-2}(\alpha_{\sigma+1} - \alpha_\sigma)p^n - 1] = (\alpha_0 - \alpha_{p^n-1} + 1)p^n - 1 \overset{(68.b)}{=} (q_{m+1} - q_m)p^n - 1$, for all m corresponding with a $\sigma_m = p^n - 1$, and this establishes the equivalence of the proposition Eq. (72) with Eq. (69) for these m.

(c) As the m-set referred to under (a) equals $\{\Phi_r + \sigma + sp^n | s \in \mathbb{Z} \;\&\; \sigma \in \{0, 1, \ldots, p^n - 2\}\}$ and the m-set under (b) equals $\{\Phi_r + p^n - 1 + sp^n | s \in \mathbb{Z}\}$, the union of both equals $\mathbb{Z}$. So, by taking (a) and (b) together, the equivalence between Eq. (72) and Eq. (69) is fully established. ■

Remarks

- The meaning of Lemma 6.1, Corollary 6.1, Lemma 6.2 and Theorem 6.1 can be illustrated in a graph which plots q_m versus m. A particular example is given in Fig. 24, but the graph is generic. It repeats the basic pattern of p^n points $\{(z, q_z) | z = m_0, m_0 + 1, \ldots, m_0 + p^n - 1\}$, by translating it over distances (sp^n, s), $s \in \mathbb{Z}$ (corresponds to Lemma 6.1). Observe that by doing so, all (m, q_m) points are positioned along different straight lines

  (a) p^n parallel lines with slope p^{-n}: the (m, q_m) points located on each of these lines have horizontal interdistance p^n. The vertical distance between (m, q_m) and $(m + 1, q_{m+1})$ equals $(\alpha_{\sigma+1} - \alpha_\sigma), \sigma = 0, 1, \ldots, p^n - 2$ (Lemma 6.2).

  (b) p^n points (m, q_m) can be found on each horizontal line: their interdistances are $p^n(\alpha_{\sigma+1} - \alpha_\sigma) - 1$. Compatibility with P-periodicity requires that these distances are a multiple of P (which corresponds to Theorem 6.1), and that the vertical distance between two points (m, q_m) and $(m + P, q_{m+P})$ is a multiple of P (Corollary 6.3). Figure 24 also shows the functions $\min Q_{p^n}(m) \triangleq \min \{q_m, q_{m+1}, \ldots, q_{m+p^n-1}\}$ and $\max Q_{p^n}(m) \triangleq$

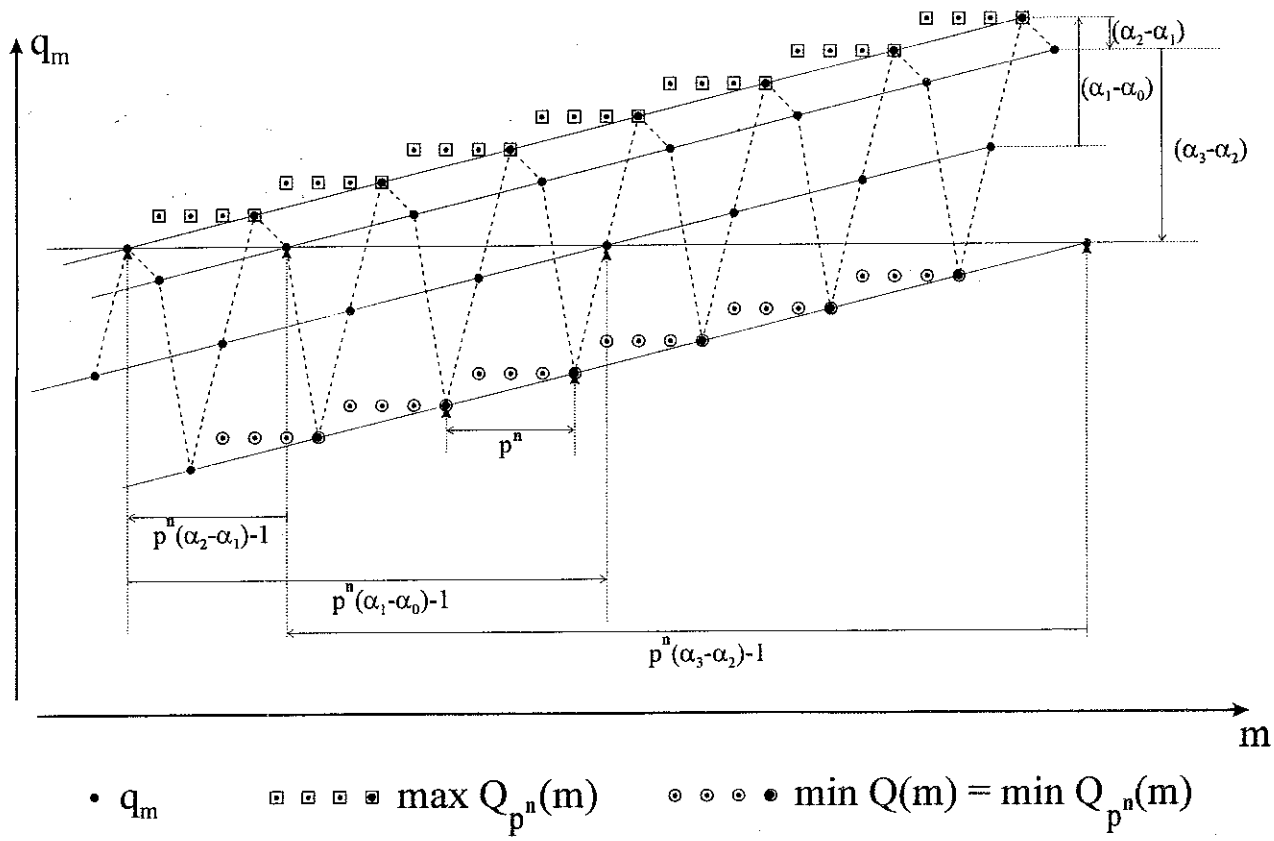

Fig. 24. The graph of q_m versus m: A generic example.

$\max\{q_m, q_{m+1}, \ldots, q_{m+p^n-1}\}$, which will be used later. Observe that these functions are discrete increasing staircase functions with step-length p^n and step-height 1.

- Theorem 6.1 provides a *necessary* condition for P to be a *possible* period of a periodic solution to the CGI-problem. It has reduced the infinite set of divisibility conditions as given by Eq. (69) to a set of (p^n-1) divisibility conditions. Observe that these conditions only involve the coarse-graining size p^n and the consecutive differences $(\alpha_{\sigma+1} - \alpha_\sigma)$ in the pattern shift-vector $\alpha = (\alpha_1, \alpha_2, \ldots, \alpha_{p^n-1})$. The other problem parameters $R(x)$, W, β do *not* enter the condition. However, the latter do determine whether a P which is a possible period will be an actual period for one of the solutions to the CGI-problem.
- The theorem was derived under the assumption of fully periodic solutions. However, it also holds for the period P of biperiodic and half-periodic solutions. Indeed, we could replay the Lemmas 6.3 and 6.4 for $m \geq M_f$ instead of $m \in \mathbb{Z}$, M_f being the leftmost point from which right P-periodicity starts (or for $m \leq L_f$ in case of left-periodicity). This would not change the condition expressed in Theorem 6.1.
- $P = 1$ is always a possible period. The trivial solution $O_R(S_0) \equiv 0$ is always a solution with $P = 1$, no matter what the particular problem-parameters are. Whether $O_R(S_0)$ with $S_0 \equiv$ *constant* is a solution, depends on the particular problem-parameters.
- The way to find all possible periods is to look for the greatest common (positive) divisor P of all $(\alpha_{\sigma+1} - \alpha_\sigma)p^n - 1$, $\sigma \in \{0, 1, \ldots, p^n - 2\}$. Then all its divisors are possible periods.

Examples

1. When $\alpha_i = \alpha_{i+1}$ for some i, then the only possible period is 1.
2. When $\alpha = (c, c+\lambda, c+2\lambda, \ldots c+(p^n-1)\lambda)$, $(c, \lambda \in \mathbb{Z})$, then the possible periods are the divisors of $\lambda p^n - 1$. For example, let $p^n = 3^2 = 9$ and $\lambda = -11$, then possible periods are the divisors of 100, i.e.: 1, 2, 3, 4, 5, 10, 20, 25, 50, 100. When $\lambda = 11$, then we have the divisors of 98, i.e.: 1, 2, 7, 14, 49, 98.
3. Let $p^n = 2^2$, and $\alpha = (1, 8, -3, 13)$. We have to look for the g.c.d of $((8-1)\cdot 2^2 - 1, (-3-8)\cdot 2^2 - 1, (13+3)\cdot 2^2 - 1) = (27, -45, 63)$. The greatest common divisor is $P_c = 9$ and so 1, 3, 9 are the *possible* periods in the solutions of any CGI-problem featuring the given (p^n, α)-parameters.

- Under the assumption that there exists a CGI-orbit with an initial state configuration with period P, this orbit can also be considered as the orbit of a $\mathbb{Z}_p$-CA of finite length P, arranged around a circle (thus enforcing periodic boundary conditions); see [Martin *et al.*, 1984]. According to Theorem 6.1, P can never be a multiple of p, and so we can apply Theorem 4.1 from the last mentioned reference, in order to find possible values for the ultimate period P_v of the resulting patterns along a column (i.e. in the vertical direction when using orthogonal display coordinates, otherwise along the skew column direction). This theorem states that P_v is a divisor of $p^{\mathrm{ord}_P(p)} - 1$ when $R(x)$ is not symmetric, and a divisor of $p^{\mathrm{sord}_P(p)} - 1$ when $R(x)$ is symmetric [$\mathrm{ord}_P(p)$ is the minimal positive integer l for which $p^l = 1 \bmod P$; $\mathrm{sord}_P(p)$ is the minimal positive integer l for which $p^l = \pm 1 \bmod P$].

6.2. *Finding the P-periodic solutions*

Recall that any solution of a CGI-problem corresponds to a good seedcode, which can be found through the procedure developed in Sec. 4. In what follows, we will present a set of sufficient conditions concerning the seedcell-states which will imply periodicity. These conditions should hold in addition to the previously obtained seed-internal equations. For this reason, these conditions will be called *additionally sufficient*. We will distinguish between conditions for right-periodicity, left-periodicity and full periodicity with a given period P (which must necessarily satisfy the conditions from Theorem 6.1). We will deal with right-periodicity conditions first.

6.2.1. *Additionally sufficient conditions for right-periodicity*

Definition 6.1.

- a solution is P-periodic to the right of $M(\in \mathbb{Z})$, when $a(k) = a(k+P)$ for $k \geq M$.
- a solution is right P-periodic, when it is P-periodic to the right of some finite M.
- a full P-periodic solution has $a(k) = a(k+P)$ for all $k \in \mathbb{Z}$.

Notation 6.1. With q_m as defined in Eq. (64), let

$$\begin{aligned} Q(m) &\triangleq \{q_m, q_{m+1}, q_{m+2}, \dots\} && \text{(a)}\\ Q_{p^n}(m) &\triangleq \{q_m,\ q_{m+1}, \dots,\ q_{m+p^n-1}\} && \text{(b)}\\ \min Q(m) &\triangleq \text{minimal element of } Q(m) && \text{(c)}\\ \min Q_{p^n}(m) &\triangleq \text{minimal element of } Q_{p^n}(m) && \text{(d)}\\ \max Q_{p^n}(m) &\triangleq \text{maximal element of } Q_{p^n}(m) && \text{(e)} \end{aligned} \tag{73}$$

The following Lemmas 6.5 to 6.7 are a prerequisite for a theorem showing that any right periodic part of a solution which is not also full-periodic, starts at some fixed location M_f.

Lemma 6.5.

$$\begin{aligned} &\text{(A)}\ \forall m \in \mathbb{Z}:\ \min Q(m) = \min Q_{p^n}(m) && \text{(a)}\\ &\quad \forall m,\ s \in \mathbb{Z}:\\ &\qquad \min Q_{p^n}(m + sp^n) = \min Q_{p^n}(m) + s && \text{(b)}\\ &\qquad \max Q_{p^n}(m + sp^n) = \max Q_{p^n}(m) + s && \text{(c)} \end{aligned} \tag{74}$$

(B) *$Q(m)$ contains all integers $k \geq \min Q_{p^n}(m)$.*

Proof

(A) (a) $Q(m) \overset{(73)}{=} \cup_{s\in\mathbb{N}} Q_{p^n}(m+sp^n) \overset{(67)}{=} \cup_{s\in\mathbb{N}}\{q_m + s, \dots, q_{m+p^n-1} + s\}$.
It is clear that $\min Q(m)$ is to be found among those elements for which $s = 0$, i.e. among $Q_{p^n}(m)$.
(b), (c): This was already illustrated in Fig. 24, and it is a straightforward consequence of the definitions and of Eq. (67).

(B) From (A). (a), we know that $\min Q(m) = \min Q_{p^n}(m) = q_{m+j}$ for some $j \in \mathcal{Z}_{p^n}$. Now $Q(m)$ contains $q_{m+j+sp^n} \overset{(67)}{=} q_{m+j} + s = \min Q_{p^n}(m) + s$, for all $s \in \mathbb{N}$. ■

Lemma 6.6. *When*

$$a(q_k) = a(q_{k+P}) \text{ for all } k \geq M\,, \tag{75}$$

then $a(m) = a(m+P)$ for all $m \geq \min Q(M) \overset{(74)}{=} \min Q_{p^n}(M)$.

Proof. Observe that

$$Q(M) = \cup_{z=0}^{P-1} Q_z(M)\,, \tag{76}$$

where

$$\begin{aligned} Q_z(M) &\triangleq \cup_{s\in\mathbb{N}} \cup_{l=0}^{p^n-1} \{q_{M+z+lP+sp^nP}\} && (77)\\ &\overset{(71,67)}{=} \cup_{s\in\mathbb{N}} \cup_{l=0}^{p^n-1} \{q_{M+z} + (j_{M,z,l} + s)P\}\,,\\ &\quad \text{(the } j_{M,z,l} \text{ are specific integers)}\\ &= \cup_{s\in\mathbb{N}}\{q_{M+z} + (\min_l j_{M,z,l} + s)P\}\\ &= \cup_{s_z=\min_l j_{M,z,l}}^{\infty}\{q_{M+z} + s_zP\} && (78) \end{aligned}$$

Combining Eq. (76) and Eq. (78) then gives

$$\begin{aligned} Q(M) = {} & \cup_{s_0=\min_l j_{M,0,l}}^{\infty}\{q_M + s_0P\}\\ & \cup_{s_1=\min_l j_{M,1,l}}^{\infty}\{q_{M+1} + s_1P\}\dots\\ & \cup_{s_{P-1}=\min_l j_{M,P-1,l}}^{\infty}\{q_{M+P-1} + s_{P-1}P\} \end{aligned}$$

Because $Q(M)$ contains all integers $k \geq \min Q(M)$ [Lemma 6.5(B)], the previous equation shows that the subsets $Q_z(M) = \cup_{s_z=\min_l j_{M,z,l}}^{\infty}\{q_{M+z} + s_zP\}$, $0 \leq z \leq P-1$ must be all disjoint and that the set of the minimal elements $\{q_{M+z} + \min_l j_{M,z,l} \cdot P | 0 \leq z \leq P-1\}$ forms a set of P consecutive integers starting with $\min Q(M) \overset{(74)}{=} \min Q_{p^n}(M)$.

Through Eq. (77) and Eq. (75), it follows that all $a(m_z)$, $m_z \in Q_z(M)$ are equal, or: $a(m_z) = a(m_z + P)$ for all $m_z \geq \min Q_z(M)$. As this holds for all $0 \leq z \leq P-1$, and because $\{\min Q_z(M) | 0 \leq z \leq P-1\}$ is a set of consecutive integers, we conclude that it holds for all $m \geq \min_z\{\min Q_z(M)\} = \min Q(M)$. This proves the lemma. ■

Lemma 6.7. *When*

$$a(m) = a(m+P) \text{ for all } m \geq M_i$$

and when

$$M_{i+1} \triangleq \min Q(M_i + \Delta) < M_i\,, \tag{79}$$

then

$$a(m) = a(m+P) \text{ for all } m \geq M_{i+1}$$

Proof. It follows from Eq. (64) that

$$\begin{aligned} a(k) - a(k+P) = {} & c_r(0)[a(q_k) - a(q_{k+P})]\\ & + \sum_{i=1}^{\Delta} c_r(i)[a(k-1) - a(k-i+P)] \end{aligned} \tag{80}$$

Suppose $a(m) = a(m+P)$ for $m \geq M_i$. Then it follows from Eq. (80) that $a(q_k) = a(q_{k+P})$ for all $k \geq M_i + \Delta$, which, by Lemma 6.6 implies that

$$a(m) = a(m+P) \text{ for all } m \geq M_{i+1}$$
$$\triangleq \min Q(M_i + \Delta). \quad \blacksquare$$

The last lemma gives conditions under which a CGI-solution which is right-periodic from M_i on, extends this right-periodicity from some $M_{i+1} < M_i$ onwards. Now this procedure can be iterated by letting $i \rightarrow i+1$, as long as $\min Q(M_{i+1} + \Delta) < M_{i+1}$ (cf. Eq. (79)), thus generating a sequence

$$M_i > M_{i+1} > M_{i+2} > M_{i+3} \cdots > M_{f-1} > M_f > \cdots$$

Observe that $M_{f-1} > M_f$ implies that $M_{f-1} + \Delta > M_f + \Delta$, and by the min $Q(*)$ definition also that $\min Q(M_{f-1}+\Delta) \geq \min Q(M_f+\Delta)$, or $M_f \geq M_{f+1}$. As a matter of fact, when it might happen that $M_f = M_{f+1} = \min Q(M_f + \Delta)$, we would subsequently find that $M_f = M_{f+1} = M_{f+2} = M_{f+3} \ldots$, so that the recursion given by the one-dimensional discrete recursive map

$$M_{i+1} = \min Q(M_i + \Delta)(M_i,\, M_{i+1} \in \mathbb{Z}) \qquad (81)$$

actually reaches a fixed point M_f. That this fixed point will eventually be reached is readily clear from the graph which plots $f(m) \triangleq \min Q(m+\Delta)$ versus m, as illustrated in Fig. 25. This graph shows that Eq. (81) has either a unique fixed point M_f [Fig. 25(a)], or two fixed points M_f and $M_f - 1$ [Fig. 25(b)]. M_f satisfies

$$M_f = \min Q(M_f + \Delta), \qquad (82)$$

and in case of two fixed points, we also have $M_f - 1 = \min Q(M_f - 1 + \Delta)$. Whatever the situation, when we start the recursion Eq. (81) from some arbitrary $M_0 > M_f$, as is the case in the present context, it is clear that M_f is reached in a finite number of steps via a sequence

$$M_0 > M_1 > M_2 > M_3 \cdots > M_{f-1} > M_f.$$

Theorem 6.2. *Any right-periodic solution for a given CGI-problem must be periodic from M_f on, where M_f is the rightmost fixed point of the iterated map*

$$M_{i+1} = \min Q(M_i + \Delta). \qquad (83)$$

(M_f depends on the parameters of the problem, but is independent of the possible period of the solution).

Proof. Any right periodic solution is certainly periodic from some $M_0 > M_f$ onwards. Then generate the sequence $M_0 > M_1 > M_2 > \cdots > M_f$ obtained by applying Eq. (83). Applying Lemma 6.7 along with this sequence proves that this right periodicity certainly extends to M_f. $\blacksquare$

Lemma 6.8. *There exists a smallest integer $X_r^{(T)}$, with T a fixed integer, such that*

$$\forall m \geq X_r^{(T)} : \ \max Q_{p^n}(m+T) \leq m + T - 1 \quad (84)$$

Proof. This is a direct consequence of the fact that the graph of the function $Q_{p^n}(m+T)$ is a discrete staircase with average slope p^{-n} (as was illustrated in Fig. 24), so that it must necessarily intersect the graph of the function $m + T - 1$, i.e. the equation

$$\max Q_{p^n}(m+T) = m + T - 1 \qquad (85)$$

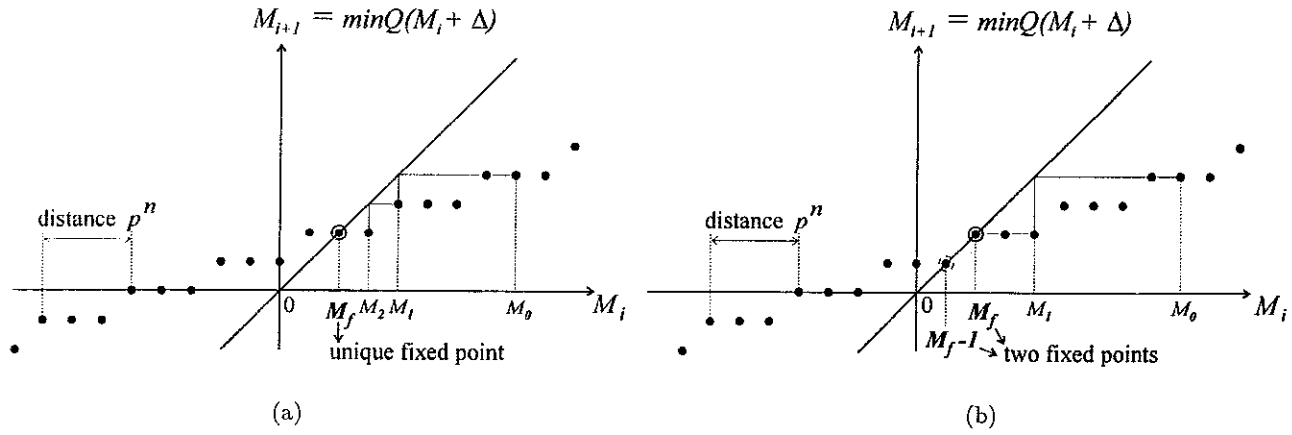

Fig. 25. The discrete recursive map $M_{i+1} = f(M_i) \triangleq \min Q(M_i+\Delta)$ (a) situation with a unique fixed point, with a trajectory $M_0 > M_1 > M_2 > M_3 = M_f$, (b) situation with two fixed points. Starting to the right of M_f always ends in M_f.

has at least one solution. Because the step-height is 1, this equation can at most have two solutions. $X_r^{(T)}$ is clearly the smallest solution of Eq. (85). ■

Corollary 6.4.

(a) $\forall m \geq X_r^{(T)}$:

$$q_{m+T} \leq m+T-1 \text{ and } q_m \leq m+T-1 \quad (86)$$

(b) $X_r^{(1)} = X_r^{(T)} + T - 1,$

$$\text{and so } X_r^{(1)} > X_r^{(T)} \text{ when } T \in \mathbb{N}_0. \quad (87)$$

Proof

(a) From the staircase-form of the function $\max Q_{p^n}(m)$, it follows that $\forall m \in \mathbb{Z}$: $q_m \leq \max Q_{p^n}(m) \leq \max Q_{p^n}(m+T)$ and $q_{m+T} \leq \max Q_{p^n}(m+T)$.

Restrict m to $m \geq X_r^{(T)}$ and apply Eq. (84) in order to find that $m+T-1$ is an upper bound for $\max Q_{p^n}(m+T)$, and so for q_m and q_{m+T}.

(b) By Lemma 6.8, $X_r^{(0)}$ is the smallest solution of the equation $\max Q_{p^n}(x) = x-1$. Hence, the smallest solution in m when $x = m+T$ is given by $X_r^{(T)} = X_r^{(0)} - T$. Equation (87) follows readily from this. ■

Theorem 6.3. *Let*

$$Y_r^{(P)} \triangleq \max\{M_f + \Delta - 1,\, X_r^{(P)} - 1\} \quad (88)$$

and let $\langle a(k)\rangle_{k\in\mathbb{Z}}$ *be the initial-state of a CGI-solution for which it is imposed that*

$$a(m) = a(m+P) \text{ for all } m:\ M_f \leq m \leq Y_r^{(P)}, \quad (89)$$

where P *is a possible period (as given by Theorem 6.1). Then the solution is right* P*-periodic, i.e.*

$$a(m) = a(m+P) \text{ for all } m \geq M_f \quad (90)$$

Proof. We actually have to show that Eq. (89) implies that $a(m) = a(m+P)$ for all $m > Y_r^{(P)}$. This will be done by induction. Fix some

$$z \geq Y_r^{(P)}, \quad (91)$$

and let

$$a(m) = a(m+P) \text{ for all } m:\ M_f \leq m \leq z. \quad (92)$$

We will show that this implies $a(z+1) = a(z+1+P)$, or

$$a(m) = a(m+P) \text{ for all } m:\ M_f \leq m \leq z+1. \quad (93)$$

Indeed, we have

$$a(z+1) - a(z+1+P) \overset{(64)}{=} c_r(0)[a(q_{z+1}) - a(q_{z+1+P})] + \sum_{i=1}^{\Delta} c_r(i)[a(z+1-i) - a(z+1-i+P)]. \quad (94)$$

Now, observe that

(a) $a(z+1-i) = a(z+1-i+P)$ for all $i = 1, 2, \ldots \Delta$, because Eq. (92) applies as $M_f \leq z+1-i \leq z$ [the first inequality holds for the minimal value of $z+1-i$, which is $Y_r^{(P)} + 1 - \Delta$ (Eq. (91)), and this is $\overset{(88)}{\geq} M_f$].

(b) $a(q_{z+1}) = a(q_{z+1+P})$, because:

1. $M_f \leq q_{z+1} \leq z+P$

$$\text{and } M_f \leq q_{z+1+P} \leq z+P \quad (95)$$

- $M_f \leq q_{z+1}$ and $M_f \leq q_{z+1+P}$ hold because $z+1+P > z+1 \geq Y_r^{(P)} + 1 \overset{(88)}{\geq} M_f + \Delta$, and $q_m \geq \min Q(M_f + \Delta) \overset{(82)}{=} M_f$ for all $m \geq M_f + \Delta$.
- $q_{z+1} \leq z+P$ and $q_{z+1+P} \leq z+P$ because $z+1 \overset{(91)}{\geq} Y_r^{(P)} + 1 \overset{(88)}{\geq} X_r^{(P)}$, and so Eq. (86) applies.

2. $q_{z+1+P} \overset{(71)}{=} q_{z+1} + s_0 P$ for some $s_0 \in \mathbb{Z}$.
3. (1) and (2) combined with the conditions imposed by Eq. (92), imply that there must be either a chain
$a(q_{z+1}) = a(q_{z+1}+P) = a(q_{z+1}+2P) = \ldots = a(q_{z+1}+s_0P) = a(q_{z+1+P})$
when $s_0 \geq 0$, or a chain
$a(q_{z+1}) = a(q_{z+1}-P) = a(q_{z+1}-2P) = \ldots = a(q_{z+1}-|s_0|P) = a(q_{z+1+P})$
when $s_0 \leq 0$.

(c) put the observations (a) and (b) together in Eq. (94) to conclude that $a(z+1) = a(z+1+P)$, from which Eq. (93) follows.

The induction Eq. (92) → Eq. (93) can be continuously repeated starting with $z = Y_r^{(P)}$, and this proves the theorem. ■

This last theorem gives us the **additionally sufficient conditions** for right P-periodicity of the

CGI solutions that we were looking for:

$$\forall m,\ M_f \le m \le Y_r^{(P)} :\ a(m) = a(m+P)\,. \quad (96)$$

The range of m for which Eq. (96) has to be imposed depends generally on P. By virtue of Eq. (87), this range can be made independent of P by taking its largest value over all possible P, i.e. by taking $Z_r \triangleq Y_r^{(1)}$ as its upper bound. This can be interesting for computational procedures and leads to

Corollary 6.5. *An additionally sufficient condition for right P-periodicity of a CGI-solution is*

$$\forall m,\ M_f \le m \le Z_r \triangleq \max\{M_f + \Delta - 1,\ X_r^{(1)} - 1\} : \\ a(m) = a(m+P)\,, \quad (97)$$

(recall that $X_r^{(1)}$ is the minimal solution of $\max Q_{p^n}(m+1) = m$).

M_f and Z_r can easily be found in a systematic way from the right propagating equations through their definitions (see Eqs. (81)–(82) for M_f, Corollary 6.5 for Z_r).

This set of equations, Eq. (97) is a sufficient addition to the set of seed-internal equations (which are necessary), and limits the solution set to the solutions which are right P-periodic (where P is a possible period as discussed in Sec. 6.1).

As all $a(k)$ which do not belong to the seed itself ultimately depend on the seed-cells (through use of the propagating equations), Eq. (96) can also be transformed into seed-internal equations. The solution of the set of original seed-internal equations together with the new additional ones will be called the right P-periodic augmented set of seed-internal equations, and will produce a reduced set of freeseed-cells with an associated reduced set of freeseed codes that guarantee right P-periodic solutions. Observe that this category of solutions also includes all possible (P', P)-biperiodic solutions, all possible full P-periodic solutions, and all possible left-complex, right P-periodic solutions. The number of right P-periodic equals $p^{N_{fa}}$, where N_{fa} is the number of free seedcells emerging from the solution of the augmented set of internal equations. Notice also that the set of P-periodic solutions contains all P_d-periodic solutions, where P_d is any divisor of P.

Example 6.1. We reconsider the $\mathbb{Z}_3$-CA problem from Example 4.2. The right-propagating equations are given in Table 1, where the indices corresponding to m, q_m and $m - \Delta$ have been indicated. The rightmost fixed point for the recursion $M_{i+1} = \min Q(M_i + \Delta)$ is indeed $M_f = 2$ (there is a second fixed point, nl. $M_f - 1 = 1$).

For example, start with $M_0 = 6$. Then

$M_1 = \min Q(M_0 + \Delta) = \min Q(12) = \min Q_3(12) = \min\{4, 3, 6\} = 3$
$M_2 = \min Q(3 + 6) = \min Q(9) = \min Q_3(9) = \min\{3, 2, 5\} = 2$
$M_3 = \min Q(2 + 6) = \min Q(8) = \min Q_3(8) = \min\{4, 3, 2\} = 2.$
As $X_r^{(1)} = 3$ [unique solution of $\max Q_3(m+1) = \max\{q_{m+1}, q_{m+2}, q_{m+3}\} = m$], we find that $Z_r = \max\{M_f + \Delta - 1,\ X_r^{(1)} - 1\} = \max\{7, 2\} = 7$.

These values $M_f = 2$ and $Z_r = 7$ give the following additionally sufficient conditions for right P-periodicity

$$\text{for } m = 2, 3, \ldots 7 :\ a(m) = a(m+P) \quad (98)$$

According to Theorem 6.1, and recalling that $\alpha = (\alpha_0, \alpha_1, \alpha_2) = (2, 1, 0)$ and $p^n = 3^1$, P must be a divisor of $(-1)\cdot 3 - 1 = -4$. So, there *may* be solutions with possible period $4, 2, 1$. Let's select $P = 4$. We explicitize the conditions of Eq. (98) and give the corresponding seed-internal equations (for the selected seed $\langle a_{-2}, a_{-1}, a_0, a_1, a_2, a_3\rangle$ in which all cells are freecells, see Example 4.2):

$$\begin{aligned}
&a_2 = a_6 \Leftrightarrow a_{-2} + 2a_1 + 2a_2 + a_3 = 0\\
&a_3 = a_7 \Leftrightarrow a_{-1} + 2a_1 = 0\\
&a_4 = a_8 \Leftrightarrow a_{-2} + a_{-1} + a_1 + 2a_2 + a_3 = 0\\
&a_5 = a_9 \Leftrightarrow 2a_{-2} + a_{-1} + a_2 + 2a_3 = 0\\
&a_6 = a_{10} \Leftrightarrow 2a_{-2} + a_{-1} + 2a_1 + a_2 + 2a_3 = 0\\
&a_7 = a_{11} \Leftrightarrow 0 = 0
\end{aligned} \quad (99)$$

(All equations in $\mathbb{Z}_3$!)

Observe that not all equations are independent: this should not be surprising as we have proven that this is a set of sufficient conditions, and redundancy may be expected. That the equation $a_7 = a_{11}$ results in $0 = 0$, just means that the CGI-equations themselves already imply that $a_7 \equiv a_{11}$. This set of seed-internal equations has to be solved in order to find the right 4-periodic solutions (in case there would already be primal seed-internal equations, these should be incorporated in the set of

equations to be solved). Solving Eqs. (99) gives four degrees of freedom: cell-states a_0, a_1, a_2, a_3 can be chosen freely, and the two seedcells a_{-2} and a_{-1} are depcells:

$$\begin{aligned} a_{-2} &= a_1 + a_2 + 2a_3 \\ a_{-1} &= a_1 \end{aligned} \tag{100}$$

This means that all good seeds which correspond to right 4-periodic solutions are of the form $\langle a_{-2}, a_{-1}, \underline{a_0}, \underline{a_1}, \underline{a_2}, \underline{a_3}\rangle = \langle a_1+a_2+2a_3, a_1, \underline{a_0}, \underline{a_1}, \underline{a_2}, \underline{a_3}\rangle$. There are $3^4 = 81$ such solutions. Notice that this set of solutions contains all solutions which are possibly fully 4-periodic, right- or fully 2-periodic, and right- or fully 1-periodic.

6.2.2. *Additionally sufficient conditions for left periodicity*

The whole development of Sec. 6.2.1. can be repeated in a left–right symmetric way, by considering the left-propagating equations for the initial state of the automaton, and will lead to a set of additionally sufficient left P-periodic equations

$$\forall m,\ Z_l \le m \le L_f :\ a(m) = a(m-P)\,, \tag{101}$$

where Z_l and L_f are the left-symmetric equivalents of Z_r and M_f defined as follows.

Let $q'_m \triangleq \lfloor \frac{m-\Phi_l}{p^n} \rfloor + \alpha_{(m-\Phi_l) \bmod p^n}$ be the equivalent of Eq. (64) for the left propagating equations, $Q'_m \triangleq \{q'_m, q'_{m-1}, q'_{m-2}, \ldots\}$ and $Q'_{-p^n}(m) \triangleq \{q'_m, q'_{m-1}, \ldots, q'_{m-p^n+1}\}$. Then:

- L_f is the minimal solution of the equation

$$m \triangleq \max Q'(m-\Delta)\,,$$

  it is also the leftmost fixed point of the iterated map

$$L_{i+1} = \max Q'(L_i - \Delta)\,.$$

- $$Z_l \triangleq \min\{L_f - \Delta + 1,\ X_l^{(1)} + 1\}$$

  with

$$\begin{aligned} X_l^{(1)} &= \text{maximal solution of } \min Q'_{-p^n}(m-1) \\ &= m\,. \end{aligned}$$

This set of equations, when reduced to a seed-internal set and combined with the original seed-internal equations, ultimately leads to a left P-periodic augmented set of equations which produces a restricted set of left P-periodic CGI solutions which includes all possible (P, P')-biperiodic solutions, all possible fully P-periodic solutions and all possible left P-periodic, right-complex solutions.

Example 6.2. We continue the previous example. The corresponding left-propagating equations can also be found in Table 1. Now we find $L_f = 1$, $X_l^{(1)} = 0$ and $Z_l = \min\{1-6+1, 0+1\} = -4$. The additionally sufficient conditions for left 4-periodicity are:

$$\begin{aligned} a_1 = a_{-3} &\Leftrightarrow 2a_{-2} + a_1 + a_2 + 2a_3 = 0 \\ a_0 = a_{-4} &\Leftrightarrow a_{-2} + 2a_1 + 2a_2 + a_3 = 0 \\ a_{-1} = a_{-5} &\Leftrightarrow 2a_{-2} + a_{-1} + a_2 + 2a_3 = 0 \\ a_{-2} = a_{-6} &\Leftrightarrow a_{-2} + 2a_{-1} + 2a_2 + a_3 = 0 \\ a_{-3} = a_{-7} &\Leftrightarrow 2a_{-2} + a_1 + a_2 + 2a_3 = 0 \\ a_{-4} = a_{-8} &\Leftrightarrow a_{-2} + 2a_1 + 2a_2 + a_3 = 0\,. \end{aligned} \tag{102}$$

It now happens that this set of equations has the same solutions as the one for right 4-periodicity. It means that right 4-periodicity implies left 4-periodicity and vice versa, and there are $3^4 = 81$ such $(4,4)$-biperiodic solutions. It does not mean that these solutions are necessarily fully 4-periodic.

6.2.3. *Additionally sufficient conditions for (P,P')-biperiodicity*

It is clear that one should solve the additionally sufficient left P-periodic equations together with the additionally sufficient right P'-periodic equations and the original seed-internal equations.

Example 6.3. We keep considering the same problem. What are its (2, 4)-biperiodic solutions? The set of equations to be solved is the sufficient set of right 4-periodic equations as given by Eqs. (99), together with the following sufficient set of left 2-periodic equations:

$$\begin{aligned} a_1 = a_{-1} &\Leftrightarrow a_{-1} + 2a_1 = 0 \\ a_0 = a_{-2} &\Leftrightarrow a_{-2} + 2a_0 = 0 \\ a_{-1} = a_{-3} &\Leftrightarrow 2a_{-2} + 2a_{-1} + 2a_1 + a_2 + 2a_3 = 0 \\ a_{-2} = a_{-4} &\Leftrightarrow a_0 + a_1 + 2a_2 + a_3 = 0 \\ a_{-3} = a_{-5} &\Leftrightarrow 2a_{-1} + a_1 = 0 \\ a_{-4} = a_{-6} &\Leftrightarrow a_{-2} + 2a_{-1} + 2a_0 + a_1 = 0 \end{aligned} \tag{103}$$

The number of free seedcells reduces to 3. A good seed is now of the form $\langle a_{-2}, a_{-1}, a_0, \underline{a_1}, \underline{a_2}, \underline{a_3}\rangle = \langle a_1 + a_2 + 2a_3,\ a_1,\ a_1 + a_2 + 2a_3,\ a_0,\ \underline{a_1}, \underline{a_2}, \underline{a_3}\rangle$, and there are $3^3 = 27$ $(2,4)$-biperiodic solutions. This set of solutions clearly contains all $(2,4)$-, $(1,4)$-, $(2,2)$-, $(1,2)$-, $(2,1)$-, $(1,1)$-biperiodic solutions (and so also all fully 2- and 1-periodic solutions). From the results of Example 6.2 and this example, we can already conclude that there are $81 - 27 = 54$ solutions which are 4- or 2- or 1-periodic to the right and 2- or 1-periodic to the left.

6.2.4. *Additionally sufficient conditions for full P-periodicity*

Full P-periodicity corresponds to (P, P)-biperiodicity with the additional requirement that there should be no phase-defect between the left and right P-periodic sequences that respectively start at L_f and M_f. The following two cases should possibly be distinguished:

(a) $L_f \geq M_f + P$: in this case, there are no additional conditions, as the overlap region between the left and right periodic sequences is sufficiently large, so that it automatically implies the absence of a phase-defect.
(b) $L_f < M_f + P$: the additionally sufficient conditions for full P-periodicity are:

$$\text{for } k = 1, 2, \ldots, M_f - L_f + P - 1: \quad a(L_f + k) = a(L_f + k - P). \quad (104)$$

Again, these equations should be reduced to their seed-internal equivalents and should be solved together with the (P, P)-periodic augmented set of seed-internal equations that are already available.

Example 6.4. Let's find all fully 4-periodic solutions of still the same problem. Therefore, we must solve the set of Eqs. (99) and Eqs. (102) for $(4,4)$-biperiodicity, augmented with the set of left–right periodic continuity equations as given by Eq. (104):

$$\begin{aligned} a_2 = a_{-2} &\Leftrightarrow a_{-2} + 2a_2 = 0 \\ a_3 = a_{-1} &\Leftrightarrow a_{-1} + 2a_3 = 0 \\ a_4 = a_0 &\Leftrightarrow a_{-2} + a_{-1} + 2a_2 + 2a_3 = 0 \\ a_5 = a_1 &\Leftrightarrow a_{-2} + a_{-1} + a_1 + 2a_2 = 0 \end{aligned} \quad (105)$$

Solving Eqs. (99), (102) and (105) gives the following good seedcode for full 4-periodicity: $\langle a_{-2}, a_{-1}, \underline{a_0}, a_1, \underline{a_2}, \underline{a_3}\rangle = \langle a_2, a_3, \underline{a_0}, a_3, \underline{a_2}, \underline{a_3}\rangle$.

So, there are 3 freecells and $3^3 = 27$ fully 4-periodic solutions for the given CGI-problem (as many as there are $(2,4)$-biperiodic solutions, but the seedcodes are different: the class of $(2,4)$-biperiodic solutions is not identical with the class of fully 4-periodic solutions (but there is certainly overlap as fully 4-periodic $\supseteq$ fully 2-periodic $\subseteq$ $(2,4)$-biperiodic)).

7. Conclusion

We have been dealing with the concept of coarse-graining invariant orbits for $\mathbb{Z}_p$-automata in a very general way (concerning CA-rule, tile-shape and weighting). A procedure for constructing all solutions to a given CGI-problem was developed. The solution patterns show a visual intricacy which may range from complete order (periodicity) to complete disorder (randomlike), by going over quasi-periodicity and quasi-randomness through intermediate complexities. Some patterns are clearly visually self-similar. Other patterns exhibit almost no structure, but may have a hidden structure which pops up in their SIP's (shift identity patterns). All solutions of a CGI-problem form a finite Abelian group.

It would be interesting to refine the morphological categorization as presented above, and which was primarily based on visual features, by some more fundamental analysis. We have presented such analysis for the unambiguously defined category of fully or partially periodic solutions. Necessary conditions for periodicity were found: these only depend on the pattern-shift vector α and the size of the tiling p^n. Also, a set of sufficient conditions was derived from which all periodic solutions for a given CGI-problem can be constructed.

In Sec. 5, while discussing the category of quasi-periodic patterns, we already have made a reference to the 2-automaticity of the initial state configuration of the particular CGI-problem presented in [Barbé *et al.*, 1995]. In the more general context of this paper, one could ask whether the initial state sequence of our CGI-solutions are perhaps p-automatic (meaning that the cell state $a(0,c)$ can be found as the output of a finite automaton whose input is the base-p representation of c). The answer seems to be positive (private communication with G. Skordev), even in the more general sense that the

complete two-dimensional orbit $\langle a(r, c)\rangle_{(r,c)\in\mathbb{N}\times\mathbb{Z}}$ is p-automatic (i.e. $a(r, c)$ is the output of a finite state machine whose input is the p-adic representation of both r and c, see [Allouche *et al.*, 1995b]). Assuming that our solutions are p-automatic, we face an interesting problem: if we can find the p-automaton with the minimal number of states that generates a particular orbit, does the complexity of its structure and its number of states somehow reflect the visual complexity of the orbit's graphical representation? Also, as p-automaticity implies the existence of a substitution system which also generates the underlying pattern [Allouche *et al.*, 1995a], we expect this substitution system to be related to the self-similarities observed in some of the examples that were discussed in Sec. 5.

A final remark: readers who are capable of stereovision when gazing at so-called stereograms, could try to do so with the patterns shown in this paper. In most cases, a three-dimensional impression will be experienced.

Acknowledgments

I am very grateful to H.-O. Peitgen, G. Skordev and F. von Haeseler, who have created the opportunity for being together, first in Oberwolfach in 1992, and then at their Institute in Bremen in 1993. The stay in Bremen was seminal for the coarse-graining invariant problem, and we had the occasion to report about it before. Without it, the present results would most likely not have come about in the form and/or at the time they have now.

Part of this work has been carried out within the framework of a Concerted Action Project of the Flemish Community, entitled "Model-Based Information Processing Systems" GOA-MIPS.

References

Allouche, J. P., Cateland, E., Peitgen, H.-O., Shallit, J. & Skordev, G. [1995a] "Automatic maps on a semi-ring with digits," *Fractals* **3**(4), 663–677.

Allouche, J. P., von Haeseler, F., Peitgen, H.-O., Petersen, A. & Skordev, G. [1995b] "Automaticity of double sequences generated by one-dimensional linear cellular automata," Report Nr. 346, Institut für Dynamische Systeme, Universität Bremen. To appear in *Theor. Comp. Sc.* [1997].

Armstrong, M. A. [1988] *Groups and Symmetry* (Springer, New York).

Barbé, A. [1988] "Periodic patterns in the binary difference field," *Complex Systems* **2**, 209–233.

Barbé, A. [1990] "A cellular automaton ruled by an eccentric conservation law," *Physica* **D45**, 49–62.

Barbé, A. [1992] "On a class of fractal matrices, (I): excess-matrices and their self-similar properties," *Int. J. Bifurcation and Chaos* **2**(4), 841–860.

Barbé, A., von Haeseler, F., Peitgen, H.-O. & Skordev, G. [1995] "Coarse-graining invariant patterns of one-dimensional two-state linear cellular automata," *Int. J. Bifurcation and Chaos* **5**(6), 1611–1631.

Bruce A. & Wallace D. [1989] "Critical point phenomena: universal physics at large length scales," in *The New Physics*, ed. Davis, P. (Cambridge Univ. Press), pp. 236–267.

Carmichael, R. D. [1956] *Introduction to the Theory of Groups of Finite Order* (Dover Publications, New York).

Graham, A. [1981] *Kronecker Products and Matrix Calculus: With Applications* (Ellis Horwood Chichester, J. Wiley & Sons, New York).

Hardy, G. & Wright, M. [1979] *An Introduction to the Theory of Numbers* (Oxford University Press, Oxford).

von Haeseler, F., Peitgen, H.-O. & Skordev, G. [1993] "Cellular automata, matrix substitutions and fractals," *Annals of Mathematics and Artificial Intelligence* **8**, 345–362.

Martin, O., Odlyzko, A. & Wolfram, S. [1984] "Algebraic properties of cellular automata," *Commun. Math. Phys.* **93**, 219–258.

Wilson, K. G. [1979] "Problems in physics with many scales of length," *Sci. Amer.* **241**, 236–267.

Appendix: Problem Table

Problem #	p^n	R(x)	α	β	Γ	W	number of core-intervals	number of solutions	nature of solutions (and their numbers)
1.	2^2	$1+x^2$	(-6,-2,2,6)	(0,1,2,3)	[0]	[1]	1	1024	full (64)- & biperiodic (64) quasirandom (896)
		seedcode = $\langle a_{-7}a_{-6}a_{-5}a_{-4}a_{-3}a_{-2}a_{-1}a_0a_1a_2a_3a_4a_5\rangle$							
2.	2^2	$1+x^2$	(0,1,2,3)	(0,0,0,0)	[0]	$\begin{bmatrix}1&0&1&0\\0&1&0&1\\1&0&1&0\\0&1&0&1\end{bmatrix}$	3	16	selfsimilar 1st kind (3) selfsimilar 2nd kind (12)
		seedcode = $\langle a_0a_1a_2a_3\rangle$							
3.	2^2	$1+x^2$	(0,1,2,3)	(0,0,0,0)	[0]	$\begin{bmatrix}1&0&0&0\\0&1&0&0\\0&0&1&0\\0&0&0&1\end{bmatrix}$	5	64	quasiperiodic (60) full-periodic (2) biperiodic (2)
		seedcode = $\langle a_{-2}a_{-1}a_0a_1a_2a_3\rangle$							
4.	3^1	$1+2x^2$	(0,7,-6)	(0,0,0)	[0]	$\begin{bmatrix}0&0&1\\0&0&0\\1&0&0\end{bmatrix}$	1	729	full-periodic (81) Lperiodic-Rselfsim.(162) Lselfsim.-Rperiodic (162) biselfsimilar (324)
		seedcode = $\langle a_j\rangle_{j=-8}^{9}$, freecells: $a_{-8},a_5,a_6,a_7,a_8,a_9$							
5.	2^2	$1+x^2$	(2,-5,3,-2)	(0,1,-3,0)	[0]	[1]	5	2048	randomlike (2047)
		seedcode = $\langle a_{-5}a_{-4}a_{-3}a_{-2}a_{-1}a_0a_1a_2a_3a_4a_5\rangle$							
6.	2^2	$1+x+x^2$	(0,1,2,3)	(0,1,2,3)	[0]	$\begin{bmatrix}1&0&0&0\\0&0&0&0\\0&0&0&0\\0&0&0&1\end{bmatrix}$	4	32	selfsimilar 3d kind (28) full-periodic (4)
		seedcode = $\langle a_{-2}a_{-1}a_0a_1a_2\rangle$							
7.	2^2	$1+x+x^2$	(0,0,0,0)	(0,0,0,0)	[0]	$\begin{bmatrix}1&0&0&0\\0&0&0&0\\0&0&0&0\\0&0&0&1\end{bmatrix}$	7	64	complex (selfsimilar 3d kind?) (63)
		seedcode = $\langle a_{-2}a_{-1}a_0a_1a_2a_3\rangle$							
8.	2^1	$1+x^2$	(0,50)	(0,0)	$\begin{bmatrix}0&1\\1&0\end{bmatrix}$	[1]	1	256	full-periodic biperiodic
		seedcode = $\langle a_j\rangle_2^{100}$, freecells $a_2,a_{68},a_{86},a_{90},a_{92},a_{96},a_{98},a_{100}$							
9.	2^2	$1+x^2$	(0,2,4,6)	(0,1,2,3)	$\begin{bmatrix}0&1&0&0\\1&0&0&0\\0&1&0&0\\1&0&0&0\end{bmatrix}$	[1]	3	128	full-periodic (4) complex (124)
		seedcode = $\langle a_{-1}a_0a_1a_2a_3a_4a_5\rangle$							
10.	2^2	$1+x+x^2$	(0,0,0,0)	(0,0,0,0)	[0]	$\begin{bmatrix}0&0&0&0\\0&1&0&0\\0&0&0&0\\0&0&0&0\end{bmatrix}$	3	4	full-periodic (2) selfsimilar 2nd kind (2)
		seedcode = $\langle a_0a_1\rangle$							
11.	2^2	$1+x^2$	(0,0,0,0)	(0,0,0,0)	$\begin{bmatrix}0&1&0&0\\1&0&0&0\\0&1&0&0\\1&0&0&0\end{bmatrix}$	[1]	8	64	selfsimilar 3d kind (63)
		seedcode = $\langle a_{-2}a_{-1}a_0a_1a_2a_3\rangle$							
12.	2^4	$1+x^3+x^6$	(0)	(0)	[0]	[1]	63	2^{60}	quasiperiodic selfsimilar 2nd kind
		seedcode = $\langle a_j\rangle_{j=-30}^{29}$, all cells are freecells							
13.	2^1	$1+x^2+x^4$	(0,4)	(0,0)	$\begin{bmatrix}0&1\\0&1\end{bmatrix}$	[1]	3	32	full-periodic (4) biperiodic (4) quasirandom(complex)(24)
		seedcode = $\langle a_2a_3a_4a_5a_6\rangle$							

Problem Table (*Continued*)

Problem #	p^n	R(x)	α	β	Γ	W	number of core-intervals	number of solutions	nature of solutions (and their numbers)
14.	3^2	$1+2x^3+x^6$	(0)	(0)	[0]	[1]	35	3^{32}	quasiperiodic
		seedcode = $\langle a_j \rangle_{j=-15}^{16}$, all cells are freecells							
15.	5^1	$1+x+x^2$	(0)	(0)	[0]	[1]	9	390625	quasiperiodic
		seedcode = $\langle a_{-3}a_{-2}a_{-1}a_0a_1a_2a_3a_4 \rangle$							
16.	5^1	$1+3x^4$	(0,5,10,15,20)	(0)	[0]	[1]	1	5^{14}	full-periodic (5^{13}) biperiodic (5^{14}-5^{13})
		seedcode = $\langle a_j \rangle_{j=4}^{27}$,freecells are $a_4,a_9,a_{10},a_{14},a_{15},a_{16},a_{19},a_{20},a_{21},a_{22},a_{24},a_{25},a_{26},a_{27}$							
17.	7^1	$5+4x+3x^2$	(0,-5,-10,-15,-20,-25,-30)	(0)	[0]	[1]	1	7^{18}	full-periodic (7^{14}) biperiodic (7^{15}-7^{14}) quasirandom (7^{18}-7^{15}) ?
		seedcode = $\langle a_j \rangle_{j=-34}^{-1}$, freecells : $a_{-34},a_{-28},a_{-22},a_{-16},a_{-14}$ to a_{-1}							
18.	2^2	$1+x+x^2$	(-2,2,1,-5)	(0)	[0]	[1]	1	64	full-periodic (4) quasirandom (60)
		seedcode = $\langle a_{-5}a_{-4}a_{-3}a_{-2}a_{-1}a_0a_1a_2 \rangle$							
19.	3^1	$1+2x^2$	(0,3,6)	(0,1,2)	[0]	$\begin{bmatrix}0&0&0\\0&1&0\\0&0&2\end{bmatrix}$	1	81	full-periodic (9) complex/bicomplex (54) Lselfsim.-Rperiodic (18)
		seedcode = $\langle a_0a_1a_2a_3a_4a_5a_6 \rangle$							
20.	3^1	$1+x^2$	(0,-1,-2)	(0,1,2)	[0]	$\begin{bmatrix}0&0&1\\0&2&0\\2&0&0\end{bmatrix}$	2	81	full-periodic (27) quasiperiodic (54)
		seedcode = $\langle a_{-3}a_{-2}a_{-1}a_0 \rangle$							
21.	5^1	$1+2x+3x^2$	(0,1,2,3,4)	(0)	[0]	$\begin{bmatrix}0&0&0&0&0\\0&0&0&0&0\\0&0&0&0&2\\0&0&0&0&0\\0&0&0&0&0\end{bmatrix}$	1	625	selfsimilar (3d kind)
		seedcode = $\langle a_0a_1a_2a_3 \rangle$							
22.	5^1	$1+4x+x^2+4x^3+x^4$	(0,1,2,3,4)	(0)	[0]	$\begin{bmatrix}0&0&0&0&0\\0&0&0&0&0\\0&0&0&0&0\\0&0&0&0&0\\0&0&0&0&1\end{bmatrix}$	16	5^{16}	full-periodic (125) biperiodic (500) selfsimilar (1st kind)
		seedcode = $\langle a_j \rangle_{j=-8}^{7}$, all cells are freecells							
23.	2^2	$1+x+x^2$	(0,2,4,2)	(0)	[0]	[1]	4	64	complex selfsimilar (3d kind)
		seedcode = $\langle a_{-1}a_0a_1a_2a_3a_4 \rangle$							